DEVELOPMENT OF PROBABILISTIC SEISMIC HAZARD MAP OF INDIA

FINAL REPORT

TECHNICAL REPORT
OF
THE WORKING COMMITTEE OF EXPERTS (WCE)
CONSTITUTED BY
THE NATIONAL DISATER MANAGEMENT AUTHORITY
GOVT. OF INDIA, NEW DELHI

PREFACE

NDMA constituted the *Working Committee of Experts for Microzonation of the Indian Landmass* on 21st September 2007 (*vide* No.NDMA/BB/S&T-1/2007). This committee met several times to discuss the technical scope of the work and decided to form a Working Group to first undertake the probabilistic seismic hazard analysis of the country and map the expected ground motion parameters for several return periods. The WCE also decided to co-opt two new members for proposing a project to NDMA for carrying out the work systematically. A Working Group consisting of four members was formed to carry out the PSHA. This working group helped SERC, Chennai as the nodal agency to put up a project proposal for funding from NDMA. This was approved by NDMA on 28th August 2008 (*vide* No. 3-7/2008/PMU) and funds released to SERC on 24th September 2008.

The present document reports the technical results of the PSHA project carried out by the working group of the WCE for NDMA. The basic frame work of PSHA is well known and details are available in the literature. However for arriving at a consensus on the mode of carrying out the PSHA a National Workshop was held by NDMA on 16th July 2008. This was attended by leading R&D specialists in geophysics, seismology and earthquake engineering representing academia, industry, government and private agencies. It was decided in the Workshop that the All India PSHA map should be prepared on a grid size of $0.2^0 \times 0.2^0$. The following nine recommendations of the Workshop were conveyed to the Working Group by NDMA, as forming the broad basis for developing the PSHA map of India.

1) The hazard may be computed by considering a circular region of 300 Km around the sample point.
2) The database to consist of all known earthquakes of magnitude 4 and above recorded in and around the subcontinent in the last ~500 years.
3) All magnitude values will be expressed in terms of moment magnitude Mw.
4) The maximum magnitude to be considered will be 0.5 units above the recorded or estimated past value for the region.
5) *(a, b)* values will be found by studying for completeness as per established statistical analysis due to Kijko, Sellvol and others.
6) Only faults identified by official agencies such as GSI, IMD, NGRI will be included in PSHA.
7) Appropriate attenuation relations will be derived and validated for Himalayan region, Indo-Gangetic plains, NE region, Central India, Gujarat and southern India separately.
8) PSHA result will be presented as contours for engineering bed rock conditions corresponding to B-type rock site.
9) Results will be shown for PGA, and Sa for one long period (1.25 sec) and one short period (0.5 sec) for different return periods.

The hazard analysis has been carried out keeping in view the above points with two minor variations. It became necessary to increase the control region to 500 km for

stations vulnerable to possible great earthquakes originating in the Himalayan region. The final results presented here refer to engineering bed rock conditions corresponding to A-type rock site (V_{30} > 1.5 km/s) instead of the recommended B-type site.

Seismic data required for the work has been collected from IMD, GSI, NGRI, CWPRS, ISR, IITR and ONGC among other organizations. EREC of IMD sent their earthquake catalogue and useful strong motion accelerogram data for Delhi.

Several individuals have contributed to the successful completion of the work presented here. Notable among these are Dr. N. Lakshmanan (Ex-Director, SERC) and Dr. N.R. Iyer, Director, SERC, Chennai. They have extended directly and through Dr. Arunachalam (Advisor-Management, SERC) all possible support for the technical and administrative work involved in bringing the PSHA mapping work to its final stage. Discussions with Prof. M. L. Sharma of IIT-Roorkee were helpful in characterizing seismicity and regional quality factors required in deriving strong motion attenuation relations. Dr. Ashok Kumar of IITR has sent strong motion data available for the Himalayan region.

An interim presentation of the PSHA work was done to the Vice-Chairman and Members of NDMA on 25th May 2009. Their comments and suggestions were helpful in understanding the societal implications and administrative perceptions behind the seismic hazard mapping work.

Dr. B. Bhattacharjee, Member, NDMA has been the inspiration and motive force behind the work reported here. He not only visualized the need for bringing in scientific approaches to the estimation of seismic hazard but also helped the WCE by organizing brain storming sessions, review meetings and workshops to elicit expert opinion at the national level.

Members of the WCE have been a source of strength for carrying out the PSHA work which in some parts involved expert judgment. As recently as 30th March, 2010 the WCE met to take a decision on identifying seismic zones for purposes of computing the *b-value* in recurrence relations. All the computational work reported in this document has been carried out by Dr. Balaji Rao and his team (SERC) and Dr. Raghukanth and his team (IITM).

A draft report was prepared by the working group and discussed at the WCE meeting held at IITM; Chennai on 2ndAugust, 2010. WCE approved the report with a few changes. The present document is the Final Report of WCE submitted to NDMA.

30th September, 2010
Bangalore

Prof. R.N. Iyengar
(Chairman WCE)
Centre for Disaster Mitigation
Jain University, Bangalore

Working Committee of Experts (WCE)-Microzonation

Prof R.N. Iyengar, Raja Ramanna Fellow, Bangalore	: Chairman
Prof D.K. Paul, IIT Roorkee	: Member
Dr. R.K. Bhandari, CDMM, Chairman VIT, Vellore	: Member
Prof. Ravi Sinha, IIT Mumbai	: Member
Dr. R.K. Chadha, NGRI, Hyderabad	: Member
Dr. Prabhas Pande, GSI, Lucknow	: Member
Prof. CVR Murthy, IIT Kanpur	: Member
Dr. A.K. Shukla, IMD, Delhi	: Member-Secretary
Dr. K.Balaji Rao, SERC,Chennai	: Member (co-opted)
Dr. S.T.G. Raghu Kanth, IIT, Guwahati	: Member (co-opted)

Working Group of WCE on PSHA

Prof R.N. Iyengar	(Presently with Jain University, Bangalore)
Dr. R.K. Chadha	
Dr. K. Balaji Rao*	
Dr. S.T.G. Raghu Kanth * *	(Presently at Dept. of Civil Engg. IIT-M, Chennai)

**Additional team members at SERC*
Dr. P. Kamatchi
Dr. M.B. Anoop
Mr. S.R. Balasubramanian
Mr. Daniel Ronald Joseph

***Additional team members at IITM*
Mr. B. Bhanu Teja

ABSTRACT

Success of earthquake disaster mitigation strategy depends on how well the stakeholders are sensitized to the necessity of reducing the vulnerability of built up structures. Past experience in seismic hazard management has highlighted the importance of having a well planned vulnerability reduction program built into the larger policy framework of sustainable development. The vulnerability of Indian habitat was dramatically demonstrated by the Kutch earthquake of 26th January 2001, which did not belong to the more frequent Himalayan sources. The looming seismic risk to our cities can be perceived in the backdrop of active faults in the Himalaya and in the Indo-Gangetic plain. Even in the less active peninsular region infrequent earthquakes can cause considerable damage. The principal cause for loss of life and damage is due to collapse of built infrastructure and resultant discontinuity in economic and social activity. While the financial loss in absolute terms is a function of the state of development, initial investment and cost of living indices, seismic vulnerability is closely dependent on the social and economic condition of the population. Prognosis of seismic hazard plays key role in planning and protecting buildings, life lines, industries and other safety sensitive structures. This necessitates estimation and quantification of future ground vibration. This motion lasting a few seconds is due to the sudden release of energy stored for centuries at the fault level influenced by the path and local soil conditions.

The present report highlights how surface level hazard at hard rock sites (A-type) can be estimated to develop charts and tables that can be used by government agencies, architects, engineers and other interested groups. All known data about past earthquakes and mapped faults are considered to characterize the seismic activity of the thirty-two source zones of the country structured into seven geological regions with differing quality factors. State-of-art probabilistic hazard analysis is carried out covering the whole country on a grid size of 0.2^0 x 0.2^0. New attenuation equations are derived for each of the regions incorporating known quality factors and near source effects due to finite source size. Well established probabilistic analysis procedure is adopted to compute the prevalent hazard in terms of peak ground acceleration (PGA), short period and long period spectral accelerations for different return periods.

A brief introduction highlighting the concept of return period along with a brief review of past PSHA efforts for estimating seismic hazard in India is presented in **Chapter 1**. The tectonic setting of the country and the fault map are discussed in **Chapter 2**, to delineate thirty-two source zones. Preparation of the national level earthquake catalogue, from the remote past till the end of year 2008 along with issues related to completeness, recurrence relations are considered in **Chapter 3**. In **Chapter 4**, finite fault stochastic seismological model of Boore is used to develop strong motion attenuation relations for seven geological provinces of India with differing stress drop and quality factors. The analytical results are validated wherever possible with available instrumental data. Standard PSHA procedures are followed to prepare All India hazard maps in **Chapter 5**. The earthquake catalogue assembled for the present work is attached as Appendix-I. A brief write up on the practical applications of the results of the report is presented in Appendix-II.

The results presented can be directly used on A-type rock sites. For other site classes, corrections have to be applied in terms of approximation prescribed in standard codes or by carrying out local geotechnical studies. The results presented in the report can be used further in city level microzonation, vulnerability analysis and risk evaluation. **Table 5.4** presents the existing hazard in forty-eight cities in terms of 500-, 2500-, 5000- and 10000-year return period PGA values. This does not represent the relative safety of the habitat which essentially depends on the vulnerability of the built up infrastructure. Numerical results presented here are subject to minor variations as and when new earthquake and fault data get accumulated.

CONTENTS

Chapter 1

INTRODUCTION

India faces threats from a variety of natural hazards such as floods, droughts, landslips, cyclones, earthquakes and tsunamis. The spate of earthquakes in the recent past, causing extensive damage has heightened the sensitivity of administrators, engineers and general public to the looming hazard due to future earthquakes occurring near densely populated Indian cities. Strong earthquakes are rare events, rarer than cyclones, windstorms and tidal waves. Nevertheless, India has seen quite a few earthquakes in the recent past. Earthquakes have occurred from pre-historic times, more or less in the same regions, where they are presently felt. The present heightened awareness towards earthquake disaster mitigation in the country is attributable to large loss of life and property suffered during the Khillari (30th September 1993), Jabalpur (22nd May 1997), Chamoli (29th March 1999) and Bhuj (26th January 2001) earthquakes. The seismic hazard or the potential of a site to experience ground motion due to an earthquake cannot be altered. The risk faced by human habitat due to earthquakes can be reduced by making man made systems and structures less vulnerable and more robust to withstand the ground motion. Seismic risk has a character to increase with time if continuous mitigating actions are not taken. This fact may be appreciated by recognizing that increasing population puts greater demands on housing, energy, water and transport needs of the society. In turn, these needs have to be met by increased construction activity of buildings, dams, reservoirs, bridges, power plants etc. Thus, even in areas of low seismic activity, the loss due to unexpected earthquakes may be high purely due to heavy infrastructure development, unless the built-up structures are engineered and maintained to withstand future earthquakes.

As we take up the question of safety of man made constructions, subtle issues crop up. It is not just new constructions that have to be made earthquake resistant. Engineers are called upon to protect existing cities, monuments and other structures built at a time when knowledge about earthquakes was limited. Moreover all types of construction may not be equally important, particularly so, when available financial resources are limited. In addition, earthquakes are low probability events with extremely high risk to the society. Damaging earthquakes are rare with their recurrence periods being of the order of several decades or centuries. But once they occur, much of the structural damage takes place within a few seconds, directly attributable to ground vibration. Hence engineers usually characterize seismic hazard in terms of the ground motion that can be experienced at the construction site. This way the dynamic response of structures can be studied to foresee where they may fail and for what level of seismic forces. This in turn helps in site selection, design and retrofitting strategies. The point to be noted here is that the quantification of hazard is needed for unpredictable future events. The nature and amplitude of ground motion at a site can be described in a probabilistic sense by combining past information with engineering methods of risk estimation.

1.1 Return Period

The most sought after ground motion descriptor is the response spectrum, which engineers use to find the most probable extra force, due to all possible future earthquakes, that a structure has to withstand in its expected life period. The life expectancy of a structure depends on socio-economic factors and hence engineering designs are not meant to assure 100% safety against every type of earthquake, for all times to come. A residential building may be expected to remain robust for a period of 50-100 years, where as a monumental structure may be envisioned to perform for 1000 years or more. Some amount of subjectivity is unavoidable here, but a consensus can be arrived at by public debate moderated by specialist opinion. Thus, one may like to know with high level of confidence what could be the foreseen peak ground acceleration (PGA) and design response spectrum (S_a) in an interval of say 50, 100, 1000 years. The level of confidence itself can be stated as a probability or percentage. At present, the popular way of describing hazard for building design is to specify that value of S_a that will be exceeded with only 2% chance in 50 years (IBC-2009). This is closely linked with the concept of return period T_r, which is the average time between consecutive occurrences of the same event in a time series. The event we are interested here is the ground motion exceeding a value y* at the chosen site, due to rupture of any fault in a wide region around the site. A given event of return period T_r is equally likely to occur in any year during the design life of N_d years. Hence, the annual probability of exceedence of y* is $p=1/T_r$. For large T_r and N_d, it can be shown that

Probability of [PGA or S_a> y* in N_d years] is ~ N_d/T_r

If N_d = 50 years, it follows T_r is nearly 2500 years. In other words the hazard for a design period of 50 years with confidence of 98% has to correspond to a return period of ~2500 years. If we are willing to reduce the confidence level to 90%, the probability of annual exceedence will be set at 0.1. This would mean we are designing for seismic hazard corresponding to 500 year return period. This is not same as postulating an earthquake that occurs once in 500 years or once in 2500 years. Actually all possible magnitudes and hypo-central distances are to be rationally combined to estimate the future ground motion to be experienced by the building during its projected life of 50 years. For safety sensitive installations such as large dams and nuclear power plants one may need still longer 5000- and 10,000-year return period ground motion values.

With the above points in view the present study aims at mapping the existing seismic hazard in terms of PGA and response spectrum corresponding to 5% damping for several return periods. Considering the sub-continental scales involved and the spatial variations to be addressed the Indian land mass is discretized into grids of 0.2^0 x 0.2^0 size. Each corner of such a grid is treated as a site for computing the hazard. The lay out of the grid points considered for estimation and further mapping of the hazard within the Indian land mass is shown in Fig.1.1.

1.2 Source, Path, Site

The standard paradigm in hazard studies is the *source, path, site* triplet. The causative seismic sources are first identified. Here, these are taken as known mapped faults in

source zones that can be associated with past earthquake activity. The quantification of the seismic potential of the sources is carried out by assembling a catalogue of past events of $M_w \geq 4$ in the respective seismogenic zones. The catalogue is statistically analyzed to characterize the identified zones in terms of the Gutenberg-Richter (G-R) recurrence relation and the maximum expected earthquake magnitude (M_{max}). The attributes of the zone are further apportioned to the line sources within the zone depending on their capacity for rupture and historical activity. A given site responds to all possible future events emanating from any of the fault in the range of influence of 300 km radius. Here the hypocentral distance and the path properties control the attenuation of ground motion depending on the quality factor of the intervening rock medium. The site is ideally a point on the surface after removing the top 1-2 m of debris or deposits. The position of the site can be geometrically fixed up with respect to every fault rupture. The subsurface geological and geotechnical condition at the site can be described in terms of the depth wise variation of material density and shear wave velocity. Since geotechnical properties of the subsurface soil can vary drastically over short distances the national level hazard map has to be for a common type of site. The effect of local soil layers can be accounted by investigations specific to a given site. Here the reference site condition is taken as the *A-type rock site* which has its average shear wave velocity in the top thirty meters to be greater than 1.5 km/s. There are many real sites in India with exposed granite satisfying the above condition. A typical section of such a site is shown in Fig.1.2. A few photographs of surface expressions of such sites are shown in Fig.1.3.

1.3 Uncertainties

Computation of seismic hazard is beset with unknowns and uncertainties. Two broad categories of uncertainties can be recognized. First is the *epistemic or model related* uncertainty. With the present knowledge of the subject we are committing ourselves to certain models which may in future get changed with better scientific knowledge. One can get a range for this uncertainty if we can use alternate models for source description and methods of statistical analysis. It is known that with more data, variance in the error estimates of the parameters can be reduced. The second type called *aleatory* uncertainty is inherent to the natural process under observation. This can not be reduced with more data or knowledge. For example, magnitude values of earthquakes with their sources and fault rupture lengths that will affect a particular site will remain uncertain. Probabilistic seismic hazard analysis (PSHA) can address both the types of uncertainties by adopting different source models and attenuation relations following the logic tree approach. However as the present work is mandated to remain within the realm of standard methods that can be verified by others, frequency dependent attenuation relations are derived by simulating large number of ground motion records following well known seismological source models, supported by validation using available recorded Indian strong motion accelerogram (SMA) data. Once the attenuation relation is available as a function of M_w and site to source distance (r), the methodology of PSHA is well known.

1.4 PSHA Efforts in India

The most popular and hence widely used seismic hazard estimation currently in the country is still based on dividing the country into four so called seismic zones (II, III, IV and V) as in the BIS code IS-1893. This approach is not only subjective but also

deterministic with no recognition for the various uncertainties that are present in the physical mechanism that dictate the looming earthquake hazard and consequent risk.

There have been several PSHA studies in the country limited to particular cities, states and regions with some controlling parameters treated as random variables. A detailed PGA hazard map with 10% annual probability of exceedence in 50 years was worked out by Khattri et al in 1984. These authors used the attenuation relation developed by Algermissen and Perkins (1976) for use in USA. Bhatia *et al* (1999) presented a PGA hazard map with 10% annual probability of exceedance in 50 years using the attenuation relation of Joyner and Boore (1981). In the above studies, the same attenuation relation has been used all over India, which remains questionable.

Seeber *et al* (1999) prepared a detailed PSHA map for the state of Maharashtra. This was based on attenuation relationships developed for Central Eastern United States (CEUS). They presented both PGA and S_a maps for 500 year return period. Jaiswal and Sinha (2006) estimated probabilistically the seismic hazard for peninsular India (10°N-26°N; 68°E-90°E) using the zoneless approach proposed by Frankel (1995). Multiple ground motion models have been combined by them using an appropriate weighting scheme. Das *et al* (2006) carried out PSHA for northeast India. They computed the uniform hazard response spectra for 100 year return period at a few cities. The limitation of this work is in the attenuation model which uses only six recorded earthquake data.

Apart from obtaining hazard maps for particular regions, there have been attempts to obtain PSHA results for important Indian cities. Iyengar and Ghosh (2004) carried out PSHA for Delhi city on a grid size of 1 km x 1 km. Nearly 300 years of past data was used to determine the regional seismic recurrence relations. The maximum potential magnitude of the Himalayan faults has been underestimated in this study. There are other limitations regarding the type of site considered and choice of the attenuation relation.

Raghukanth and Iyengar (2006) developed uniform hazard response spectra for Mumbai city valid for different site conditions. The major limitation with this study is the point source attenuation relation used for estimating the hazard. The proximity of Mumbai city to major faults indicates that near source effects will have significant influence on hazard estimation. Menon *et al* (2010) estimated probabilistic seismic hazard for the State of Tamilnadu by identifying eleven areal source zones. To account for epistemic uncertainty they considered additionally zone less model and weighted attenuation based on three different relations available in the literature. Mahajan *et al* (2010) prepared PSHA map for the north-western region of Himalaya. Nineteen different seismogenic areal source zones have been considered in their study. For the attenuation relationship weighted average of the equation of Abrahamson and Litcheister (1989) developed for USA and the equation of Hasegawa *et al* (1981) valid for Canada has been used in preparing PGA contour maps.

Due to continuous efforts by different researchers, there is considerable improvement in our knowledge about seismo-tectonic characterization and relevant data. For instance, Geological Survey of India (GSI) has compiled and integrated all available data on

geological, geophysical and seismological attributes for the entire country and has brought out the Seismotectonic Atlas of India and its Environs (GSI 2000). Similarly, paleoseismic investigations (Sukhija *et al.*, 1999, 2006; Kumar *et al.*, 2001; Rajendran *et al.*, 2004, 2008; Lave *et al.*, 2005) and identification of historical events (Iyengar *et al.*, 1999; Ambraseys and Jackson, 2003) helps us to build a robust earthquake catalogue. Further, important information on the quality factors of different regions of India are available (Singh *et al*, 1999, 2004; Bodin *et al*, 2004; Sharma *et al*, 2007; Parvez *et al*, 2008; Raghukanth and Somala 2009; Mohanty *et al*, 2009). Integrating all the above scientific information, it is now possible to carry out PSHA of the entire country. Mapping of the PSHA result will be useful to engineers, planners and to agencies interested in disaster mitigation. This would also represent the existing seismic hazard of the country in line with international standards such as the International Building Code. The PGA and the response spectrum can be used as basic inputs to prepare detailed microzonation maps for important cities.

The present study aims at developing All India PSHA map avoiding the major limitations of the previous studies briefly reviewed above. This exercise is presented in this report under the following heads.

Chapter 2: Seismogenic Zones and Fault Map
Chapter 3: Catalogue of Earthquakes and Recurrence Relation
Chapter 4: Quality Factors and Regional Attenuation of Strong Motion
Chapter 5: PSHA Computation and Hazard Mapping

Appendix I: Earthquake Catalogue
Appendix II: Application of the PSHA results

[Note: The international borders of India shown in the figures of this report are approximate and meant for scientific purposes only.]

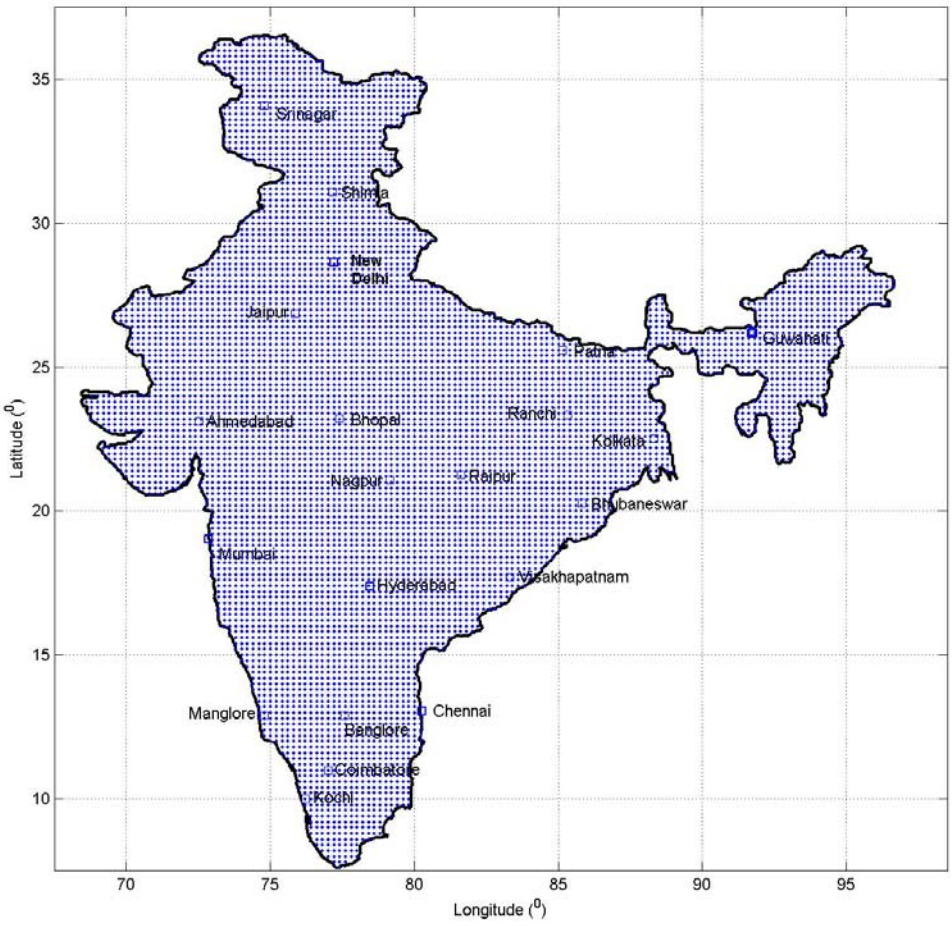

Figure 1.1 Seismic Hazard Estimation at 7156 Grid Points

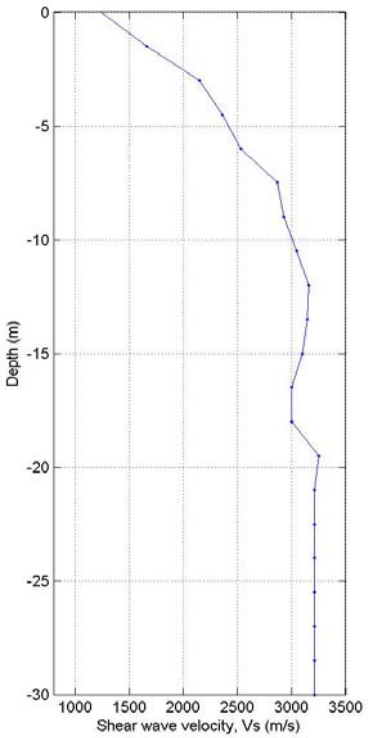

Figure 1.2 Typical shear wave velocity profile at a granitic outcrop.

Fig.1.3 (a)

Fig. 1.3 (b)

Fig. 1.3 (c)

Chapter 2

SEISMOGENIC ZONES AND FAULT MAP

2.1 Introduction

The Indian subcontinent is not homogeneous with respect to its seismogenic characters. This is clear from observing the varying spatial density of past epicenters in a fixed period of time. Any seismicity map of India will show that the Andaman-Nicobar Islands, the North East, the Himalayas are more active than the stable continental region (SCR) of Peninsular India. A map of epicenters superposed on fault lines is shown in Figure 2.1 for ready reference. For PSHA it is necessary to delineate the spatial structure of the seismic zones and the faults within these zones that can be associated with past epicenters. Further this activity has to be quantified in terms of recurrence relations, fault lengths and potential maximum magnitude.

2.2 Tectonic Setting

India broadly consists of three distinct geological units namely the tertiary mobile belt namely, the Himalaya-Arakan Yoma-Andaman Nicobar Island Arc, the Indo-Gangetic plain and the Indian shield. It is now well established that Himalayas are a result of collision between the Indian and the Eurasian plates about 50-60 Million years ago (Valdiya 2001). The current penetrating rate of the Indian plate into the Eurasian plate is estimated to be 45 mm/year (Bilham 2004). Due to this continuous under-thrusting of the Indian plate beneath the Eurasian plate, stresses are increasing and accumulating progressively in the Himalayas. This makes the Himalayas seismically very active. The 2,500 km long Himalayan mountain chain is convex southwards and embodies big bulges and knee-bends at the ends (Valdiya 2001). The width of this unit extending from Kashmir to Arunachal Pradesh varies from 250 to 300 km. In the northeast, the Himalaya takes a bend and meets the Indo-Burmese arc. This eastern extremity of the Himalaya is known as the Assam syntaxis. Similarly, the turning point of the Himalayan mountain system in the north-western region is known as the Hazara syntaxis, where the northwest end of the Himalaya meets the Pamir-Hindukush region. The structure and tectonics of these two syntaxis zones are complex and largely unknown (Chandra 1978). Moreover the geology at the two syntaxis zones is quite different. These syntaxis zones are also the locations of high stress concentrations and intense seismic activity. The Chaman fault in the west and Sagaing fault in the east cut the Himalayan mountain chain at its two extremities. These faults are further linked to much longer and fundamental faults of the Indian ocean and they act as links in transmitting the movements of the oceanic faults to the Indian plate. A general tectonic picture of the Indian region with the topography is presented in Figure 2.2.

The plate collision process gave rise to several active faults in the Himalayan region, namely the Main Central Thrust (MCT), the Main Boundary Thrust (MBT), and the Himalayan Frontal Thrust (Valdiya 1976). The location of these faults as per the Seismo-tectonic Atlas of India (GSI 2000) is shown in Figure 2.3. The Indus Tsangpo Suture Zone (ITSZ) is considered to be the plate boundary where the Tethys Ocean was consumed by the subduction process. The Main Karakuram Thrust (MKT) marks the

southern boundary of the Hindu Kush and the Karakuram. The curvilinear ITSZ and MCT are traced to the south of MKT. The Main Mantle Thrust (MMT) in the Hazara syntaxis is the western extension of the MCT. The Chaman fault joins the Herat fault and the two bend eastward and split into the Karakuram and the Altayan Tagh fault systems in the Pamir region (Figures 2.2 and 2.3). The Balochistan arc comprising of Sulaiman and the Kirthar ranges are aligned in a north-south direction. The fault plane solutions in Himalayas have thrust solutions with nodal planes dipping toward the north, indicating under thrusting of the Indian plate along the entire Himalayan region.

The Indo-Gangetic plain also known as the Himalayan fore-deep lies in between the Indian shield and the Himalayas (Figure 2.2). The formation of Aravali hills in Indo-Gangetic plain is related to tectonic movements before 2500 BC which changed the drainage pattern of the Northwest India drastically (Valdiya 2002). The Vedic River Saraswati which flowed from the Himalayas to the present day Rann-of-Kutch in the Holocene period got desiccated due to tectonic activities in the Indo-Gangetic plain. This East-West tectonic basin is characterized by several hidden faults and ridges in the basement of the Ganga basin (Gansser 1974; Valdiya 1976). The Delhi-Haridwar ridge which is demarcated by a pair of faults is the continuation of the Aravali Mountain into the Himalaya through Haridwar. Similarly Faizabad ridge and Munger-Saharsa ridge denotes the prolongation of the Bundelkhand and Satpura massifs. All the ridges are bounded by faults and are in tectonic continuation from the Indian shield. The North-South Dhubri fault in northeast India separates the north Bengal basin from Shillong plateau. These faults have oblique and transverse alignment across the Himalayan tectonic trend. Gansser (1974) pointed out that Gangetic plain is not a sediment filled fore-deep, but it represents the depressed part of the peninsular shield in which several hidden faults exist.. The earthquake activity in the Gangetic plain is broadly associated with strike-slip faulting (Gupta 2006). The Gangetic plain is moderately seismic when compared to the Himalaya (Quittmeyer and Jacob 1979).

North East India (NEI) is considered as one of the most intense seismic regions in the world. This part of India has an extremely complex tectonic and geologic set up. Most of the earthquakes in NEI are caused due to the south–north and the west–east movement of the Indian plate (Chen and Molnar 1990). The most striking feature in this region is that the Himalaya takes a sharp bend along the Assam syntaxis and continues in a broadly north-south arcuate direction to the east of Burma and joins the Andaman arc giving rise to a complex plate boundary. Another important geomorphologic feature of NEI is the Brahmaputra River which runs almost parallel to the MBT along the Assam valley, and suddenly takes a 90^0 turn to run parallel to the Dhubri fault (Figure 2.2). The Shillong plateau and Mikir hills are considered as fragment of Peninsular Shield which moved to the east along the Dauki fault. Due to its proximity to Himalayas and Burmese arc, the earthquakes in the Shillong Plateau and Assam valley area may be referred to as plate-boundary earthquakes (Kayal 2008). The seismic activity in this region is very high compared to the shield area of other part of peninsular India.

The 5000 km long Andaman-Sumatra-Sunda arc from Burma to Sumatra and Java to Australia defines the boundary between the Indo-Australian and Eurasian plates (Fitch,

1970; Curray *et al*., 1979). The under thrusting of the Indian plate in northeast direction beneath the Andaman-Nicobar Islands can be observed in the focal mechanism solutions of earthquakes of this region. The nature of convergence in the Andaman-Sunda arc is of oceanic type, where as in the Indo-Burmese arc, it is continental type (Kayal 2008). This region is highly active and falls in the zone of most severe seismic hazard. The Andaman-Sunda arc has produced great earthquakes in the past which have generated damaging tsunamis.

The Indo-Eurasian collision resulted in the flexure of the Indian plate. The flexural stresses along with the northwest compressive stress of collision are responsible for sporadic earthquake occurrences within the Indian plate (Bilham *et al* 2008). The great structural disturbances during the geological past resulted in the development of local zones of weakness along which crustal adjustments are likely to take place. It is generally held that seismic activity is more at the intersections of the Dharwar, Aravalli and Singhbhum proto-continents which together constitute Peninsular India (Rao and Rao 1983). These three proto-continents are separated by rifts. The most striking feature in the fault map of Peninsular India is the Son-Narmada-Tapti (SONATA) rift zone which is an ENE-WSW trending zone and runs across the Indian shield from west coast to east coast (Figure 2.2). This rift zone of about 1600 km in length separating the northern and southern blocks of the Indian shield is a region of moderate seismic activity with infrequent earthquakes.

In Southern India, sporadic and low-level seismicity is observed along the old shear zones. The faults associated with the Godavari Graben namely, the Kaddam Fault and the Gundlakamma Fault near Ongole on the coast trending NW-SE are regarded to be moderately active in PI. These faults separate the Singhbum and the Dharwar proto-continents. Another prominent rift zone in PI is the Kutch rift located at the northwest margin of the Indian shield. The formation of Kutch, Cambay and Narmada rift basins in PI is mainly attributed to the reactivation of Precambrian structures during the rifting of Gondwanaland in the early Jurassic or late Triassic period. The structural trend of the Kutch rift basin is controlled by a number of E-W faults. The 26th Jan 2001 (M_w 7.7) intra-plate earthquake occurred in this region. The focal mechanisms of some earthquakes in this region indicate reverse faulting. The Kutch region is bounded by the south-dipping Nagar Parkar fault in the north and the north-dipping Kathiawar fault in the south. The other major faults in the region are the E-W trending Allah Bund fault, Island Belt fault, Kachchh Mainland Fault (KMF), Kathiawar Fault, Nagar Parkar Fault and Katrol Hill Fault (Figure 2.3). Among these, the Allah Bund Fault, KMF and Katrol Hill Fault are active and have been associated with devastating earthquakes in the past. Apart from the Kutch and the SONATA rifts and Godavari Graben, the Cambay Graben, the West Coast Zone, the Cuddapah Basin, and the parts of southern India are known areas of significant seismic activity. Earthquakes in PI can be classified into rift and non-rift events. The Koyna (1967) and the Killari (1993) earthquakes were non-rift events where as the Jabalpur (1999) and the Kutch (2001) earthquakes were rift events. Based on the occurrence of earthquakes, it is observed that the hazard in PI is less severe than in the Himalayan region, but the damages caused due to intraplate events are generally very

high. These events are also felt over a much larger area than the Himalayan earthquakes (Singh *et al* 2004; Kayal 2008).

Grady (1971) notified a submerged volcano in Bay of Bengal which reportedly had erupted in the 17th Century. He indicated that this volcano might be located near a hidden fault in the sea (Fig. 2.2). Recently Balakrishnan *et al* (2009) based on three dimensional geophysical data located this hidden fault in the Bay of Bengal, as marked in Fig. 2.3. Some past events with their epicentres in the Bay of Bengal (Fig. 2.1) may be attributed to this fault.

2.3 Seismogenic Zones

The various maps show that there are some regions that are more active than others. This activity is correlated with the number of occurrence of past earthquakes and also with the presence of faults and lineaments. There is a possibility that not all past epicentres can be uniquely identified with particular faults. This gives rise to the postulation of diffuse aerial sources in some places to be the cause of seismic activity. However for the purpose of the present work it has been accepted that only line sources will be considered and all known activity will be attributed to mapped faults only.

The distribution of faults varies spatially as seen from Fig.2.3. Some specific patterns can be recognized about the faults and epicentres being dense in some regions. This pattern and the known tectonic disposition of India help us to demarcate thirty-two seismic source zones for further work.

In the past Khattri *et al* (1984) identified twenty-four source zones in India and neighbouring region on the basis of seismotectonics and historical seismicity. They recognized six zones in the Indian shield region, four in the Indo-Gangetic plain and the remaining fourteen zones distributed in the Himalayas, NEI and ANI. The region around the Killari earthquake of 1993 (M_w 6.3) was not recognized in this study. Bhatia *et al* (1999) identified eighty-five source zones based on past data. The Killari source zone was included in this study. The identified areal sources were smaller in size compared to that of Khattri *et al* (1984). Based on seismicity, tectonics and geodynamics, Parvez *et al* (2003) delineated forty seismogenic zones. Recently, Gupta (2006) identified eighty-one sources encompassing India and adjoining regions. In these studies, boundaries of the zones have been demarcated based on the presence of historical seismicity clusters. The source zones are spatially dense and contiguous in the Himalayas, Indo-Burmese range and the Andamans, whereas in the stable continental part of India large gaps are assumed. Because earthquakes are frequent in the Himalayas and NEI, the catalogues are statistically complete for such regions and hence epicentre clusters can be used as a means of marking homogeneous regions. However in the Indo-Gangetic plain and the Indian shield, due to their weak activity historic information is scarce and hence the past seismic source zones are not robust. Seeber *et al* (1999) pointed out that location of future earthquakes in shield regions may differ substantially from known patterns. Hence based on historic data and geology, these authors divided the Indian shield into seven seismogenic zones without gaps. This hints at the necessity of incorporating large-scale geological features in identifying source zones when past data is not sufficient.

In the present study we are primarily interested in ground motion which, at a given site, can be caused due to strong sources in distant locations or weak sources situated nearby. Hence it is necessary to avoid gaps between source zones. Hence in the present grouping there will be no region with zero seismic activity. The land mass under study is grouped into thirty-two seismogenic zones based on historical seismicity, tectonic features and geology. To capture the major tectonic and geological features large zone sizes are selected. The Indian shield region is divided into seven tectonic zones following Seeber *et al* (1999). The past efforts of Bhatia *et al* (1999) and Gupta (2006) have been utilized to identify seismogenic zones in the Himalayas, NEI and ANI. Source zones in Pakistan which can induce ground motion across the international borders are selected as per the publication of the Pakistan Meteorology Department (PMD 2007). In Fig. 2.4 the thirty-two source zones are shown along with the faults within each zone.

Sources *1-4* correspond to contiguous segments of the Himalayas. These sources represent the plate boundary regions where lie the MBT, MCT, Indus-Tsangpo suture and the Tethys suture. Source zone *5* represents the Mishmi Block and it contains a part of the Tethys suture. Source *6* includes the Altyn Tagh and Karakoram faults. Source *30* in the extreme northwest part contains the Hindukush and Pamir regions which are known for their high levels of seismicity. Sources *21 to 26* are demarcated based on the variation in the intensity of activity over the Chaman Fault and the Kirthar-Sulaiman ranges. Source *8* occupies the Shillong plateau and the Assam valley region. This region has active linear structures like the Dauki, Dhubri, and Kopili faults. A narrow inactive corridor known to exist in the NEI region is marked as zone *7*. The Bengal basin region is in source *9*. Source zones *10-15* are connected with the subduction of the Indian plate below the Burmese plate. Source zone *27* represents the Gujarat region which is seismically quite active. This comprises of the Saurastra Craton, the Kutch Rift and the Cambay Rift. Source zone *28* corresponds to the Aravalli ranges and the Bundelkhand Craton separated by the Great Boundary Fault. Source zone *16* corresponds to the Son Narmada and Tapti region, a very prominent tectonic feature in the Indian Shield. Source zone *19* represents the Godavari Graben and zone *18* consists of the Mahanadi Graben and the Eastern Craton of the Indian Shield. The Western and Eastern passive margins are represented by source zones *20 and 17*. Source *29* represents Southern Craton in PI. Damodar Graben and Singhbum Craton lie in source *31*. Source *32* encloses the new fault identified in Bay of Bengal by ONGC (Balakrishnan *et al* 2009). This also includes the submerged volcano said to have shown activity in 1756 off the Pondicherry coast. The position of this is marked in Fig.2.3 and Fig.2.4 as stated by Grady (1971)

Characterization of the seismicity of the identified thirty-two source zones in terms of the Gutenberg-Richter recurrence relation is possible after assembling an All India earthquake catalogue. This is detailed in the next chapter.

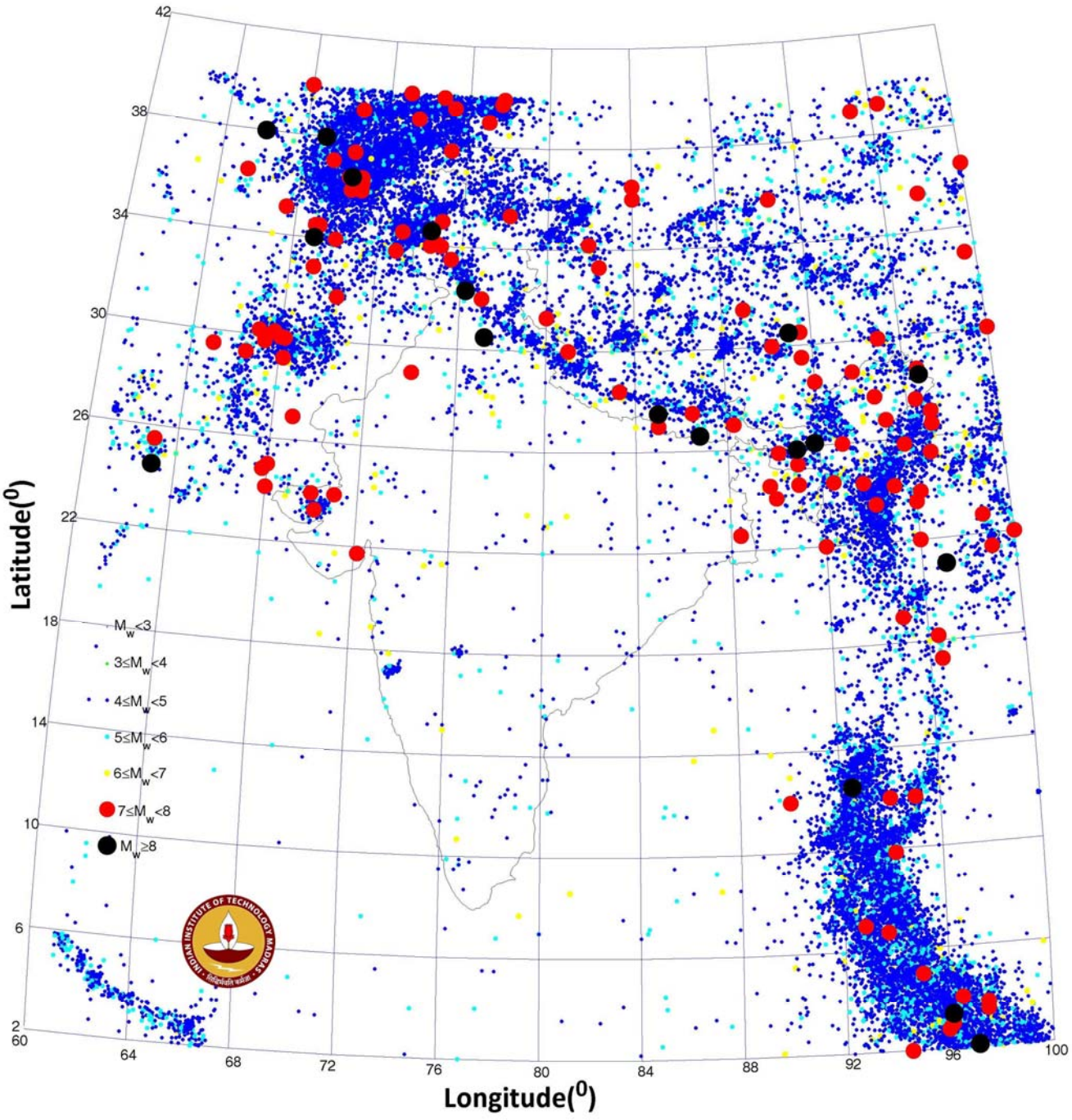

Figure 2.1 Historic Seismicity superposed on known Faults

(38860 events of Mw ≥4 including foreshocks and aftershocks)

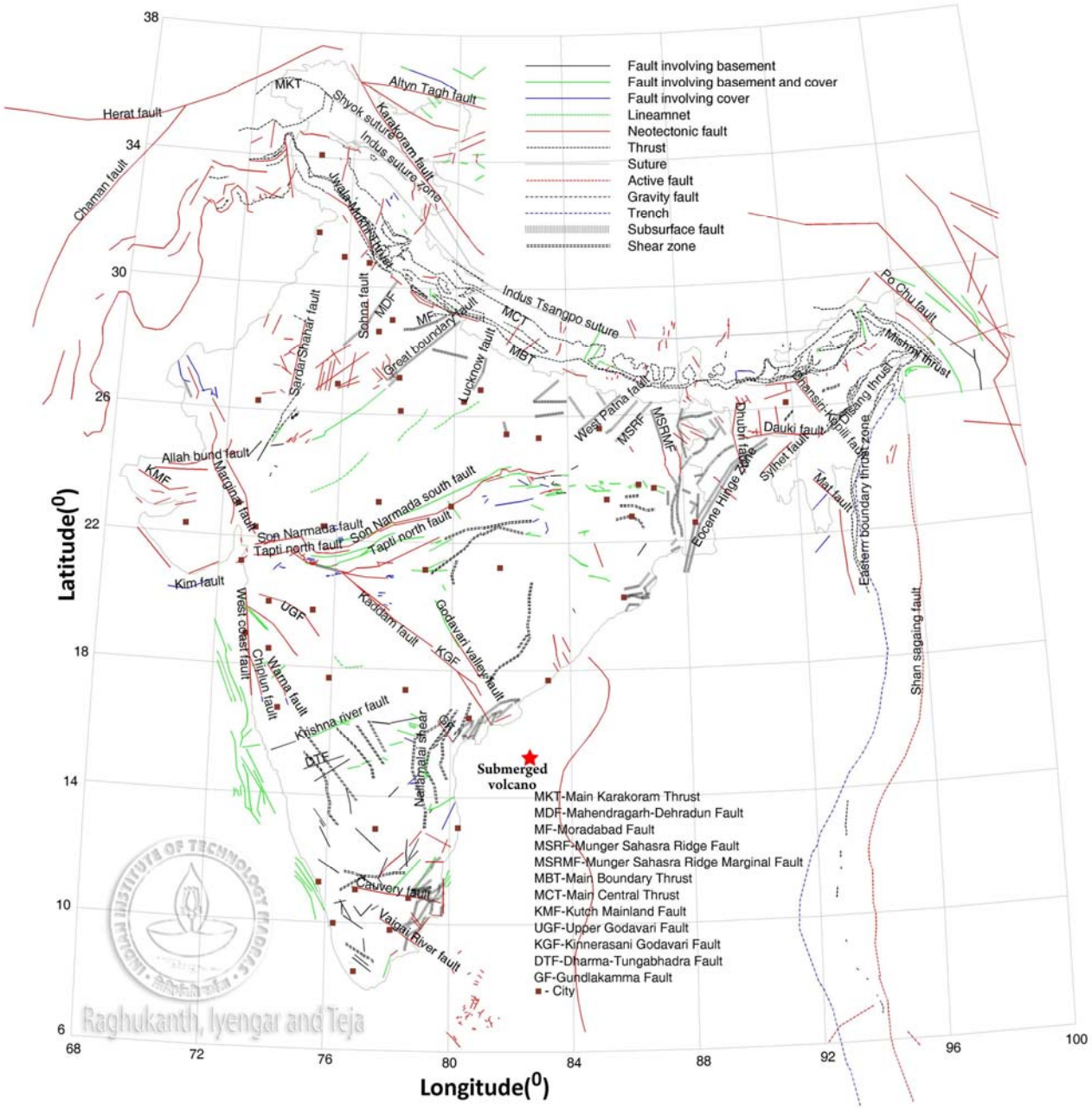

Figure 2.2 Fault Map of India. (Seismo-tectonic Atlas of GSI 2000; Valdiya 1976; Balakrishnan *et al* 2009)

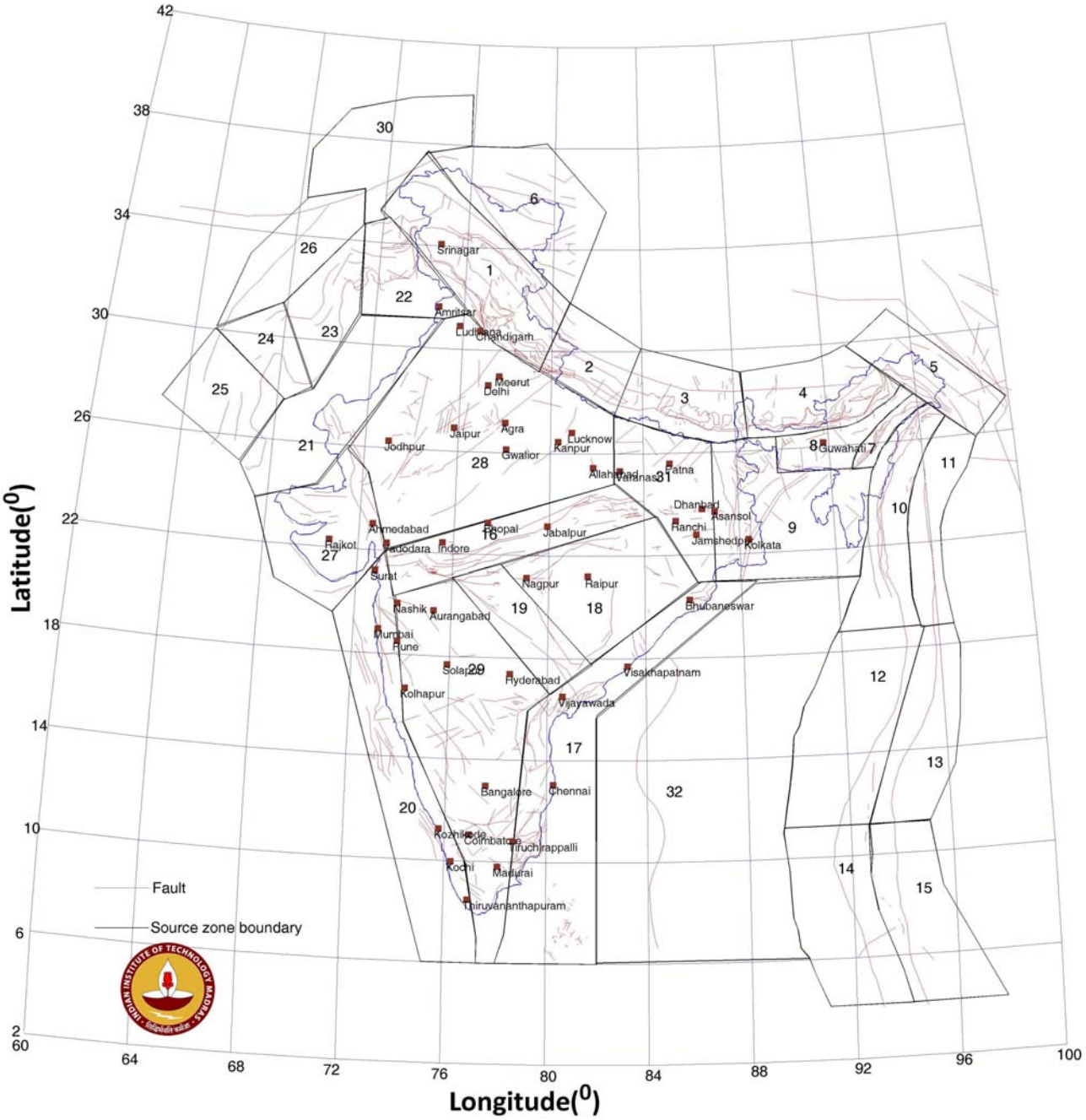

Figure 2.3 Thirty-two Seismogenic Zones of India

Chapter 3

EARTHQUAKE CATALOGUE AND RECURRENCE RELATION

3.1 Introduction

In the previous chapter we have identified the spatial structure of the seismogenic zones. These are the regions with concentration of faults and also of past epicenters. The next step is to quantify the seismic activity in these source zones by developing the Gutenberg-Richter recurrence relations. A comprehensive database of location, date and magnitude of past earthquakes is required, for deriving such recurrence relations. Generally it is known that accurate data is available for events that have happened in the last 50-100 years only. Since damage causing earthquakes are rare the length of the catalogue (sample size) influences our conclusions on the occurrence of strong earthquakes. This situation is common to countries which started sophisticated instrumentation in the middle of the 20^{th} Century. In India after 1964 reliable information on instrumental magnitudes and locations are available (Chandra 1992; Guha and Basu 1993). Prior to this period damage reports and historical records are the major sources for building up a database. In the past several investigators attempted to prepare earthquake catalogues for the Indian subcontinent. Notable efforts are by Oldham (1883), Chandra (1977, 1992); Bapat *et al* (1983), Rao (2005) and IMD. There have been efforts to derive earthquake recurrence relationships for some special regions of India by combining data from several sources (Kaila *et al* 1972; Seeber *et al* 1995; Shanker and Sharma 1998; Iyengar and Ghosh 2004; Raghukanth and Iyengar 2006; Jaiswal and Sinha 2007). All these studies provide valuable information on Indian seismic parameters for further work and comparison. However, it may be noted here that comprehensive quantification of seismic activity for the whole country has not yet been attempted. This provides the impetus to develop an All India catalogue of past earthquakes. The collected earthquake data is naturally assigned to the thirty-two source zones of the previous chapter. The methodology proposed by Kijko and Graham (1999) combining prehistoric, historic and instrumental data is used to estimate the potential maximum magnitude (M_{max}) and the *(a,b)* values in the recurrence relation.

The primary sources for earthquake data are the national repository with the India Meteorological Department (IMD) and the reports of the Geological Survey of India (GSI). Instrumental magnitude and location of recent earthquakes are presently available on the internet also. In the present study, the earthquake catalogue for the region (4^0N-40^0N; 63^0E-100^0 E) has been assembled. The considered region overlpas with parts of Afghanistan, Bhutan, Burma, Nepal, Pakistan, and Sri Lanka. Hence special efforts have been made to collect instrumental, historical and paleo-earthquake data from diverse sources.

3.2 Instrumental Data

The most accurate and complete information on instrumental earthquakes for India is from permanent global seismic network observations. This data from 1922 to early 1960 is available in the International Seismological Summary (ISS) reports and in ISC

bulletins. The ISC took over the service from ISS in 1964 and data from 1900 till date is available on the ISC website. The USGS (http://neic.usgs.gov/) website also contains information for location, date, origin time and magnitude. This is considered to be one of the reliable data repositories since 1973. Apart from these global databases, the IMD data base is comprised of historical and instrumentally recorded earthquakes. Only local magnitude M_L is assigned to the recorded earthquakes. The USGS database reports 23,540 events of magnitude $M_w \geq 4$ for the study region for the region (2^0- 40^0N; 61^0-100^0 E) starting from 1973. The ISC website reports 36,335 events covering the period 1904 to 2008. The catalogue supplied by IMD lists about 16,396 events for the period 1505-2008.

3.3 Historical Data

Oldham was perhaps of the earliest to create an earthquake catalogue for India. A list of significant Indian earthquakes up to 1869 was prepared by Oldham (1883). Chandra (1977) compiled *378* events from 1594 to 1975 and prepared an earthquake catalogue for Peninsular India. The historical events in this catalogue were taken from the publications of Oldham (1883), Turner (1911), Milne (1911), Tandon and Choudhary (1968), and Guha *et al.* (1968). Instrumentally located earthquakes listed by IMD and USGS were also included in this catalogue. Quittmeyer and Jacob (1979) prepared a list of Himalayan earthquakes. The catalogue of Bapat *et al* (1983) lists about *40* earthquakes in India and its neighbouring region prior to 1800 AD. Rao and Rao (1984) reported *295* events in Peninsular India from 1340 AD to 1983. Chandra (1992) compiled *711* events from the Himalayan region for the period 1505-1986. Guha and Basu (1993) prepared a list of earthquakes of magnitude ≥ 3 for Peninsular India. Vitanage (1998) reported *58* historical earthquakes for the period AD 1614-1993 in Sri Lanka. Iyengar *et al* (1999) carried out an intensive search of ancient Indian literature for earthquake related information. They identified *38* damaging events in India in the medieval period. Ambraseys and Jackson (2003) identified seven historical events with estimated magnitudes $M_w > 7$ in North India and Tibet. Rao (2005) reviewed several earthquake catalogues prepared for the Indian region and identified fifty important events from 1250 BC to 1963 AD. Iyengar and Ghosh (2005) and Raghukanth and Iyengar (2006) developed earthquake database in a region of 300 km radius around Delhi and Mumbai cities. Jaiswal and Sinha (2007) prepared an earthquake catalogue with *640* events for Peninsular India after removing aftershocks. The website (http://isr.gujarat.gov.in/) contains a list of earthquakes from earliest time till 2008 for Gujarat and Northeast India. Pakistan Meteorological Department compiled a list of *58* historical events during AD 25-1905 that occurred in Kashmir and in Pakistan. Ambraseys and Bilham (2009) searched historical Persian documents, British and French Consular reports to identify *52* earthquakes in Afghanistan for the period AD 734-2004.

3.4 Paleo-earthquake Data

Paleo-seismology is a science which interprets geological evidences such as surface faulting, earthquake induced liquefaction and deformation features to identify the location, time and size of the prehistoric events (McCalpin 2009). Such studies are considered reliable to identify only large earthquakes of $M_w \geq 6.5$. Paleo-seismic investigations are widely used in many countries to supplement historical and

instrumental data (Giardini et al 2004, Petersen et al., 2008, McCalpin 2009). In India, recurrence intervals of large and great earthquakes exceed the duration of instrumental and historical records. Hence prehistoric events identified by paleo-seismic investigations would be valuable in building up a national earthquake catalogue. This is all the more important for India since the Harappan city of Dholavira belonging to the Bronze Age has been excavated by archaeologists in the Kutch region of Gujarat with telltale effects of an ancient earthquake in the 3rd Millennium BC.

Sukhija *et al* (1999) obtained evidences for three large seismic events (M_w >7) from paleo-liquefaction studies in the epicentral region of the Great Assam earthquake of 1897. Two of these occurred during 1450-1650 AD and 700-1050 AD. The third one is dated around 600 AD. Kumar *et al* (2001) carried out paleo-seismic investigations on the Himalayan Frontal Thrust (HFT) and obtained evidences for a great earthquake (M_w > 8) in 260 AD and two major events (M_w >7) in 1294 AD and 1423 A.D near Chandigarh. Investigations by Malik *et al* (2003) support the identificatioin of the above three HFT events. In NEI evidence for a very large event (M_w>8) *circa* 830 AD near Guwahati City has been obtained by Rajendran *et al* (2004). Lave *et al* (2005) obtained geological evidences for an earthquake of magnitude (M_w > 8.5) on HFT *c* 1100 AD in Far East Nepal.

Sukhija *et al* (2006) have observed paleo-seismic signatures like liquefaction features in the meizoseismal area of the 1993-Latur (Killari) earthquake. Based on radiocarbon dating of organic samples and archaeological artifacts in the region, this paleo-event has been dated to the broad period 190 BC-410 AD. The data also indicated that the magnitude of this event could have been greater than that of the 1993-Latur earthquake. Rajendran *et al* (2008) carried out paleoseismic studies in Gujarat. They identified two events of magnitude M_w > 7 near the Allah Bund Fault. The first is dateable to 2474±656 BC and the second to 893 AD. They also reported a historical event of magnitude M_w > 7 around 325 BC in the Kutch region. It may be remarked here that the first of the above paleo-event matches closely with the 3rd millennium earthquake said to have damaged the flourishing city of Dholavira.

3.5 All India Catalogue

A catalogue containing all known events of magnitude $M_w \geq 4$ for the region (2^0- 40^0N; 61^0-100^0 E) has been assembled for further work. The catalogue starts with the 2474 BC Dholavira earthquake in Gujarat with an approximated M_w of 7.5. A total of 38,860 events of magnitude $M_w \geq 4$ known up to 31st December 2008 are listed in the catalogue. The temporal distribution of the events is admittedly too uneven as shown in Fig. 3.2.

A common problem faced in assembling a catalogue is due to the different magnitude values reported in the literature. Here this is handled by converting all reported values to moment magnitude numbers. For the pre-instrumental period of the catalogue only MMI estimates were available. These have been converted to magnitude numbers using the empirical relation M_w= (2/3 MMI+1). For many events IMD has reported only the local magnitude M_L. This has been converted to M_w following the approach of Idriss (1985). For events from ISC, USGS catalogues with surface wave magnitude M_S and body wave

magnitude m_b the following conversion formulae of Scordilis (2006) derived on the basis of global data are used.

M_S - M_W

$$M_w = 0.67M_S + 2.07, \quad \text{for } (3.0 \le M_S \le 6.1)$$
$$M_w = 0.99M_S + 0.08, \quad \text{for } (6.2 \le M_S \le 8.2) \qquad (3.1)$$

m_b - M_w

$$M_w = 0.85m_b + 1.03, \quad \text{for } (3.5 \le m_b \le 6.2) \qquad (3.2)$$

The body wave magnitude saturates at the value of 6.2. The complete catalogue is presented on a CD attached as an appendix at the end of this report.

3.6 Declustering

Estimation of the recurrence parameters assumes the sample data series to be temporally statistically independent. Aftershocks and foreshocks are admittedly dependent on the main shock and hence such events get clustered in a general catalogue. The widely used declustering approach introduced by Gardner and Knopoff (1974) and modified by Uhrhammer (1986) is used here to remove time-dependent events from the earthquake catalogue. The procedure essentially removes a space and time window after each main shock. A total of 19319 aftershocks and foreshocks have been removed from the above main catalogue. The final catalog after foreshock and aftershock removal is shown in Figure 3.1. This database used further is pictorially shown in Figure 3.2 as a function of magnitude and time.

3.7 Completeness of the catalogue

The All India catalogue developed in the present study is a combination of instrumental, historic and pre-historic data. As such completeness of magnitudes in time has to be established before proceeding further. Here the widely used procedure proposed by Stepp (1972) is applied to determine the interval in a magnitude class over which the class is complete. The earthquake data is grouped into seven magnitude classes namely, $4 \le M_w < 5$, $5 \le M_w < 6$, $6 \le M_w < 7$, $7 \le M_w < 8$ and $8 \le M_w < 9$. With a time interval of 10 years, the average number of events per year in each magnitude range is determined. If $x_1, x_2, \ldots x_n$ are the number of events per year in a magnitude range, then the mean rate for this sample is

$$\chi = \frac{1}{n}\sum_{i=1}^{n} x_i \qquad (3.3)$$

where n is the number of unit time intervals. The variance is given by

$$\sigma_\chi^2 = \frac{\chi}{T} \qquad (3.4)$$

where T is the duration of the sample. If χ were to be constant, σ_χ would vary as $1/\sqrt{T}$. Following Stepp (1972) the standard deviation of the mean rate as a function of sample length are plotted along with nearly tangent lines with slope $1/\sqrt{T}$. The deviation of standard deviation of the estimate of the mean from the tangent line indicates the length up to which a particular magnitude range may be taken to be complete. The standard

deviation shows stability in shorter windows for smaller earthquakes and in longer time windows for large magnitude earthquakes. The standard deviation of the mean of the annual number of events as a function of sample length for the All India data is shown in Figure 3.3. This provides a easy criteria for testing the completeness of the data. The results show that the All India data is complete for the sets $4 \le M_w < 5$, $5 \le M_w < 6$, $6 \le M_w < 7$, $7 \le M_w < 8$ and $M_w > 8$ for the past 50 (1958-2008), 110 (1898-2008), 130 (1878-2008), 340 (1668-2008) and 600 (1408-2008) years respectively. These intervals are marked also on Figure 3.2. The completeness for larger magnitudes is not verifiable for all the source zones since the average return period of great earthquakes would be longer than the time period spanned by the catalogue. Hence the catalogue is assumed to be complete for large magnitude earthquakes over the entire duration.

3.8 Regional Recurrence

The seismic activity of a source zone is characterized by the Gutenberg-Richter (G-R) recurrence relation

$$Log_{10} N(m) = a - bm \qquad (3.5)$$

Here, *N(m)* is the number of earthquakes greater than or equal to magnitude *m*. The (*a*, *b*) values characterize the seismicity of the region. A lower *b* value means that out of the total number of earthquakes, a larger fraction occurs at the higher magnitudes, whereas a higher *b* value implies a larger fraction of low magnitude events in the catalogue. Although the value of *b* varies from region to region, it lies typically in the range $0.6 < b < 1.5$. The general level of earthquake activity in a given area during the study period is represented by the parameter *a.* The value of *a* directly indicates the number of ($M_w > 4$) earthquakes per year. The seismic hazard at any site is controlled by the parameters (*a*, *b*). Knopoff and Kagan (1977) demonstrated that an upper bound magnitude (M_{max}) has to be introduced if the G-R relation is to be applied further in a realistic fashion. The catalogue developed for India is a combination of instrumental, historic and pre-historic data of differing quality. Large uncertainties in the magnitude value and location have to be accounted for by probabilistic hazard analysis.. These issues can be addressed using the procedure of Kijko and Graham (1998) and Kijko (2002). This method assumes Poisson distribution for earthquake occurrence with activity rate $N(m)$ and a truncated G–R relationship for magnitude values. The uncertainty in the estimation of magnitudes and time of occurrence of earthquakes can be incorporated in deriving the parameters. Further computation of the parameters (*a*, *b*) by the maximum likelihood method of Kijko and Graham (1998) requires the earthquake catalogue to be partitioned into two parts called extreme and complete. The extreme part refers to the time interval where information only on large historical events is available. The complete part represents the time period in which information on both large as well as small magnitude earthquakes is available. This partitioning of the catalogue is carried out systematically using the method of Stepp (1972).

3.9 Zonal Recurrence Relation

The seismic parameters, namely (*a,b)* in equation 3.3 and the potential maximum magnitude (M_{max}) are estimated for the thirty-two tectonic units. Since earthquakes with magnitude less than four do not cause structural damage, the threshold magnitude (m_0) is

taken as *4*. Based on the completeness test of magnitude class $4 \leq M_w < 5$, the data set is divided into *complete part* (1959-2009) and *extreme part* (-1958) for all the 32 regions. The starting point of the extreme part of the catalogue for each region is different and taken as the year of first occurrence of an earthquake in that particular region. Once the catalogue is divided in time, the standard computer program developed by Kijko and Graham (1998) is used for determining the earthquake recurrence relation. The uncertainty in the reported magnitudes is taken as 0.5 in the extreme part. For the complete part the magnitude uncertainty is assumed to be 0.3 (Giardini *et al* 2004). The three seismic parameters [$N(4)$, b and M_{max}] for all the thirty-two zones are reported in Table 3.2. The standard deviation of the *b*-value is also reported in this table. Since earthquakes occur frequently in the Himalayas, ANI and NEI, catalogues in these zones are fairly complete for both small and large earthquakes. Hence uncertainty in the estimated parameters is low in these regions. In the Indo-Gangetic Plain, Gujarat, Central India and Peninsular India, the catalogues contain fewer samples and hence the errors in the estimates are higher. The recurrence relation for all the 32 regions is shown in Figure 3.4.

The Hindukush-Pamir region exhibits highest activity at $N(4) > 40$ per year. The source zones of ANI, Quetta-Sebi and Indo-Burma Region also have high activity with $N(4) > 5$ per year. The corresponding activity rate of the Gangetic plain (zones 28 and 31) is between 0.17–1.16. Gujarat region shows annual activity of $N(4) > 1.31$. The lowest values of $N(4)$ are observed in the shield region.

The other activity parameter *b* also shows considerable spatial variation over India. In the Himalayan plate boundary region *b* varies from 0.66 to 0.88. In NEI the b-value varies from 0.66 to 0.74. The *b*-value for Andaman region lies in between 0.62-0.71. High b-values of the order of 1.2 occur in the southern parts of PI.

The potential maximum magnitude for all the 32 source zones, estimated by the method of maximum likelihood in Kijko's approach is reported in Table 3.2 The M_{max} for the Mishmi Block, Western Himalaya, Eastern Afghanistan is as high as 8.8. In the Himalayan region, M_{max} ranges 7.4-8.8. The M_{max} for Gujarat region is estimated as 8.0. In the Gangetic Plain M_{max} varies from 6.5 to 8.5. The maximum potential magnitude in Central and Peninsular India is less than 7.0.

The work reported in this chapter takes further the dilineation and characterization of the seismic sources in and around India. This essentially refers to estimating the (a,b) values in the G-R recurrence relation and the potential maximum magnitude that can be expected in a particular source zone. The G-R relation obtained for all the zones which covers the whole of the country is shown in Figure 3.4. It is popularly held that the standard G-R relation graph would be a straight line. The present results appear to be bilinear with a slope change at higher magnitudes. It is possible the scarcity of high magnitude events in the catalogue have contributed to this shape. On the other hand it is also possible the mechanics of fracture associated with small and large magnitude events follow different power law, leading to a bilinear graph. Previously Scholz (1997) has shown that every region has a charecteristic dimension which separates the scaling of

small and large magnitude earthquakes. These two sets of events may not be self-similar to each other. In such a case for a large region with several faults belonging to different geological strata the recurrence relation could be bilinear.

With the country completely structured into seismic source zones of varying potential we can claim that any future event will originate within one of these zones. The actual event will be due to the rupture of a fault, amounting to a particular M_w, within a given zone. This rupture creates seismic waves propagating towards target sites through the intervening medium. It is clear the ground motion depends significantly on the source to site distance and the material properties of the rock medium that forms the path for the seismic waves. How the path affects the ground motion in different parts of the country is investigated in the next chapter by deriving appropriate empirical strong motion attenuation relations.

Table 3.1. Earthquake catalogue for India

Long (^{0}E)	Lat (^{0}N)	Year	Mon.	Date	M_w	Depth (km)	Time		Ref.
							Hrs	Mins	
71.00	24.00	-2474	-	-	7.5	-	-	-	4
71.00	24.00	-325	-	-	7.5	-	-	-	4
72.90	33.72	25	-	-	7.7	-	-	-	6
69.50	37.10	50	-	-	7.0	-	-	-	6
76.47	18.10	110	-	-	6.5	-	-	-	10
74.50	34.60	250	-	-	8.5	-	-	-	5
77.20	30.50	260	-	-	8.0	-	-	-	8
60.50	31.60	734	-	-	6.4	-	-	-	7
60.50	29.50	805	12	2	6.9	-	-	-	4
60.50	29.50	815	-	-	6.9	-	-	-	7
65.40	36.40	819	6	-	7.3	-	-	-	6
91.80	26.10	825	-	-	8.0	-	-	-	13
62.20	34.30	849	-	-	5.6	-	-	-	6
67.80	24.80	894	-	-	7.7	-	-	-	9
68.90	26.93	980	-	-	7.6	-	-	-	7
69.13	32.85	1053	-	-	7.0	-	-	-	8
80.10	17.30	1063	12	-	3.7	-	-	-	14
85.00	27.50	1100	-	-	8.5	-	-	-	7
62.20	34.40	1102	2	28	5.6	-	-	-	12
77.20	30.50	1294	-	-	7.5	-	-	-	8
.	.	.	.	.	.	.	.	.	.
.	.	.	.	.	.	.	.	.	.
.	.	.	.	.	.	.	.	.	.
.	.	.	.	.	.	.	.	.	.
70.35	37.21	2008	12	31	4.0	-	17	12	1

1-ISC, 2-IMD, 3-USGS, 4-Rajendran *et al* (2004,2008), 5-Iyengar *et al* (1999), 6-PMD, 7- Ambraseys and Bilham (2009), 8- Kumar et al (2001), 9-Lave *et al* (2005), 10- Sukhija *et al* (2006), 11- Rao and Rao(1984), Rao(2005), 12-Ambraseys and Jackson (2003), 13 - Bilham *et al* (2007), 14- De Ballore (1911), 15-Oldham (1883). 16- Milne (1911), 17- Ambraseys (2000), 18- Jaiswal and Sinha (2004)

Table 3.2. Seismicity parameters for thirty-two zones in India

Source No.	Zones	*b*-value	*N(4)*	Max. Potential Magnitude (M_{max})	No. of earthquakes
1	Western Himalaya	0.88±0.02	5.37	8.8	901
2	Central Himalaya-I	0.73±0.04	3.15	7.8	306
3	Central Himalaya-II	0.78±0.04	2.30	8.8	340
4	Eastern Himalaya	0.71±0.04	3.12	8.0	223
5	Mishmi Block	0.66±0.03	3.72	8.8	219
6	Altya Tegh & Karakoram	0.91±0.03	7.10	7.3	726
7	Naga Thrust	0.67±0.08	0.18	6.8	32
8	Shillong Plateau & Assam valley	0.73±0.04	1.46	8.4	181
9	Bengal Basin	0.74±0.04	1.99	8.1	289
10	Indo-Burmese Arc	0.80±0.02	11.40	7.8	1055
11	Shan-Sagaing Fault	0.66±0.04	5.28	8.1	260
12	West Andaman-I	0.70±0.03	3.62	8.4	239
13	East Andaman-I	0.63±0.03	5.83	7.5	331
14	West Andaman-II	0.71±0.02	2.55	7.5	158
15	East Andaman-II	0.62±0.01	16.53	7.6	985
16	SONATA	0.64±0.08	0.24	6.8	24
17	Eastern Passive Margin	0.74±0.08	0.27	6.1	40
18	Mahanandi Graben & Eastern Craton	0.77±0.09	0.24	5.3	15
19	Godavari Graben	0.85±0.09	0.13	6.0	10
20	Western Passive Margin	0.76±0.07	0.37	6.8	70
21	Sindh-Punjab	0.77±0.06	0.60	8.0	89
22	Upper Punjab	1.01±0.05	1.68	7.8	224
23	Koh-e-Sulaiman	0.84±0.04	5.03	7.3	358
24	Quetta-Sibi	0.74±0.04	5.22	7.8	293
25	Southern Baluchistan	0.74±0.05	2.58	7.3	190
26	Eastern Afghanistan	0.89±0.04	5.59	8.3	534
27	Gujarat Region	0.87±0.06	1.31	8.0	93
28	Aravali-Bundelkhand	0.81±0.06	1.16	7.0	114
29	Southern Craton	1.19±0.08	0.47	6.8	45
30	Hindukush and Pamirs	0.93±0.01	83.54	8.0	6790
31	Gangetic region	0.84±0.09	0.17	6.3	25
32	Bay of Bengal	0.60±0.08	0.49	6.7	53

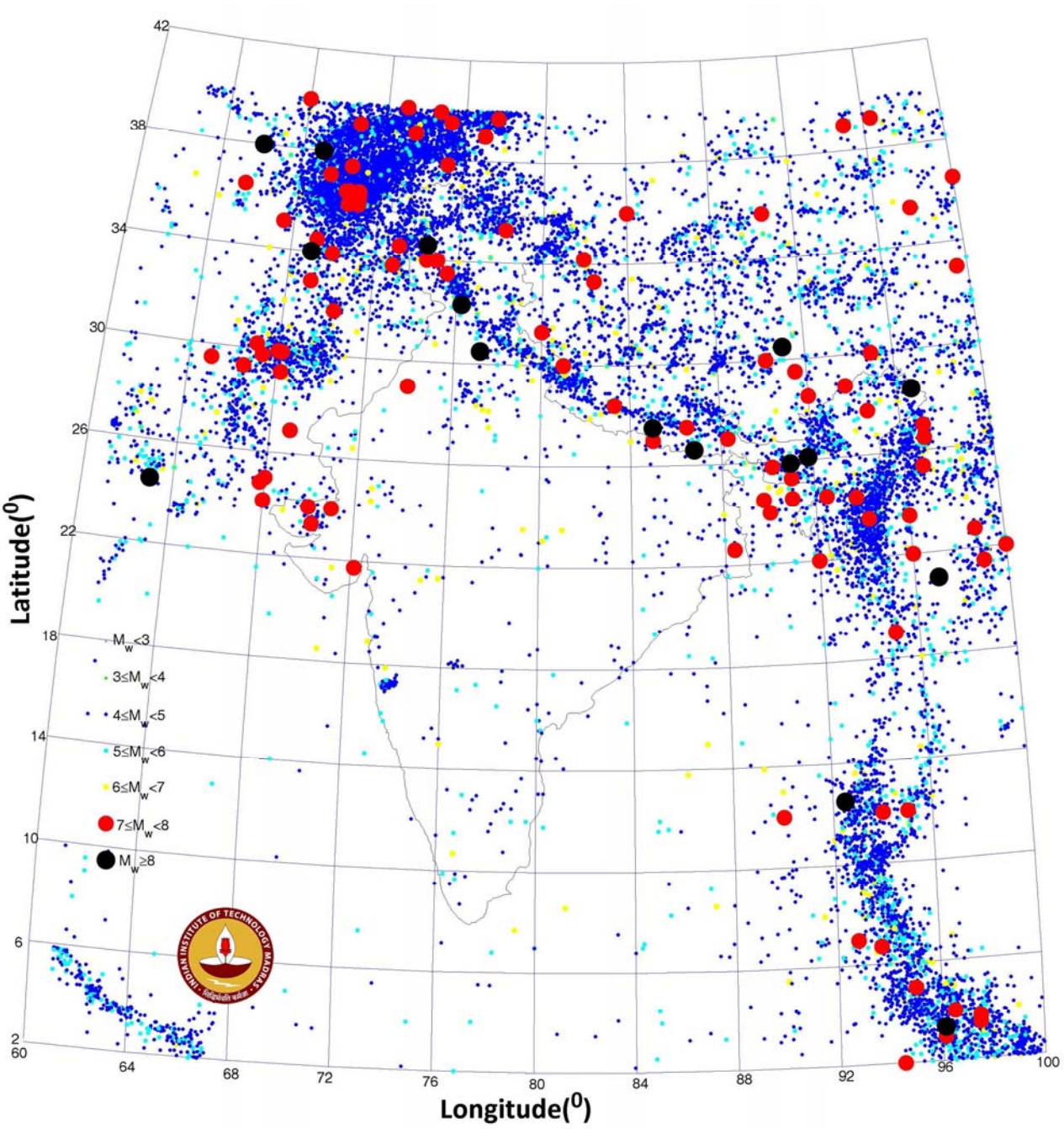

Figure 3.1 Seismicity of India (2474 BC-2008 AD)
(Excluding 19319 foreshocks and aftershocks)

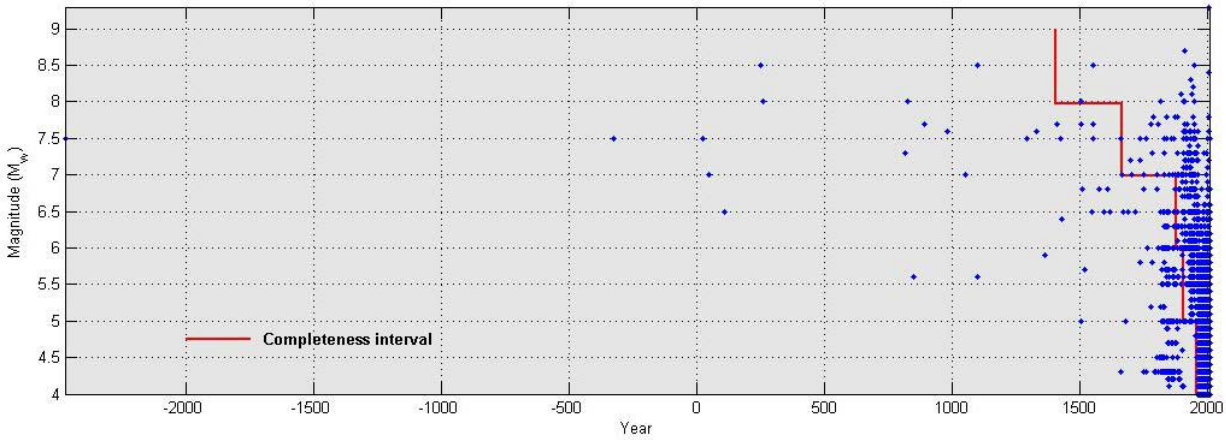

Figure 3.2 Time distribution of earthquakes

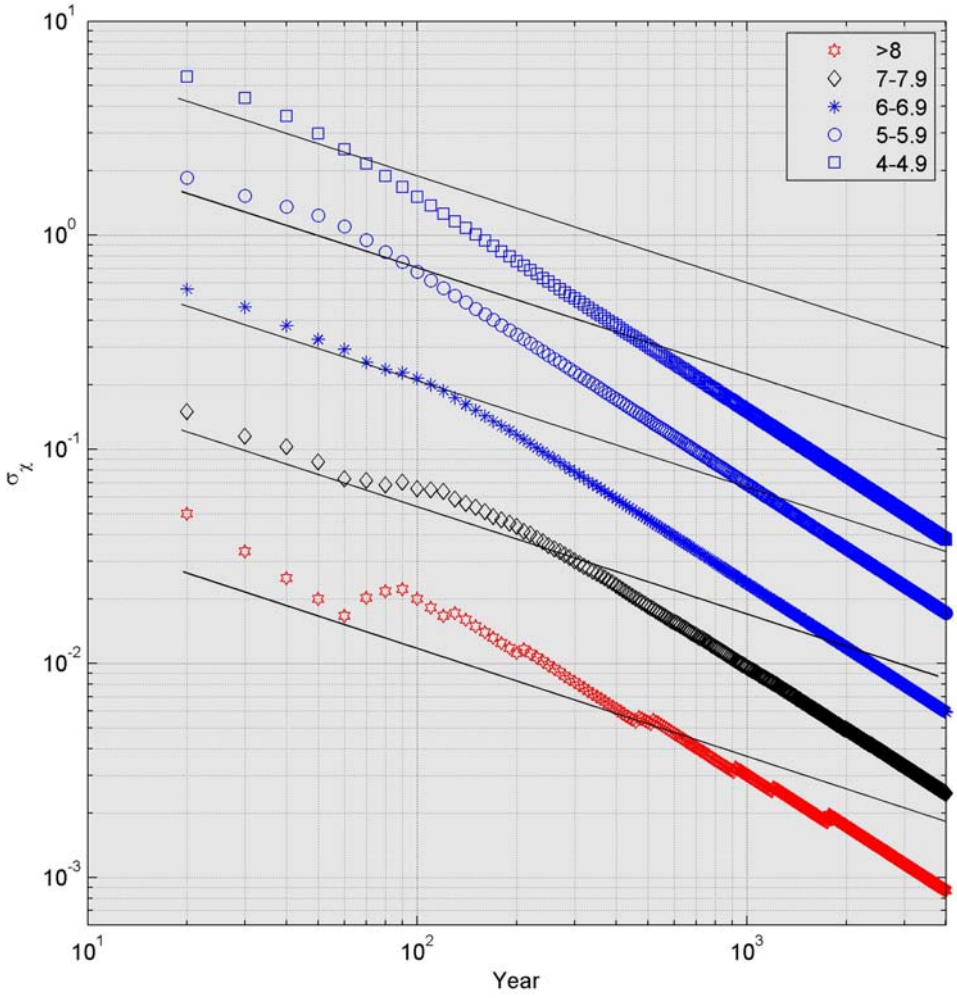

Figure 3.3 Completeness test of All India earthquake data. Variation of σ_χ versus time interval and magnitude and line with slope ($1/\sqrt{T}$).

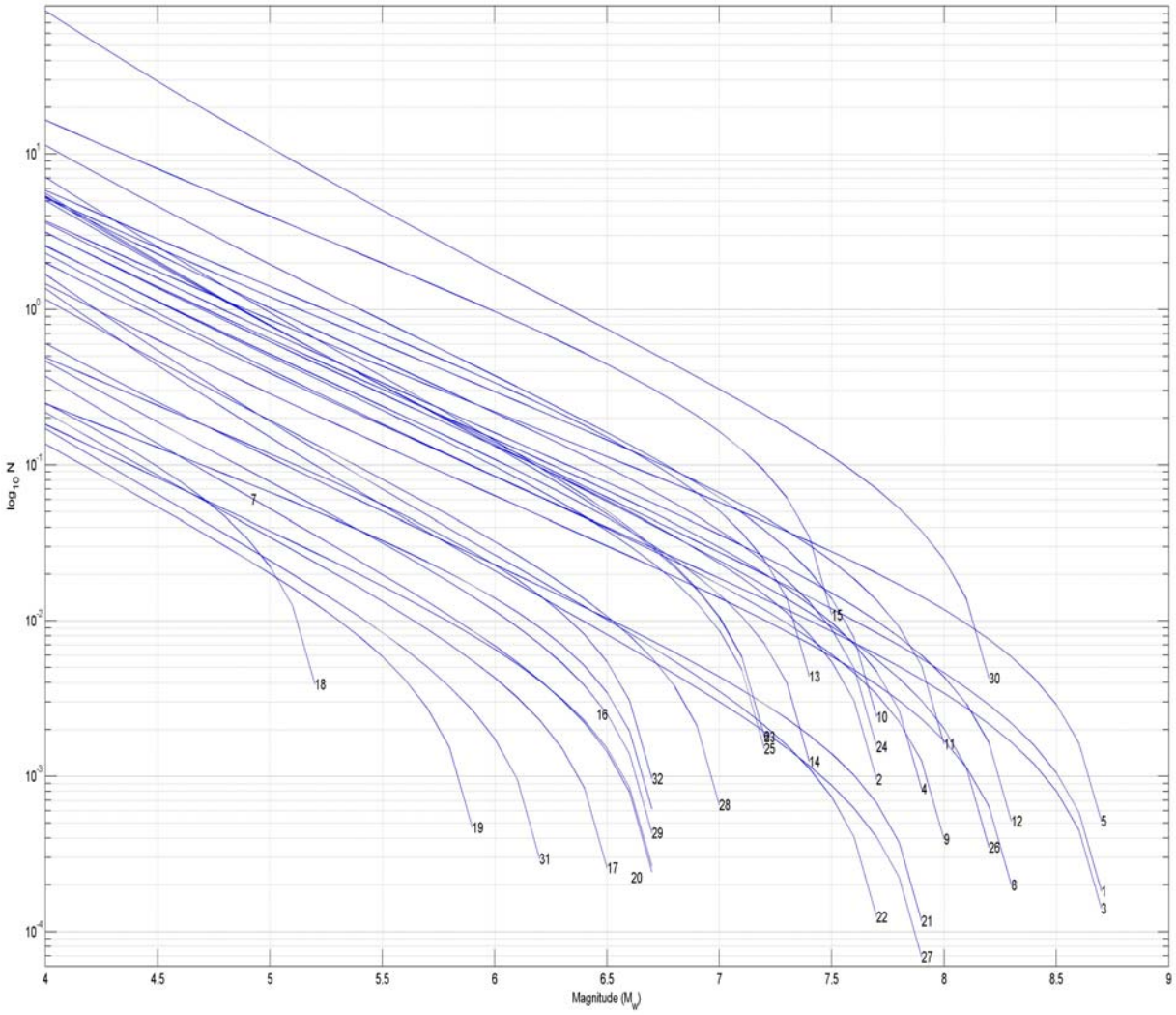

Figure 3.4. Source Zone Magnitude-Frequency Relationship

Chapter 4

REGIONAL QUALITY FACTORS AND ATTENUATION OF STRONG MOTION

4.1 Introduction

Past experience shows that a site vibrates due to earthquake events originating anywhere in a region of about 300 km radius around the site. Hence, besides the source geometry and strength, regional properties play major role in dictating the seismic hazard at the site. Computation of ground motion by solving the wave equation in three dimensions for all possible fault ruptures incorporating several uncertain parameters is almost impossible. Hence it is the usual practice to utilize empirical relations known as attenuation equations to estimate the probable ground motions at a site due to all competing potential fault ruptures. These relations normally describe the average and standard deviation of the frequency dependent spectral acceleration in terms of the earthquake magnitude and source to site distance. The acceptance of such an empirical relation depends essentially on how best it can represent the regional geology as reflected by the density and quality factor in the horizontal direction and the vertical velocity structure of the rocks through which the seismic waves propagate. Hence such predictive equations should be able to capture the essence of the subsurface set up at the target site in terms of the geometric spread and vertical modification of the energy release which happens on the fault several kilometers below the surface. In addition it would be advantageous if they can incorporate effects due to directivity, fault type, dip angle etc. As in other problems in engineering where empirical relations are common one may expect experimental results will lead to the required answer. While this optimism may not be wrong, the amount of data required to develop such an empirical relation based on recorded data and validated with respect to independent set of observations is not available for any part of the world. At this stage it is advantageous to briefly review the available India strong motion data base.

4.2 Strong Motion Database

Since earthquakes are quite common in Himalayas and in NEI, in 1985 three strong-motion arrays comprising of 135 stations were established in these regions (Chandrasekaran and Das 1992). The Kangra array is in the Himachal Pradesh region, the Shillong array is in NEI, and the Uttarakhand array is in northwest Himalayas. These arrays have recorded twenty-one individual earthquakes, with magnitudes lying between 4.5 and 7.2, recording 156 three component accelerograms. The strong-motion data for all these events are available in the global data base (http://db.cosmos-eq.org/). The stations are either located on firm ground or on soft rock sites. Site condition at stations located on granite, quartzite and sand stone is taken as soft rock. Firm ground sites are those sites which are deployed on exposed soil cover on the basement (Sharma 1998). Out of the recorded earthquakes, seven occurred in NEI and remaining triggered in the Himalayas. Among the seven in NEI, four events occurred in Indo-Burma ranges are related to subduction tectonics where as remaining three earthquakes are of crustal nature.

The Delhi Strong Motion Array was established by CBRI around 1995 (Iyengar 1997). A few records originating from the long distance Chamoli earthquake are available from this array. Records for small magnitude local shocks are also recorded by this array.

The only region with SMA data in the Indian shield is the Koyna-Warna region of western India. The earliest available record is for the Koyna earthquake of 11th December 1967. After this, a large number of records of smaller magnitudes were obtained in the Koyna region. This set of data is available from the reports of Gupta *et al.* (1992). SMA records have been obtained by Baumbach *et al.* (1994) for a few aftershocks of the 1993-Khillari earthquake. A few instrumental velocity records within epicentral distances of 300 km are available for the Jabalpur earthquake of 1997 (Singh *et al.,* 1999). Similarly, a few data are available for the main event and aftershocks of the Kutch earthquake of 2001 (Singh *et al.,* 2003).

Openly available SMA data of India is shown Fig.4.1 as a function of magnitude and hypocentral distance. It is observed that even if we take the whole country as a homogenous unit the SMA database is seriously deficient in all magnitude and distance ranges. Hence any empirical attenuation relation proposed purely on past data can not be used as a credible tool in hazard estimation.

A valid attenuation relation is a prerequisite for PSHA. Since the subcontinent is too much varied in its geological structure a single equation to cover all the land mass is unacceptable. Proposals to adopt equations from other regions of the world to Indian sites based on arguments of similarity are essentially intuitive in nature, lacking objectively verifiable rationale. Some of the PSHA efforts in the past have used attenuation relations that were not the most appropriate to Indian conditions. Another serious limitation of the available relations is their inability to predict ground motion at near source distances of the order of the fault rupture. Even a cursory look at the Indian source zone map of Fig. 3.4 indicates that too many sites are located in the near source region particularly for events of magnitude greater than 6.5 which can have rupture lengths greater than 20 km. These points compel one to derive attenuation relations for seven important geological provinces differentiated in terms of their quality factors, and probable range of stress drop during future earthquakes. Validation of these equations is possible by comparing their predictions with actual recorded past strong motion data. This approach of deriving empirical attenuation relations through large scale computer simulation of synthetic accelerograms, has been previously used by Iyengar and Raghukanth (2004) and Raghukanth and Iyengar (2007). The major limitation of this effort was the point source assumption and hence it was unable to predict ground motion at sites near the faults. However the stochastic source mechanism model (Boore 1983, Atkinson and Boore 1995, Joyner and Boore 2000, Boore 2003) can be improved to include sources of finite dimension.

4.3 Stochastic Seismological Model

The stochastic finite fault approach of Boore (2009) which is an improved version of the methodology proposed by Motazedian and Atkinson (2005) is used to simulate ground motion samples for engineering soil conditions. A brief description of the method starting

with the frequency domain representation of the ground acceleration will bring out the advantages of this approach. In this method, the rectangular fault plane is divided into N number of subfaults and each subfault is represented as a point source. The Fourier amplitude spectrum of ground motion [$A(r,f)$] due to the j^{th} subfault at a site is derived from the point source seismological model, expressed as

$$A_j(r,f) = CH_jS_j(f)F(f)D(r,f)P(f) \tag{4.1}$$

Here C is a scaling factor, $S_j(f)$ is the source spectral function, $D(r,f)$ is the diminution function characterizing the quality of the region, $P(f)$ is a filter function, $F(f)$ is the site dependent function that modifies the bed rock motion in the vertical direction and H_j is a scaling factor used for conserving the energy of high-frequency spectral level of sub-faults. In the present study, following Brune (1970), the principal source model $S_j(f)$ is taken

$$S_j(f) = (2\pi f)^2 \frac{\mathrm{M}_{0j}}{\left[1+\left(f/f_{0j}\right)^2\right]} \tag{4.2}$$

Here f_{0j} is the corner frequency and M_{oj} is the seismic moment of the j^{th} subfault. The three important seismic source parameters M_o, f_{oj} and the stress drop ($\Delta\sigma$) are related through

$$f_{0j} = 4.9\mathrm{x}10^6(\mathrm{N_{Rj}})^{-1/3}\mathrm{N}^{1/3}V_s\left(\frac{\Delta\sigma}{\mathrm{M}_{0j}}\right)^{1/3} \tag{4.3}$$

Here V_s stands for the shear wave velocity in the source region, corresponding to bedrock conditions. $\mathrm{N_{Rj}}$ is the cumulative number of ruptured subfaults by the time rupture reaches the j^{th} subfault. The spatial modifying function $D(f)$ is given by

$$D(r,f) = G\exp\left[\frac{-\pi fr}{V_sQ(f)}\right] \tag{4.4}$$

where G is the geometric attenuation factor. The other term denotes anelastic attenuation with hypocentral distance $\boldsymbol{r}$ and the quality factor as Q. The spatial spread of the ground motion depends sensitively on the quality factor of the local region. The constant C of equation (4.1) is

$$C = \frac{\left\langle R_{\theta\phi}\right\rangle\sqrt{2}}{4\pi\rho V_s^3} \tag{4.5}$$

where $\langle R_{\theta\phi}\rangle$ is the radiation coefficient averaged over an appropriate range of azimuths and take-off angles and ρ is the material density at the focal depth. The coefficient $\sqrt{2}$ in the above equation arises as the product of the free surface amplification and partitioning of energy in orthogonal directions. The scaling factor for j^{th} sub-fault, H_j based on the squared acceleration spectrum is taken as (Boore 2009)

$$H_j = \sqrt{N}\frac{f_0^2}{f_{0j}^2} \tag{4.6}$$

Where f_0 is the corner frequency at the end of the rupture, which can be obtained by substituting $N_R(t) = N$ in equation (4.3). The filter function $P_j(f)$ is taken as

$$P_j(f) = \frac{\sqrt{N}}{H_j} \frac{1+(f/f_{0j})^2}{1+(f/f_0)^2} \tag{4.7}$$

The moment of j^{th} subfault is computed from the slip distribution as follows

$$M_{0j} = \frac{M_0 D_j}{\sum_{j=1}^{N} D_j} \tag{4.8}$$

Here, D_j is the average final slip acting on the j^{th} subfault. M_0 is the total seismic moment on the fault. To further account for earthquake rupture Motazedian and Atkinson (2005) introduced the concept of pulsing area where the cumulative number of active subfaults, $N_R(t)$ increases with time at the initiation of rupture and becomes constant at some fixed percentage of the total rupture area. This parameter determines the number of active subfaults during the rupture of j^{th} subfault. These many subfaults are used in computing the corner frequency in equation (4.3).

The above is a general finite source model expressed in the frequency domain, valid for any region if only the various controlling parameters can be selected suitably. Here lies strength of this approach since almost all required parameters for India have been worked out in the past by geophysicists and seismologists using various types of instrumental data from small and large earthquakes. The parameters applicable at All India level are listed first. The spatial modifier of eq (4.4) consists of a general geometrical attenuation term G. This is taken following Singh et al, (1999) as

$$G = \begin{cases} \dfrac{1}{r}, & for\ r \le 100 \\ \dfrac{1}{10\sqrt{r}}, & for\ r > 100 \end{cases} \tag{4.9}$$

The shear wave velocity and density at the focal depth are fixed at 3.6 km/s and 2900 kg/m^3 respectively corresponding to compressed hard granite (Singh *et al* 1999; Mitra *et al* 2005).

4.4 Regionalization in terms of geology

The effects that are specific to Indian geological regions appear in the quality factor *Q(f),* stress drop value ($\Delta\sigma$), focal depth and the site amplification function *F(f).* At this stage a brief discussion on the geological structure of India to extract useful information for further work is necessary.

India can be naturally divided into three geological provinces namely, the Himalayas, the Indo-Gangetic Plain and the Indian Shield (Figure 4.2). The Siwalik range which defines the southern boundary of the Himalayas contains sediments deposited by ancient Himalayan Rivers. The elevation of Siwalik ranges lies in between 0.25 km to 0.8 km.

The lesser Himalaya which lies in between MBT and MCT consists of mostly Palaeozoic sedimentary rocks. The average elevation in lesser Himalaya is 2.5 km. The Great Himalaya which is the most northerly sub-province comprises of crystalline metamorphic and igneous rocks. The average elevation in this part is about 5 km.

The Indo-Gangetic region consists of the vast alluvial plains. The sagging of the basement in this part is attributed to the collision of the Indian and the Eurasian plates. The Indo-Gangetic region is filled with sediments flowing from the Himalayas and parts of the peninsular shield region. The thickness of the alluvial deposits in the Indo-Gangetic Plains is of the order of 1.5-6 km. This conceals the solid nature of its basement. The average elevation in this region is about 200m (Figure 2.2).

The peninsular shield consists of complex system of folds and faults in the basement rock, attributed to the intense tectonic activity during its evolution. This region contains majority of the rock formations and stratigraphical units in India. The rocks of the oldest Archean era known as Dharwars occupy more than half of the India shield (Figure 4.2).

In northeast India, the Archean rocks occur in Shillong plateau and Mikir hills. Orogenic movements during the Precambrian period, which is the next oldest era after Archean period, resulted in the formation of some isolated basins. Sedimentary rocks got deposited over the eroded surface of Archean rocks. Precambrian rocks in PI occur in Cuddapah and Vindhyan basins.

The Gondwana rocks which are younger than Precambrian rocks occur in three linear tracts along Sone-Narmada-Damodar rivers alignment, along Mahanadi and Godavari rivers. The basaltic lava flows during the Mesozoic era resulted in the formation of Deccan traps. The area covered by these rocks is approximately about three hundred thousand square kilometres.

The above, while not a detailed review of the geology of the land mass still helps us to identify broadly seven important regional blocks with differing quality factors. These regions can be broadly identified as Gujarat, Indo-Gangetic Plains, Himalayas, NEI, ANI, Central India, and the remaining Peninsular India. These regions are marked in Fig.4.3.

4.5 Quality Factors

Among the source parameters stress drop, focal depth and quality factor vary from region to region depending on the seismo-tectonic setup and geology. In the past several seismologists have analysed instrumental data to arrive at estimates of the frequency dependent quality factor, which is similar to the damping coefficient in elastic materials. On similar lines the value of stress drop that can happen in different regions for a given magnitude of earthquake is available. Large amount of literature exists on the estimation of these parameters. Rao *et al.* (1998) used strong-motion records of small-magnitude earthquakes and estimated Q value to be $460f^{0.83}$ for the southern part of peninsular India, excluding the Koyna-Warna region. Singh *et al* (1999) derived Q as $508f^{0.48}$ from the broadband records of the Jabalpur earthquake, for the central India. The derived stress drop for events in Central India, Peninsular India and Gujarat region lies in the range of

100-300 bars. The focal depth of events that occur more frequently in these three regions varies from 5 km to 25 km. Singh *et al* (2004) studied the Uttarkashi and Chamoli event records to arrive at the quality factor for Himalayan region as $253f^{0.8}$. Bodin *et al* (2004) modeled the ground motion data of aftershocks in size from about M_w 2 to M_w 5.2 of the Bhuj earthquake of 2001 and derived the quality factor for Gujarat region as $790f^{0.22}$. The estimated stress drop of the aftershocks varied from 150 to 200 bars. The Koyna-Warna region in PI has large number of instrumental recordings. Sharma *et al* (2007) analysed these to arrive at $Q = 169f^{0.77}$. Parvez *et al* (2008) analyzed data from several earthquakes in the magnitude range of M_w 2 to M_w 4.9 that occurred in ANI and determined the quality factor as $119f^{0.80}$. Raghukanth and Somala (2009) calibrated a point source seismological model for NEI. The range of stress drop and the quality factor for Indo-Burma, Shillong plateau and Bengal basin were obtained based on strong motion data of seven events. For earthquakes originating in Indo-Burma tectonic domain Q has been estimated to be $431f^{0.73}$. For the Shillong plateau and Bengal basin region Q is found to be $280f^{0.89}$. Mohanty *et al* (2009) studied the strong motion data of fifty-five earthquakes of magnitude 1.5 to 4.2 acquired from the Delhi telemetric network and derived the quality factor for Indo-Gangetic Plain as $142f^{1.04}$. The quality factors for all the seven regions are shown in Table 4.1.

The other important regional parameter is the focal depth which can vary from as low as 5 km to as deep as 100 km or deeper. The variation in focal depth is fairly well known for the different regions in India (Nandy 2001; Shukla et al 2007; Kayal 2008). The range of focal depth, stress drop and dip in the seven regions are reported in Table 4.2. Apart from the above parameters, the S-wave radiation coefficient ($<R_{\theta\phi}>$) varies randomly within particular intervals. Here, following Boore and Boatwright (1984), the S-wave radiation coefficient is taken to be in the interval 0.48–0.64. In addition to the above parameters the slip distribution and pulsing percentage area is also required in the simulation. The slip field on the rupture plane is treated as uniform for all the sub-faults and pulsing percentage area is varied from 25% - 75% (Boore and Atkinson 2006).

The varying subsurface condition in the seven regions highlights the importance of selecting a common reference site for mapping seismic hazard. As already mentioned, PSHA is carried out here for A-type rock sites which has to be modified by the users to account for local soil deposits. It remains to fix up the amplification function *F(f)* for A-type sites further work.

4.6 Amplification Function for A-type sites

The velocity structure from the basement to the surface can vary in a variety of ways. The A-type reference site can also be made of different layers of rocks making up the average value of $V_{30} > 1.5$ km/s. Such sites are quite common in PI and are also met with in Central and Northeast India. It can be observed that, since V_{30} is an average value, one can have several combinations of soil profiles leading to the same average value. Thus, in addition to uncertainties in seismological parameters, one has to consider the statistical variation in soil profiles for simulating representative surface level spectral accelerations. Here, a random sample of fifty profiles matching with A-type site categories is selected for further study. These are realistic as they are drawn from actual field investigations

(Katti *et al* 1975; Boominathan 2004; Parvez *et al* 2002; Mitra *et al* 2005). These sample profiles along with their corresponding attenuation factor (Q_v) are shown in figure 4.4. Modification between bedrock and A-type site is a linear problem in one dimension and hence for such sites amplification can be directly found by the quarter-wavelength method of Boore and Joyner (1997) which is described below.

The three most important properties that influence site amplification are shear wave velocity, density and material damping. It can be shown that the amplification factor when seismic waves travel from the bedrock to A-type site is given by the square root of the ratio between the seismic impedance at the source to the seismic impedance at the site (Boore and Joyner 1997).

$$F = \sqrt{\frac{\rho V_S}{\rho_A V_A}} \tag{4.10}$$

Here, ρ and V_s are the density and shear wave velocity at the bedrock and ρ_A, V_A are the average density and shear wave velocity at the site. The amplification factor can be made frequency dependent, by averaging the density and shear wave velocity in the A-type site to a depth corresponding to a quarter-wavelength of the frequency of interest. With this modification and accounting for attenuation due to site damping, eq. 4.10 can be rewritten as

$$F(f) = \sqrt{\frac{\rho V_s}{\overline{\rho}(z)\,\overline{V_S}(z)}}\ \exp(-\pi \xi f) \tag{4.11}$$

Here $\overline{\rho(z)}, \overline{V_S(z)}$ are weighted averages of density and shear wave velocity, ξ is the equivalent damping ratio of the rock profile. In the above equation the first term represents the amplification of the ground motion amplitudes due to the rock layers. The second term $exp(-\pi\xi f)$ represents the attenuation effect due to the damping properties of the rock layers. The time averaged density and shear wave velocity are computed from the quarter wavelength method as

$$\overline{\rho}(z) = \frac{1}{d}\int_0^d \rho(z)\ dz$$
$$\overline{V_S}(z) = \frac{d}{t(d)} \tag{4.12}$$

where $t(d)$ is the travel time from the surface to a depth d computed from the shear wave velocity profiles as

$$t(d) = \int_0^d \frac{dz}{V_S(z)} \tag{4.13}$$

The depth and the travel time corresponding to a quarter wavelength is found from the condition

$$t(d) = \frac{1}{4f} \tag{4.14}$$

In this method, first the travel times for different depths are calculated from eq. (4.13) from the rock shear wave velocity profiles. For a particular frequency, corresponding depth and travel time are determined from eq. (4.14) and these values are used in eq. (4.12) for calculating ρ(z) and Vs(z). These time averaged values are substituted in eq. (4.11) for determining the amplification function and the procedure is repeated for all frequencies. The damping ratio in eq. (4.11) is computed from the quality factor Q(f) of the rock layers as

$$\xi = \int_0^D \frac{dz}{VsQ_V} \tag{4.15}$$

where D is the total thickness of the rock layers. Sample amplification functions for fifty typical A-type sites (Fig. 4.4) are presented in Fig. 4.5.

4.7 Sample Ground Motion

From the above discussion it is seen that once the stress drop, site amplification and Q factors are known, the Fourier amplitude spectrum of ground acceleration for any combination of magnitude (M_w) and hypocentral distance ($\boldsymbol{r}$) can be expressed within the limitations of a finite source seismological source mechanism model. This is a random process and hence in the time domain this represents an ensemble of accelerograms. These samples can be retrieved from eq.(4.1) in three steps. First, a Gaussian stationary white noise sample of length equal to the strong motion duration (Boore and Atkinson 1987)

$$T = (1/f_c + 0.05\,\boldsymbol{r}) \tag{4.16}$$

is simulated for each sub-fault. This sample is multiplied by a suitable the nonstationary modulating function. Here we use the function suggested by Saragoni and Hart (1974), which is a generalization of the function previously developed by Iyengar and Iyengar (1969). The simulated sample is Fourier transformed into the frequency domain. This Fourier spectrum is normalized by its root mean-square value and multiplied by the seismological source-path-site function $A(f)$ of eq.(4.1). The resulting function is transformed back into the time domain to get a sample of the ground motion accelerogram for each subfault. The simulated acceleration time histories for all the sub-faults are summed up with time delay of Δt_j to account for the rupture velocity to obtain the final ground acceleration,

$$a(t) = \sum_{j=1}^{N} a_j(t + \Delta t_j) \tag{4.17}$$

Any number of accelerograms can be simulated in this fashion to compute samples of response spectra corresponding to 5% damping.

Here spectral acceleration values have been simulated for moment magnitude (M_w) ranging from 4 to 8.5 in increments of 0.5 units, at 20 values of hypocentral distances ranging from 1 to 500 km. To capture finiteness of the source the ground motions are also simulated for eight azimuths ranging from 0^0 to 315^0 in increments of 45^0. Thus a total number of 160 distance samples are considered for each magnitude. In all, there are 1600

pairs of magnitudes and distances. Since the stress drop, focal depth, dip, amplification function, radiation coefficient and pulsing percentage area are random variables, we have included the uncertainty arising out of these parameters also. Accordingly, fifty samples of these six seismic parameters are generated and these are combined using the Latin Hypercube sampling technique (Iman and Conover 1980) to select for each magnitude value fifty sets of random seismic parameters. Thus, a database of 80,000 PGA and S_a samples corresponding to 1600 simulated earthquake events are generated. This synthetic database is developed separately for each of the seven regions previously described using their respective quality factors.

Among the seven regions PI and NEI need further area weighted refinement. This happens because the Koyna-Warna region and the remaining part of South India have different Q-factors. To account for this the simulated samples are individually simulated for each of the above sub-regions and combined in the ratio of 1:5 to assemble the final set of 80,000 samples for PI. Similarly the subduction zone and the shallow active zone in North East India are in the ratio 1:3 with differing Q-factors. Here also the samples have been generated separately and mixed together in the above ratio.

4.8 Regional Attenuation Equations

Several functional forms of ground motion attenuation have been proposed in the literature to reflecting salient aspects of the spread of ground motion (Sadigh *et al* 1997, Toro *et al* 1997, Campbell 2003, Atkinson and Boore 2006). Since all the proposals are empirical the particular form selected are justified heuristically and some times by limited comparison with instrumental records. After reviewing the various available forms of equations, it has been decided to develop the attenuation relation for all the seven regions in the form

$$\ln\left(\frac{S_a}{g}\right) = \mathrm{C}_1 + \mathrm{C}_2 M + \mathrm{C}_3 M^2 + \mathrm{C}_4\, r + \mathrm{C}_5 \ln\left(r + \mathrm{C}_6 e^{\mathrm{C}_7 M}\right) + \mathrm{C}_8 \log(r)\mathrm{f}_0 + \ln(\varepsilon) \qquad (4.18)$$

$$\mathrm{f}_0 = \max(\ln(r/100), 0)$$

Here S_a is the spectral acceleration, M is the moment magnitude, $\boldsymbol{r}$ is the hypocentral distance in kilometers. This form of the attenuation accounts for geometrical spreading, anelastic attenuation and magnitude saturation similar to the finite source seismological model discussed previously. The coefficients of the above equation are obtained from the simulated database of 80,000 samples by a two-step stratified regression following Joyner and Boore (1981). Since the equation is empirical there would be other forms that can equally well represent the data. The sufficiency of a particular equation can be verified by plotting the residuals in the goodness of fit to detect systematic trends that indicate existence of bias. In figure 4.6, residuals ($ln\ \varepsilon$) are plotted as function of magnitude and hypocentral distance for the Himalayan region. Absence of discernable trend verifies the sufficiency of the above equation to represent ground motion for further work. This sufficiency has been verified for the other six regions also.

The coefficients C_1, C_2….C_8 and the standard error are shown in Tables 4.3-4.9 as functions of period (1/frequency) for all the seven regions. These results can be used to construct the mean and (mean+sigma) response spectrum on A-type rock in any part of

India. In Figure 4.7 the attenuation of PGA in the all the seven regions is shown for different magnitude values.

4.9 Validation

As mentioned earlier the SMA data available for India is limited. Hence, it would be interesting to see how the derived synthetic attenuation relation matches with available observations. Comparison between instrumented PGA values from the Koyna-Warna region (Iyengar and Raghukanth 2004) with values estimated from the derived attenuation relation is presented in Table 4.10. The Koyna earthquake of 11 December 1967 is still the only large magnitude event in PI for which instrumental strong motion records are available. The actual response spectrum of the horizontal component is compared with the estimated spectrum in Fig. 4.8. It is seen from this figure the instrumental spectrum compares well with the mean spectrum estimated using the frequency dependent attenuation coefficients of Table 4.5. The sample fluctuations inevitably present in any single record are within the sigma band.

In Figs 4.9 and 4.10 the estimated PGA values for the Himalayan region are compared with recorded instrumental values of the Uttarkashi and Chamoli earthquake are shown. The present estimation are only expected values with considerable variation.

Similarly Fig. 4.11 shows the comparison between the SMA data of 6th August 1988 Indo-Burmese earthquake with the estimated ground motion. Since not all the instrument sites can be considered to be hard rock matching with A-type site, in the above cases recorded data some times goes beyond the sigma band. Nevertheless, the comparison between the estimated and the observed PGA values is satisfactory.

With the development of the seven attenuation relations we have at our disposal all required information for carrying out hazard mapping incorporating uncertainties due to source, path and site.

Table 4.1 Q-factors considered for the all the seven regions

Region	Q - factor	Investigator
Himalaya	$Q = 253f^{0.8}$	Singh et al (2004)
North East India	Indo-Burmese arc $Q = 431f^{0.73}$ Bengal basin- Shillong plateau $Q = 224f^{0.93}$	Raghukanth and Somala (2009)
Indo-Gangetic	$Q=142f^{1.04}$	Mohanty *et al* (2006)
Gujarat	$Q=790f^{0.22}$	Bodin *et al* (2004)
Central India	$Q=508f^{0.48}$	Singh et al (1999)
Peninsular India	Koyna-Warna $Q =71f^{1.32}$ South India $Q=460f^{0.83}$	Sharma et al (2007) Rao et al (1998)
Andaman-Nicobar	$Q = 119f^{0.80}$	Parvez et al (2008)

Table 4.2. Uncertainties in Earthquake Model Parameters

Region	**Stress drop $\Delta\sigma$ (bars)**	**Dip (^{0})**	**Focal depth (km)**	**Reference**
Himalaya	50-200	2^0-30^0	5-40	Kayal (2008)
Northeast India-crustal	100-300	10^0-80^0	5-50	Kayal (2008)
Northeast India-Subduction	100-300	50^0-90^0	50-140	Satyabala (2003)
Indo-Gangetic Plain	50-200	10^0-80^0	5-40	Kayal (2008)
Gujarat	100-300	10^0-80^0	5-40	Bodin *et al* (2004)
Central India	100-300	10^0-80^0	5-30	Singh *et al* (2004)
Peninsular India	100-300	10^0-80^0	5-25	Singh *et al* (2004)
Koyna-Warna	100-300	10^0-80^0	5-15	Talwani *et al* (1998)
Andaman-Nicobar	50-200	10^0-80^0	5-100	Parvez *et al* (2005)

Table 4.3 Coefficients in the attenuation relation for Andaman region

Period	C_1	C_2	C_3	C_4	C_5	C_6	C_7	C_8	$\sigma(\varepsilon)$
0.0000	-2.4965	0.7886	0.0446	-0.0078	-1.5282	0.0273	1.0030	0.0645	0.4090
0.0100	-2.5002	0.7864	0.0448	-0.0078	-1.5272	0.0272	1.0036	0.0647	0.4055
0.0150	-1.5514	0.6563	0.0529	-0.0082	-1.5006	0.0257	1.0055	0.0586	0.4223
0.0200	-1.4400	0.6278	0.0539	-0.0085	-1.4597	0.0205	1.0298	0.0632	0.4119
0.0300	-1.5031	0.6302	0.0523	-0.0086	-1.4133	0.0164	1.0524	0.0696	0.4050
0.0400	-1.6368	0.6485	0.0502	-0.0086	-1.3935	0.0154	1.0563	0.0738	0.3621
0.0500	-1.8045	0.6791	0.0476	-0.0086	-1.3852	0.0149	1.0585	0.0756	0.4028
0.0600	-2.0570	0.7300	0.0436	-0.0085	-1.3767	0.0154	1.0528	0.0777	0.3796
0.0750	-2.3964	0.7862	0.0390	-0.0085	-1.3566	0.0142	1.0600	0.0776	0.3796
0.0900	-2.7262	0.8535	0.0338	-0.0084	-1.3438	0.0140	1.0600	0.0786	0.3596
0.1000	-2.9836	0.9072	0.0298	-0.0084	-1.3398	0.0146	1.0541	0.0777	0.3567
0.1500	-4.2457	1.1969	0.0084	-0.0081	-1.3235	0.0178	1.0266	0.0762	0.3862
0.2000	-5.5321	1.4971	-0.0136	-0.0080	-1.3000	0.0199	1.0093	0.0737	0.3740
0.3000	-7.9032	2.0991	-0.0565	-0.0078	-1.2989	0.0306	0.9545	0.0742	0.3817
0.4000	-9.9729	2.6180	-0.0929	-0.0076	-1.2864	0.0365	0.9317	0.0742	0.3767
0.5000	-11.6848	3.0527	-0.1228	-0.0075	-1.2873	0.0432	0.9103	0.0750	0.3757
0.6000	-13.4260	3.4724	-0.1513	-0.0074	-1.2761	0.0465	0.9007	0.0726	0.3748
0.7000	-14.6203	3.7696	-0.1709	-0.0073	-1.2783	0.0531	0.8881	0.0716	0.3997
0.7500	-15.1806	3.8953	-0.1792	-0.0072	-1.2711	0.0518	0.8905	0.0704	0.3796
0.8000	-15.7691	4.0461	-0.1887	-0.0072	-1.2822	0.0562	0.8815	0.0727	0.3795
0.9000	-16.8876	4.3018	-0.2050	-0.0071	-1.2799	0.0581	0.8770	0.0729	0.4027
1.0000	-17.4428	4.4232	-0.2125	-0.0070	-1.2773	0.0570	0.8802	0.0727	0.4040
1.2000	-19.0194	4.7593	-0.2325	-0.0069	-1.2736	0.0596	0.8780	0.0759	0.3811
1.5000	-20.4267	5.0465	-0.2478	-0.0066	-1.2894	0.0669	0.8674	0.0769	0.3533
2.0000	-22.1132	5.3545	-0.2616	-0.0064	-1.3079	0.0714	0.8653	0.0821	0.3845
2.5000	-23.1519	5.4901	-0.2650	-0.0062	-1.3055	0.0685	0.8724	0.0840	0.3929
3.0000	-23.8338	5.5345	-0.2602	-0.0060	-1.3334	0.0724	0.8697	0.0877	0.4074
4.0000	-24.4244	5.4829	-0.2453	-0.0057	-1.3652	0.0784	0.8653	0.0921	0.4059

Table 4.4 Coefficients in the attenuation relation for Indo-Gangetic region

Period	C_1	C_2	C_3	C_4	C_5	C_6	C_7	C_8	$\sigma(\varepsilon)$
0.00	-3.1373	0.9365	0.0258	-0.0076	-1.4326	0.0183	1.0198	0.1047	0.4095
0.010	-3.1396	0.9342	0.0259	-0.0076	-1.4319	0.0182	1.0205	0.1047	0.4177
0.015	-2.1117	0.7802	0.0369	-0.0079	-1.4170	0.0153	1.0409	0.1009	0.4646
0.020	-1.9868	0.7638	0.0375	-0.0080	-1.3899	0.0131	1.0576	0.1029	0.4508
0.030	-1.9837	0.7637	0.0369	-0.0080	-1.3619	0.0116	1.0713	0.1036	0.4178
0.040	-2.0880	0.7815	0.0353	-0.0079	-1.3512	0.0114	1.0712	0.1047	0.4167
0.050	-2.2463	0.8145	0.0328	-0.0078	-1.3483	0.0117	1.0672	0.1044	0.4041
0.060	-2.5145	0.8703	0.0285	-0.0078	-1.3403	0.0119	1.0630	0.1043	0.3999
0.075	-2.8025	0.9134	0.0250	-0.0077	-1.3231	0.0116	1.0655	0.1024	0.3965
0.090	-3.1251	0.9829	0.0198	-0.0076	-1.3135	0.0118	1.0623	0.1014	0.4033
0.100	-3.3506	1.0305	0.0164	-0.0076	-1.3135	0.0124	1.0555	0.1017	0.3986
0.150	-4.6406	1.3309	-0.0058	-0.0074	-1.2986	0.0168	1.0142	0.1001	0.3982
0.200	-5.8750	1.6228	-0.0271	-0.0072	-1.2808	0.0195	0.9920	0.0974	0.3943
0.300	-8.2728	2.2294	-0.0707	-0.0070	-1.2741	0.0312	0.9292	0.0973	0.4029
0.400	-10.3671	2.7647	-0.1084	-0.0069	-1.2662	0.0438	0.8854	0.0978	0.4018
0.500	-12.0415	3.1774	-0.1369	-0.0068	-1.2593	0.0481	0.8718	0.0972	0.4120
0.600	-13.7659	3.5922	-0.1652	-0.0068	-1.2467	0.0533	0.8573	0.0964	0.4134
0.700	-14.9423	3.8804	-0.1843	-0.0067	-1.2458	0.0576	0.8494	0.0949	0.4145
0.750	-15.5104	4.0075	-0.1928	-0.0067	-1.2376	0.0561	0.8516	0.0940	0.4154
0.800	-16.0963	4.1523	-0.2020	-0.0066	-1.2440	0.0601	0.8438	0.0951	0.4068
0.900	-17.2437	4.4035	-0.2181	-0.0066	-1.2309	0.0555	0.8520	0.0931	0.4083
1.000	-17.7686	4.5126	-0.2248	-0.0066	-1.2251	0.0533	0.8567	0.0926	0.4083
1.200	-19.2437	4.8024	-0.2414	-0.0066	-1.2137	0.0476	0.8705	0.0927	0.4072
1.500	-20.5601	5.0418	-0.2534	-0.0066	-1.2151	0.0457	0.8775	0.0915	0.3960
2.000	-22.0981	5.2587	-0.2612	-0.0068	-1.2009	0.0315	0.9236	0.0931	0.3941
2.500	-22.9997	5.3216	-0.2595	-0.0068	-1.1763	0.0190	0.9836	0.0901	0.3988
3.000	-23.5081	5.2531	-0.2468	-0.0068	-1.1617	0.0090	1.0789	0.0869	0.3975
4.000	-23.8099	5.0255	-0.2198	-0.0069	-1.1298	0.0017	1.2845	0.0845	0.4056

Table 4.5 Coefficients in the attenuation relation for Peninsular India

Period	C_1	C_2	C_3	C_4	C_5	C_6	C_7	C_8	$\sigma(\varepsilon)$
0.0000	-5.2182	1.6543	-0.0309	-0.0029	-1.4428	0.0188	0.9968	0.1237	0.3843
0.0100	-5.2204	1.6523	-0.0307	-0.0029	-1.4422	0.0187	0.9971	0.1237	0.3837
0.0150	-4.1862	1.4952	-0.0197	-0.0030	-1.4265	0.0162	1.0135	0.1209	0.4159
0.0200	-4.1018	1.5037	-0.0209	-0.0030	-1.4096	0.0146	1.0237	0.1202	0.4022
0.0300	-4.1365	1.5228	-0.0227	-0.0030	-1.3888	0.0137	1.0298	0.1161	0.3873
0.0400	-4.2520	1.5430	-0.0244	-0.0029	-1.3783	0.0137	1.0266	0.1149	0.3827
0.0500	-4.4128	1.5817	-0.0271	-0.0029	-1.3801	0.0142	1.0227	0.1140	0.3822
0.0600	-4.7225	1.6531	-0.0327	-0.0028	-1.3730	0.0159	1.0077	0.1132	0.3835
0.0750	-5.0947	1.7235	-0.0383	-0.0028	-1.3572	0.0146	1.0136	0.1121	0.3842
0.0900	-5.5186	1.8218	-0.0460	-0.0028	-1.3441	0.0145	1.0117	0.1113	0.3856
0.1000	-5.8239	1.8911	-0.0511	-0.0028	-1.3409	0.0157	1.0018	0.1103	0.3868
0.1500	-7.4663	2.2950	-0.0816	-0.0027	-1.3179	0.0213	0.9581	0.1055	0.3888
0.2000	-9.0431	2.6930	-0.1115	-0.0026	-1.2965	0.0239	0.9374	0.1020	0.3941
0.3000	-11.9934	3.4705	-0.1687	-0.0025	-1.2861	0.0384	0.8713	0.0989	0.4008
0.4000	-14.3305	4.0665	-0.2112	-0.0025	-1.2686	0.0462	0.8467	0.0984	0.4052
0.5000	-16.2504	4.5566	-0.2457	-0.0024	-1.2614	0.0533	0.8254	0.0975	0.4082
0.6000	-18.1350	5.0060	-0.2767	-0.0024	-1.2419	0.0473	0.8363	0.0949	0.4106
0.7000	-19.3494	5.3013	-0.2962	-0.0024	-1.2399	0.0508	0.8309	0.0934	0.4119
0.7500	-19.8904	5.4156	-0.3035	-0.0023	-1.2316	0.0472	0.8388	0.0922	0.4130
0.8000	-20.4426	5.5522	-0.3118	-0.0023	-1.2423	0.0529	0.8273	0.0938	0.4120
0.9000	-21.4875	5.7648	-0.3246	-0.0023	-1.2309	0.0473	0.8383	0.0922	0.4129
1.0000	-21.9767	5.8581	-0.3297	-0.0023	-1.2258	0.0438	0.8487	0.0927	0.4134
1.2000	-23.1660	6.0486	-0.3372	-0.0023	-1.2204	0.0401	0.8659	0.0939	0.4139
1.5000	-24.2031	6.1891	-0.3402	-0.0022	-1.2281	0.0371	0.8833	0.0924	0.4137
2.0000	-25.1523	6.2202	-0.3308	-0.0022	-1.2390	0.0324	0.9107	0.0975	0.4173
2.5000	-25.5577	6.1153	-0.3139	-0.0022	-1.2275	0.0213	0.9687	0.0982	0.4248
3.0000	-25.5807	5.8957	-0.2871	-0.0021	-1.2341	0.0150	1.0215	0.1003	0.4274
4.0000	-25.2671	5.5029	-0.2436	-0.0021	-1.2511	0.0122	1.0627	0.1034	0.4346

Table 4.6 Coefficients in the attenuation relation for Central India

Period	C_1	C_2	C_3	C_4	C_5	C_6	C_7	C_8	$\sigma(\varepsilon)$
0.0000	-3.7671	1.2303	-0.0019	-0.0027	-1.4857	0.0385	0.8975	0.1301	0.3940
0.0100	-3.7649	1.2254	-0.0015	-0.0027	-1.4845	0.0379	0.8992	0.1300	0.3926
0.0150	-2.6575	1.1024	0.0068	-0.0028	-1.4778	0.0434	0.8804	0.1282	0.4602
0.0200	-2.5364	1.1017	0.0064	-0.0028	-1.4555	0.0363	0.9000	0.1257	0.4315
0.0300	-2.5474	1.1146	0.0050	-0.0028	-1.4276	0.0316	0.9131	0.1219	0.3966
0.0400	-2.6973	1.1508	0.0020	-0.0027	-1.4164	0.0314	0.9112	0.1213	0.3829
0.0500	-2.8567	1.1830	-0.0003	-0.0026	-1.4120	0.0289	0.9212	0.1184	0.3773
0.0600	-3.1317	1.2335	-0.0041	-0.0026	-1.3984	0.0274	0.9272	0.1161	0.3752
0.0750	-3.5059	1.3089	-0.0101	-0.0026	-1.3831	0.0276	0.9225	0.1149	0.3721
0.0900	-3.9446	1.4148	-0.0183	-0.0026	-1.3716	0.0273	0.9209	0.1152	0.3724
0.1000	-4.2782	1.4909	-0.0242	-0.0026	-1.3652	0.0288	0.9126	0.1140	0.3718
0.1500	-5.9110	1.8819	-0.0535	-0.0025	-1.3352	0.0336	0.8876	0.1078	0.3753
0.2000	-7.5046	2.2741	-0.0829	-0.0024	-1.3075	0.0320	0.8878	0.1026	0.3787
0.3000	-10.4006	3.0324	-0.1384	-0.0023	-1.2968	0.0456	0.8386	0.1006	0.3886
0.4000	-12.8011	3.6427	-0.1822	-0.0023	-1.2748	0.0494	0.8251	0.0985	0.3947
0.5000	-14.6664	4.1214	-0.2156	-0.0022	-1.2735	0.0601	0.7992	0.0987	0.3979
0.6000	-16.5796	4.5750	-0.2469	-0.0022	-1.2498	0.0512	0.8157	0.0935	0.4001
0.7000	-17.7618	4.8571	-0.2653	-0.0022	-1.2458	0.0539	0.8121	0.0940	0.4001
0.7500	-18.3078	4.9783	-0.2730	-0.0021	-1.2414	0.0523	0.8160	0.0933	0.4009
0.8000	-18.8559	5.1126	-0.2811	-0.0021	-1.2515	0.0579	0.8068	0.0935	0.3990
0.9000	-19.9069	5.3340	-0.2944	-0.0021	-1.2459	0.0531	0.8172	0.0919	0.3997
1.0000	-20.3915	5.4297	-0.2996	-0.0020	-1.2441	0.0512	0.8229	0.0932	0.3987
1.2000	-21.5917	5.6300	-0.3079	-0.0020	-1.2435	0.0498	0.8342	0.0948	0.3931
1.5000	-22.5895	5.7652	-0.3100	-0.0018	-1.2601	0.0512	0.8393	0.0962	0.3890
2.0000	-23.5769	5.8344	-0.3034	-0.0017	-1.2867	0.0584	0.8352	0.1037	0.3877
2.5000	-23.9621	5.7445	-0.2875	-0.0017	-1.2917	0.0491	0.8633	0.1067	0.3923
3.0000	-24.0289	5.5676	-0.2637	-0.0016	-1.3173	0.0508	0.8699	0.1131	0.3962
4.0000	-23.7515	5.2307	-0.2245	-0.0015	-1.3626	0.0644	0.8526	0.1198	0.4066

Table 4.7 Coefficients in the attenuation relation for Gujarat region

Period	C_1	C_2	C_3	C_4	C_5	C_6	C_7	C_8	$\sigma(\varepsilon)$
0.0000	-4.7653	1.3935	-0.0162	-0.0020	-1.4183	0.0187	0.9899	0.1243	0.3596
0.0100	-4.7654	1.3925	-0.0162	-0.0020	-1.4180	0.0186	0.9906	0.1243	0.3597
0.0150	-3.7890	1.2437	-0.0057	-0.0020	-1.4138	0.0170	1.0015	0.1226	0.3661
0.0200	-3.4369	1.2058	-0.0033	-0.0021	-1.3996	0.0150	1.0151	0.1218	0.3650
0.0300	-3.2520	1.2062	-0.0038	-0.0020	-1.3782	0.0146	1.0161	0.1178	0.3631
0.0400	-3.2479	1.2148	-0.0045	-0.0020	-1.3680	0.0140	1.0203	0.1165	0.3638
0.0500	-3.3558	1.2533	-0.0074	-0.0020	-1.3690	0.0143	1.0155	0.1167	0.3643
0.0600	-3.6403	1.3297	-0.0132	-0.0019	-1.3622	0.0165	0.9978	0.1157	0.3664
0.0750	-3.9514	1.3939	-0.0184	-0.0019	-1.3468	0.0158	0.9996	0.1149	0.3681
0.0900	-4.3288	1.4850	-0.0254	-0.0019	-1.3347	0.0165	0.9904	0.1141	0.3688
0.1000	-4.6321	1.5609	-0.0310	-0.0019	-1.3326	0.0177	0.9826	0.1123	0.3696
0.1500	-6.1285	1.9439	-0.0597	-0.0018	-1.3206	0.0263	0.9280	0.1095	0.3758
0.2000	-7.6691	2.3366	-0.0890	-0.0018	-1.2994	0.0327	0.8962	0.1057	0.3798
0.3000	-10.5848	3.1084	-0.1458	-0.0017	-1.2888	0.0486	0.8389	0.1044	0.3886
0.4000	-12.9478	3.7214	-0.1896	-0.0017	-1.2751	0.0612	0.8082	0.1039	0.3950
0.5000	-14.8383	4.1990	-0.2231	-0.0017	-1.2652	0.0657	0.7974	0.1021	0.3964
0.6000	-16.6838	4.6394	-0.2532	-0.0016	-1.2477	0.0644	0.7973	0.0983	0.3964
0.7000	-17.9334	4.9467	-0.2737	-0.0016	-1.2447	0.0703	0.7889	0.0972	0.3949
0.7500	-18.4834	5.0638	-0.2811	-0.0016	-1.2368	0.0650	0.7976	0.0964	0.3959
0.8000	-19.0245	5.1951	-0.2890	-0.0016	-1.2468	0.0702	0.7914	0.0983	0.3954
0.9000	-20.0872	5.4162	-0.3023	-0.0016	-1.2375	0.0622	0.8044	0.0974	0.3949
1.0000	-20.5927	5.5113	-0.3075	-0.0016	-1.2298	0.0575	0.8143	0.0973	0.3944
1.2000	-21.8734	5.7343	-0.3176	-0.0014	-1.2272	0.0525	0.8334	0.0963	0.3904
1.5000	-22.8904	5.8770	-0.3202	-0.0013	-1.2438	0.0522	0.8446	0.0972	0.3882
2.0000	-23.9486	5.9483	-0.3140	-0.0012	-1.2567	0.0516	0.8548	0.1027	0.3902
2.5000	-24.3712	5.8437	-0.2969	-0.0011	-1.2440	0.0334	0.9136	0.1023	0.3970
3.0000	-24.4438	5.6416	-0.2715	-0.0011	-1.2528	0.0237	0.9662	0.1034	0.4019
4.0000	-24.1841	5.2717	-0.2297	-0.0011	-1.2726	0.0229	0.9826	0.1103	0.4096

Table 4.8 Coefficients in the attenuation relation for Northeast India

Period	C_1	C_2	C_3	C_4	C_5	C_6	C_7	C_8	$\sigma(\varepsilon)$
0.0000	-4.2427	1.3100	-0.0097	-0.0031	-1.3159	0.0172	1.0279	0.1083	0.4424
0.0100	-4.2462	1.3069	-0.0095	-0.0031	-1.3145	0.0168	1.0306	0.1083	0.4410
0.0150	-3.2699	1.1651	0.0002	-0.0032	-1.2902	0.0119	1.0720	0.1046	0.4988
0.0200	-3.1139	1.1599	0.0002	-0.0032	-1.2834	0.0115	1.0743	0.1049	0.4759
0.0300	-3.0689	1.1659	-0.0004	-0.0032	-1.2760	0.0114	1.0734	0.1041	0.4453
0.0400	-3.1870	1.1912	-0.0023	-0.0032	-1.2705	0.0120	1.0666	0.1043	0.4331
0.0500	-3.3512	1.2267	-0.0050	-0.0031	-1.2696	0.0127	1.0581	0.1048	0.4271
0.0600	-3.6194	1.2894	-0.0096	-0.0031	-1.2684	0.0146	1.0392	0.1047	0.4226
0.0750	-3.9007	1.3424	-0.0136	-0.0031	-1.2617	0.0157	1.0292	0.1041	0.4193
0.0900	-4.2122	1.4221	-0.0196	-0.0030	-1.2619	0.0201	0.9982	0.1041	0.4177
0.1000	-4.4638	1.4880	-0.0242	-0.0030	-1.2695	0.0240	0.9758	0.1062	0.4162
0.1500	-5.8209	1.8267	-0.0487	-0.0029	-1.2711	0.0445	0.8973	0.1056	0.4164
0.2000	-7.1113	2.1560	-0.0724	-0.0029	-1.2706	0.0687	0.8408	0.1070	0.4182
0.3000	-9.5795	2.8058	-0.1183	-0.0029	-1.2853	0.1340	0.7572	0.1092	0.4240
0.4000	-11.6654	3.3577	-0.1566	-0.0028	-1.2962	0.2120	0.7011	0.1120	0.4303
0.5000	-13.4385	3.7880	-0.1860	-0.0028	-1.2841	0.2313	0.6899	0.1104	0.4328
0.6000	-15.1386	4.2035	-0.2137	-0.0028	-1.2828	0.2685	0.6716	0.1111	0.4344
0.7000	-16.2898	4.4858	-0.2320	-0.0027	-1.2874	0.2832	0.6681	0.1103	0.4344
0.7500	-16.8403	4.5993	-0.2392	-0.0027	-1.2769	0.2676	0.6733	0.1091	0.4345
0.8000	-17.4118	4.7372	-0.2477	-0.0027	-1.2831	0.2763	0.6710	0.1117	0.4330
0.9000	-18.5053	4.9764	-0.2624	-0.0027	-1.2779	0.2687	0.6757	0.1095	0.4325
1.0000	-19.0253	5.0821	-0.2686	-0.0026	-1.2738	0.2580	0.6804	0.1084	0.4323
1.2000	-20.5318	5.3671	-0.2844	-0.0025	-1.2595	0.2229	0.6984	0.1073	0.4270
1.5000	-21.8434	5.5932	-0.2946	-0.0024	-1.2622	0.1930	0.7206	0.1060	0.4229
2.0000	-23.3177	5.7719	-0.2982	-0.0023	-1.2473	0.1237	0.7830	0.1039	0.4201
2.5000	-24.1965	5.7795	-0.2916	-0.0022	-1.2027	0.0485	0.8985	0.0979	0.4223
3.0000	-24.6659	5.6577	-0.2737	-0.0020	-1.1729	0.0131	1.0680	0.0919	0.4233
4.0000	-24.7444	5.3029	-0.2351	-0.0019	-1.1223	0.0008	1.4322	0.0849	0.4319

Table 4.9 Coefficients in the attenuation relation for Himalayan region

Period	C_1	C_2	C_3	C_4	C_5	C_6	C_7	C_8	$\sigma(\varepsilon)$
0.0000	-3.7438	1.0892	0.0098	-0.0046	-1.4817	0.0124	0.9950	0.1249	0.4094
0.0100	-3.7486	1.0877	0.0099	-0.0046	-1.4804	0.0123	0.9955	0.1247	0.4083
0.0150	-2.7616	0.9550	0.0188	-0.0049	-1.4649	0.0111	1.0051	0.1234	0.4678
0.0200	-2.7051	0.9588	0.0179	-0.0049	-1.4387	0.0092	1.0246	0.1223	0.4445
0.0300	-2.7582	0.9755	0.0162	-0.0048	-1.4121	0.0081	1.0372	0.1179	0.4137
0.0400	-2.9321	1.0173	0.0126	-0.0047	-1.4014	0.0087	1.0248	0.1165	0.4001
0.0500	-3.0839	1.0461	0.0106	-0.0046	-1.3992	0.0089	1.0217	0.1124	0.3941
0.0600	-3.3069	1.0905	0.0075	-0.0046	-1.3958	0.0095	1.0129	0.1150	0.3910
0.0750	-3.6744	1.1532	0.0024	-0.0046	-1.3738	0.0086	1.0202	0.1145	0.3885
0.0900	-4.1011	1.2448	-0.0045	-0.0046	-1.3582	0.0086	1.0173	0.1146	0.3873
0.1000	-4.4163	1.3088	-0.0092	-0.0045	-1.3480	0.0089	1.0131	0.1095	0.3873
0.1500	-5.8898	1.6365	-0.0331	-0.0043	-1.3168	0.0101	0.9903	0.1011	0.3882
0.2000	-7.3244	1.9682	-0.0572	-0.0043	-1.2859	0.0096	0.9891	0.0987	0.3929
0.3000	-9.9600	2.6152	-0.1031	-0.0040	-1.2659	0.0134	0.9404	0.0926	0.4010
0.4000	-12.1052	3.1363	-0.1391	-0.0040	-1.2445	0.0166	0.9136	0.0878	0.4060
0.5000	-13.8894	3.5767	-0.1691	-0.0039	-1.2403	0.0188	0.8940	0.0906	0.4069
0.6000	-15.6887	3.9957	-0.1974	-0.0038	-1.2192	0.0181	0.8930	0.0876	0.4085
0.7000	-16.8075	4.2512	-0.2137	-0.0038	-1.2118	0.0187	0.8939	0.0863	0.4078
0.7500	-17.3641	4.3748	-0.2219	-0.0038	-1.2038	0.0183	0.8934	0.0842	0.4096
0.8000	-17.9297	4.5173	-0.2306	-0.0037	-1.2175	0.0221	0.8745	0.0847	0.4070
0.9000	-19.0065	4.7521	-0.2452	-0.0037	-1.2109	0.0231	0.8670	0.0861	0.4072
1.0000	-19.5191	4.8564	-0.2515	-0.0037	-1.2044	0.0224	0.8699	0.0854	0.4081
1.2000	-20.8567	5.1139	-0.2652	-0.0036	-1.2027	0.0236	0.8720	0.0868	0.4007
1.5000	-22.0907	5.3398	-0.2751	-0.0035	-1.2231	0.0254	0.8731	0.0871	0.3958
2.0000	-23.4263	5.5337	-0.2796	-0.0034	-1.2496	0.0283	0.8733	0.0946	0.3898
2.5000	-24.1315	5.5606	-0.2742	-0.0033	-1.2525	0.0245	0.8965	0.0971	0.3924
3.0000	-24.6217	5.5327	-0.2635	-0.0032	-1.2779	0.0238	0.9092	0.1009	0.3951
4.0000	-24.8660	5.3573	-0.2394	-0.0031	-1.3022	0.0224	0.9280	0.1076	0.4023

Table 4.10 Comparison of estimated and recorded PGA in Koyna region

Date	Magnitude	Epicentral distance (km)	Focal depth (km)	Recorded PGA (g)	Estimated PGA (g)
13-Sep-67	5.6	13	3	0.1640	0.3142
13-Sep-67	4.3	11	5	0.0200	0.0854
10-Dec-67	6.5	13	10	0.4860	0.5181
12-Dec-67	4.5	14	13	0.0360	0.0589
13-Dec-67	4.4	12	15	0.0410	0.0515
24-Dec-67	4.8	7	20	0.0500	0.0742
24-Dec-67	4.8	7	20	0.0350	0.0742
4-Mar-68	4	4	10	0.0190	0.0682
4-Mar-68	4	9	10	0.0090	0.0503
1-Jan-70	4.1	9	11	0.0130	0.0532
27-May-70	4.2	11	3	0.0698	0.0815
26-Sep-70	4.2	11	13	0.0420	0.0471
17-Feb-74	4.5	17	19	0.0214	0.0393
29-Jul-74	4.1	8	24	0.0360	0.0235
2-Sep-80	4.1	18	13	0.0293	0.0284
2-Sep-80	4.1	18	13	0.0110	0.0284
20-Sep-80	4.5	21	8	0.0310	0.047
20-Sep-80	4.7	17	8	0.0220	0.0773
20-Sep-80	4.7	17	8	0.0219	0.0773
25-Apr-82	4.1	18	13	0.0293	0.0284
25-Apr-82	4.1	18	13	0.0110	0.0284
12-Mar-95	4.5	20	10	0.0130	0.0473
13-Mar-95	4.2	25	10	0.0055	0.0245

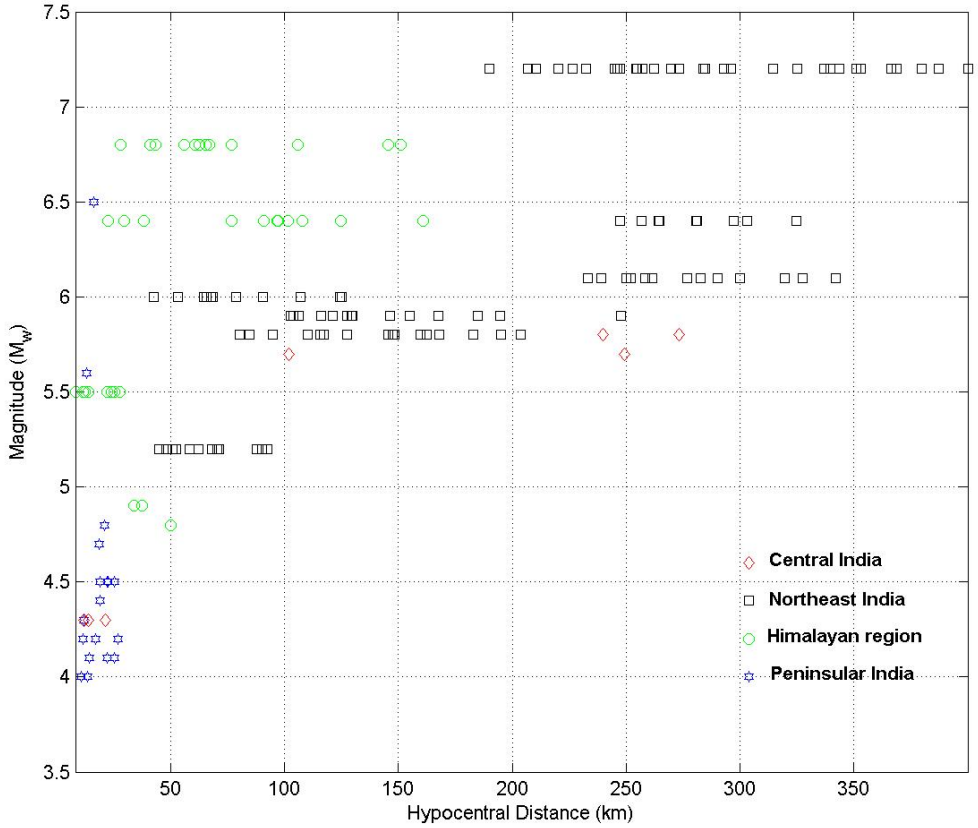

Fig.4.1 Indian Strong Motion Database. Magnitude-Distance Distribution

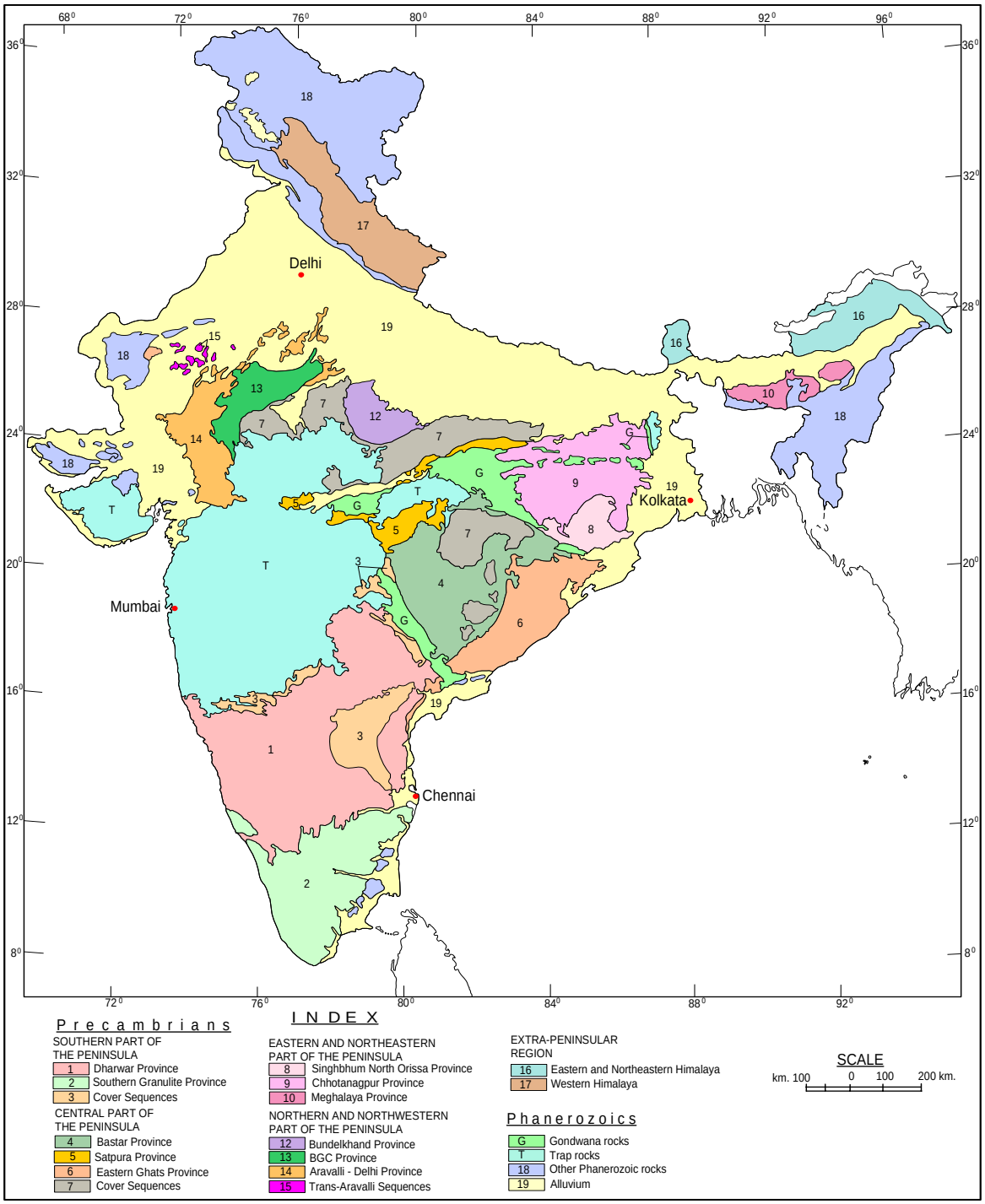

Fig. I.04 Map showing distribution of Geological Provinces in India

Figure 4.2 Geological Map of India (GSI)

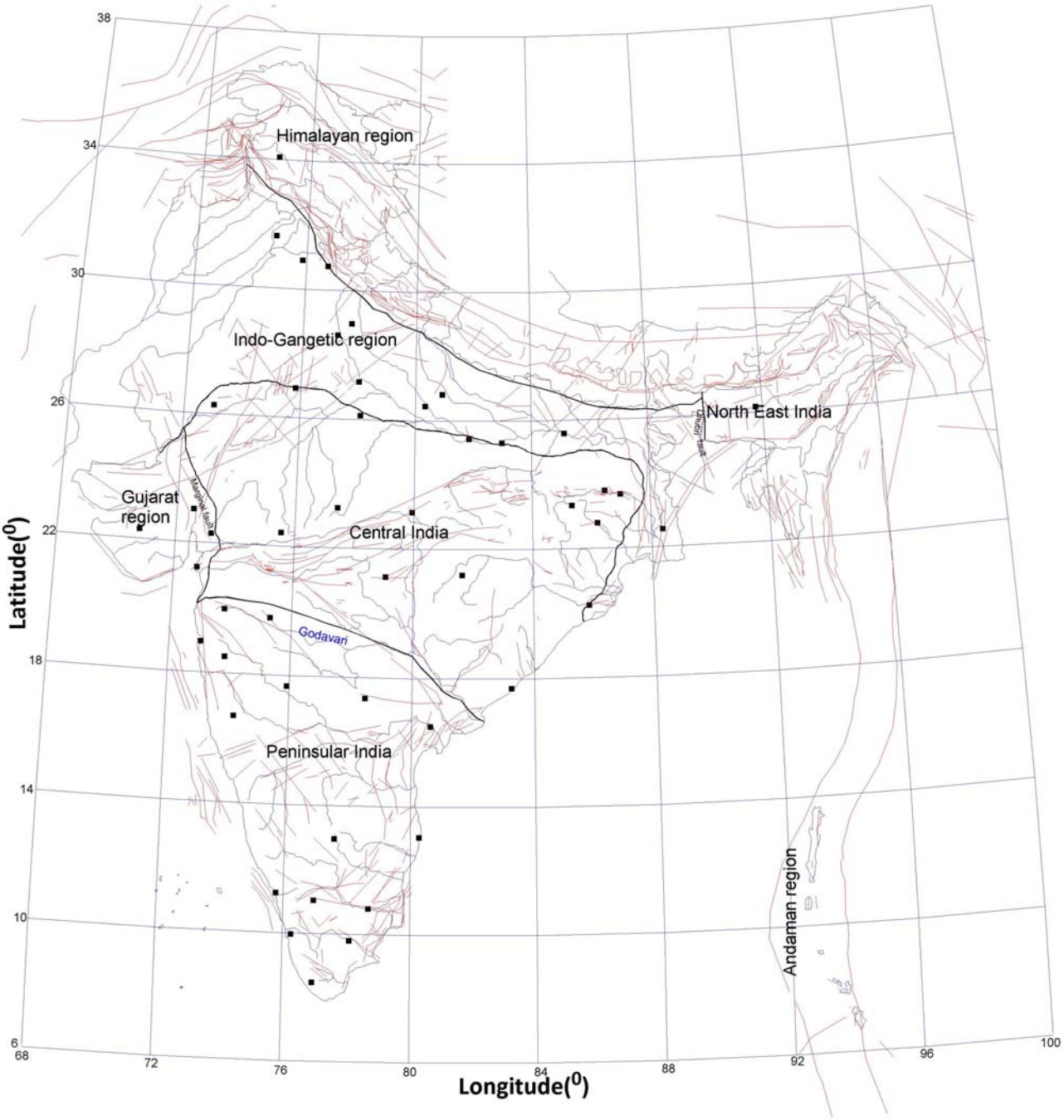

Figure 4.3 Seven Geological Provinces with differing Quality Factors (Dots indicate cities with population > 1 Million)

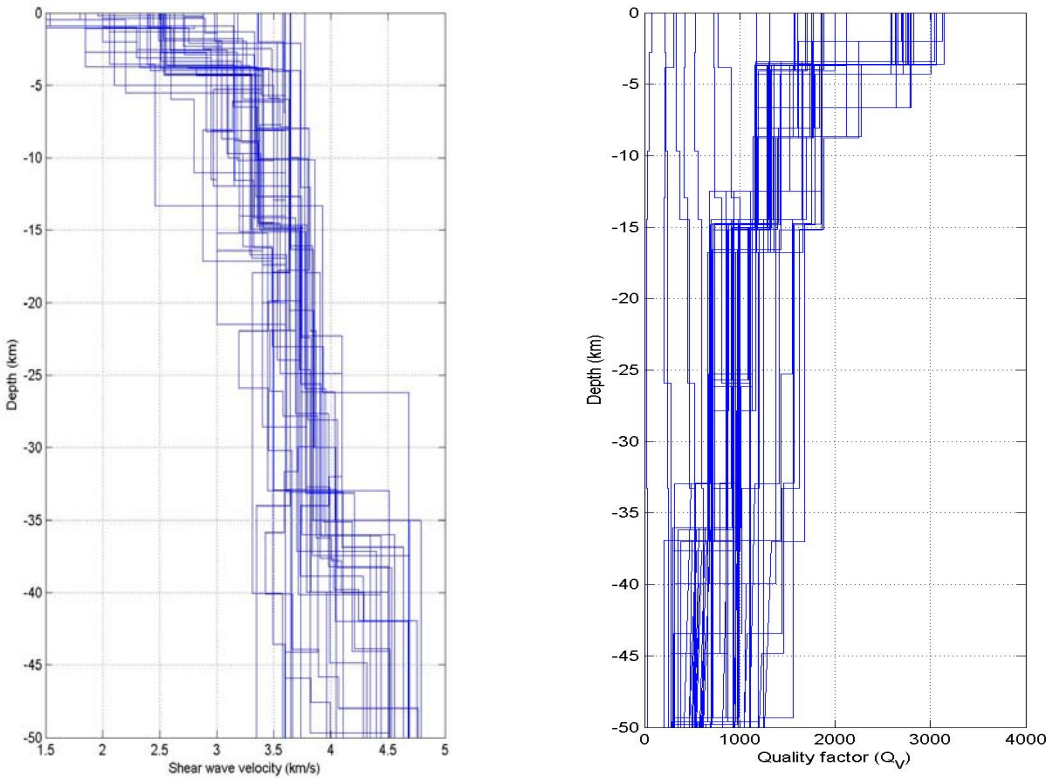

Figure 4.4 Sample Shear Wave Velocity Profiles at A-type Sites

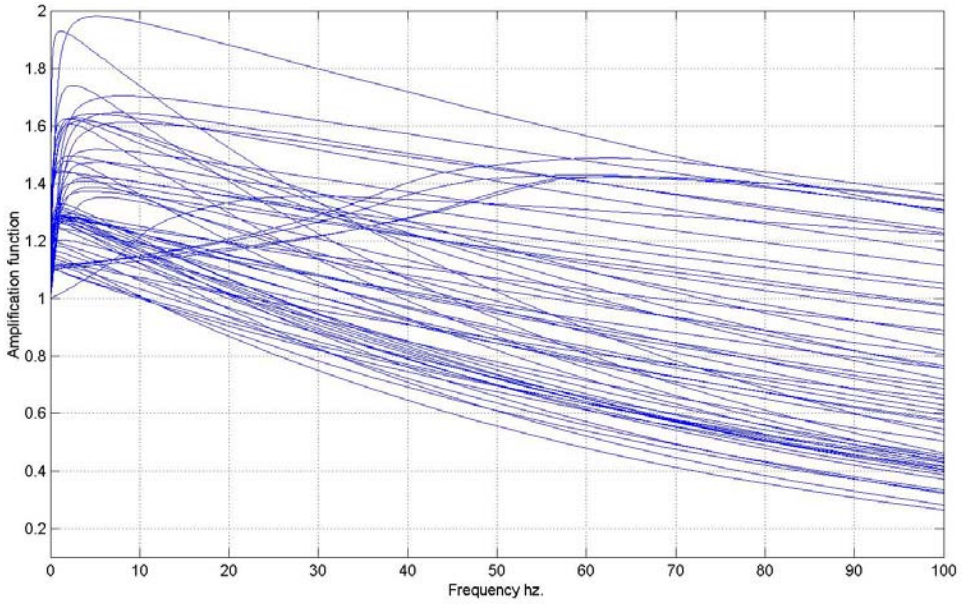

Fig. 4.5 Sample Amplification Functions at A-type Sites

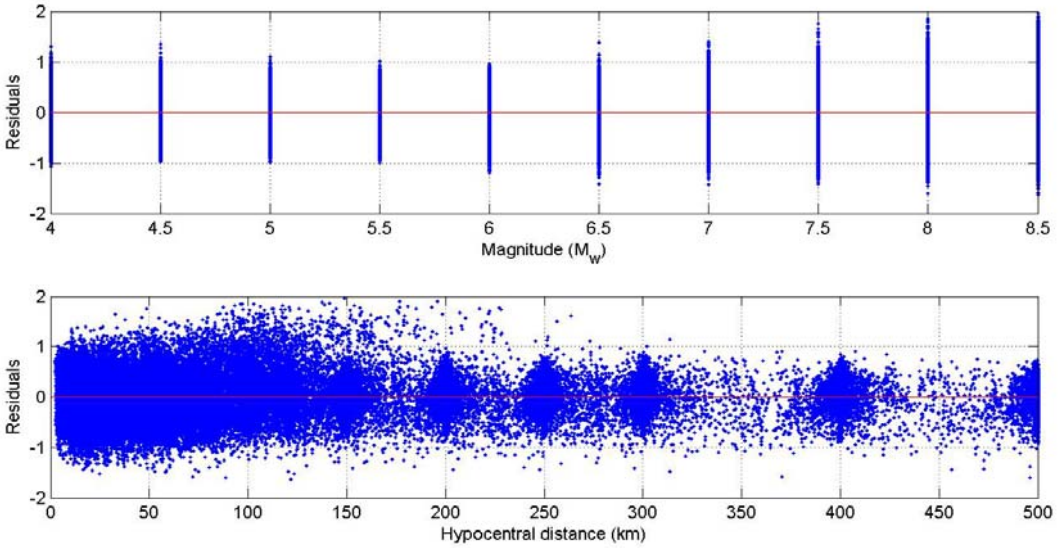

Figure 4.6 Residual *vs* M_w
Residual *vs* Hypo-central Distance (Himalayan Region)
Residual = [log (simulated PGA) - log (PGA of eq. 4.18)]

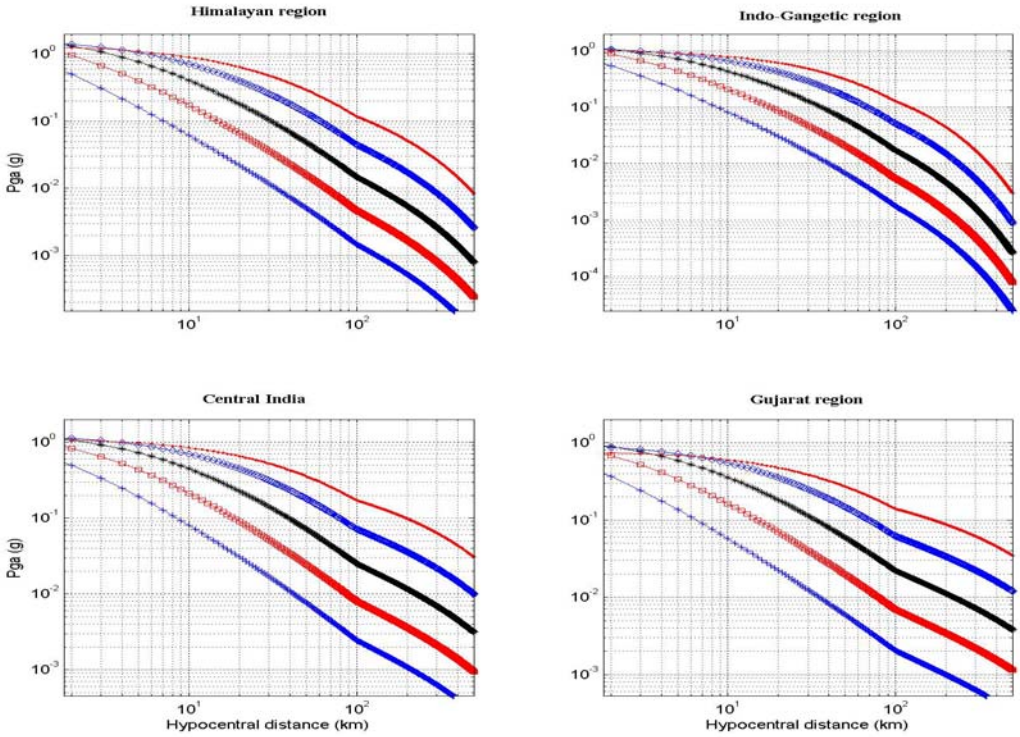

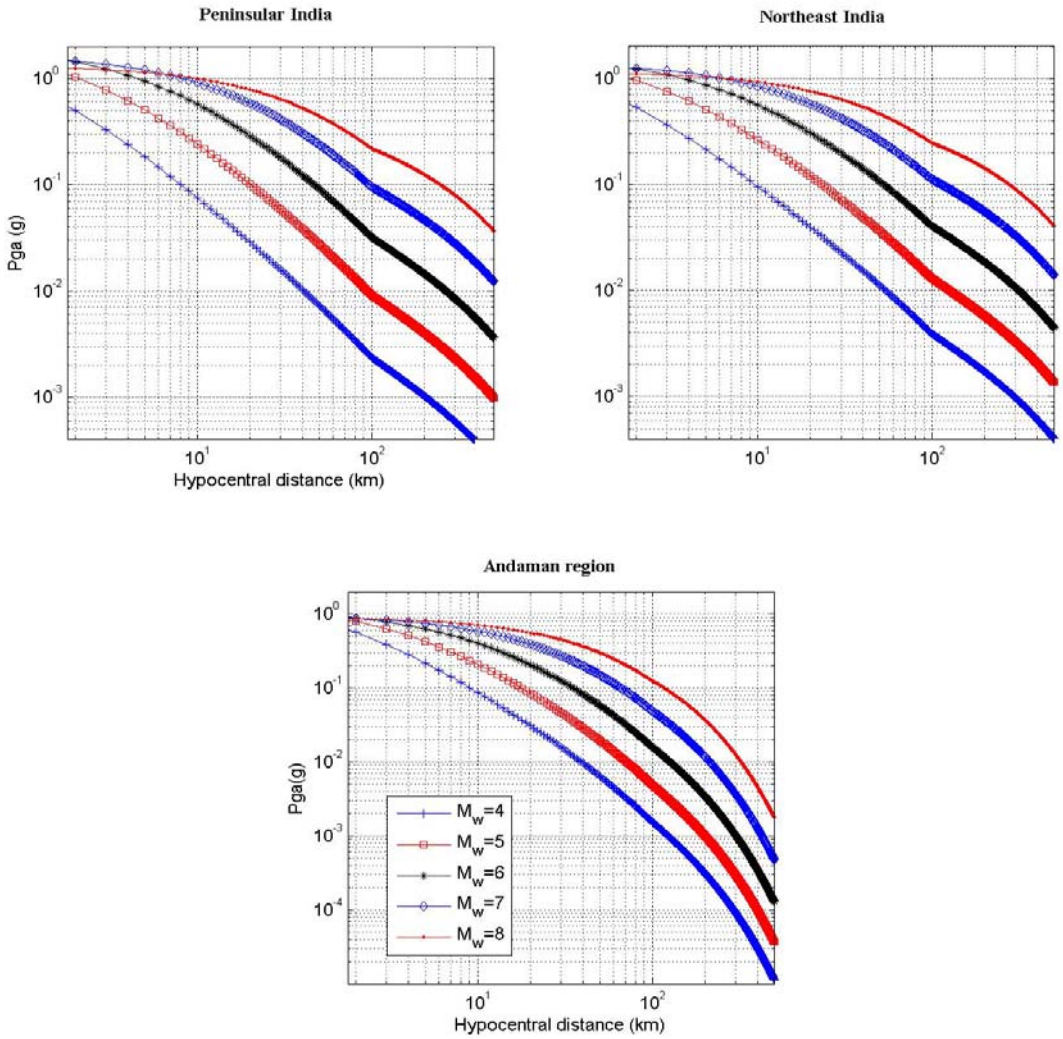

Fig. 4.7 Attenuation of PGA (g) with Hypocentral Distance at Type-A rock level

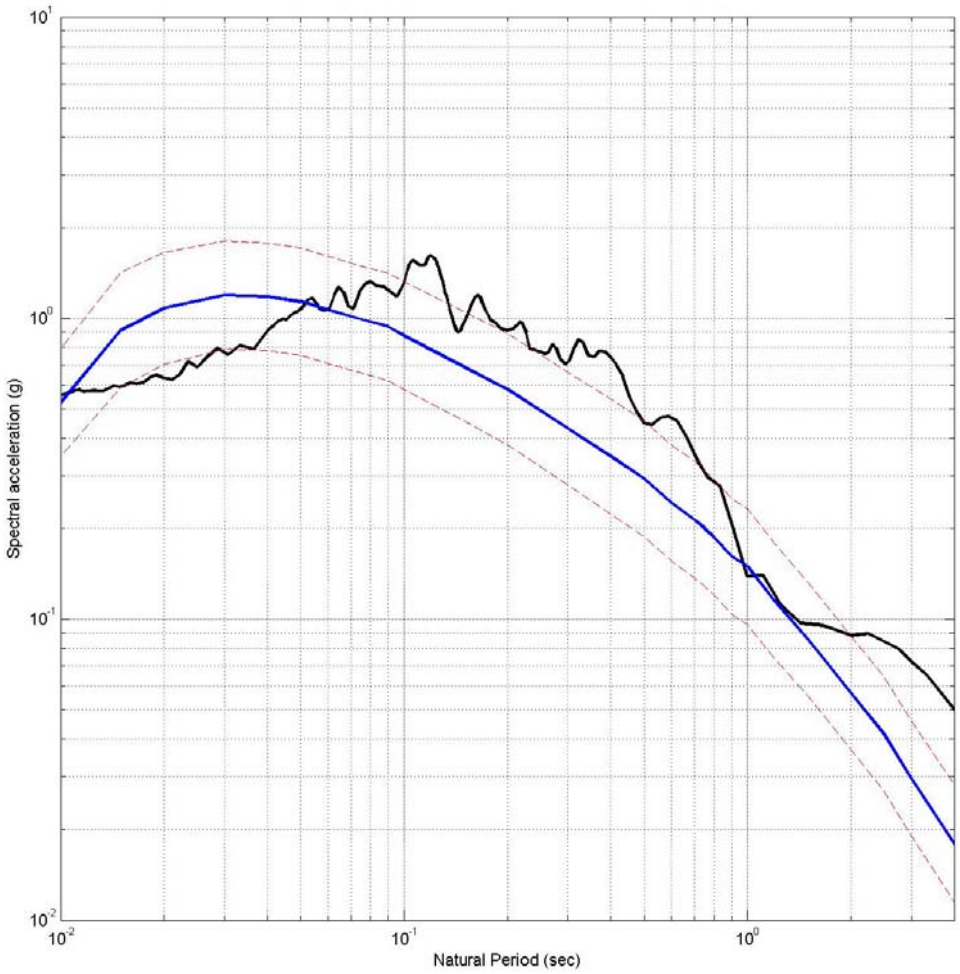

Fig. 4.8 Comparison between estimated response spectra and computed spectra from recorded strong motion data of the Koyna earthquake of 11 December 1967. (M_w = 6.5, hypocentral distance = 16 km, damping = 5%). Mean and ± sigma bands are shown.

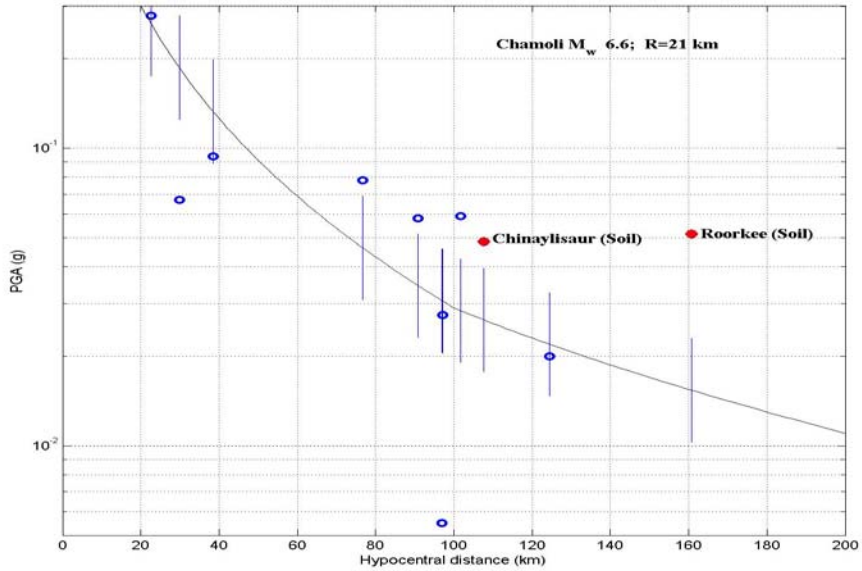

Fig. 4.9. Attenuation in the Himalayan region**.** Comparison between empirical estimates and recorded PGA data of Chamoli earthquake of 29th October 1999 (M_w 6.6). Vertical bands indicate ± sigma width about the mean value.

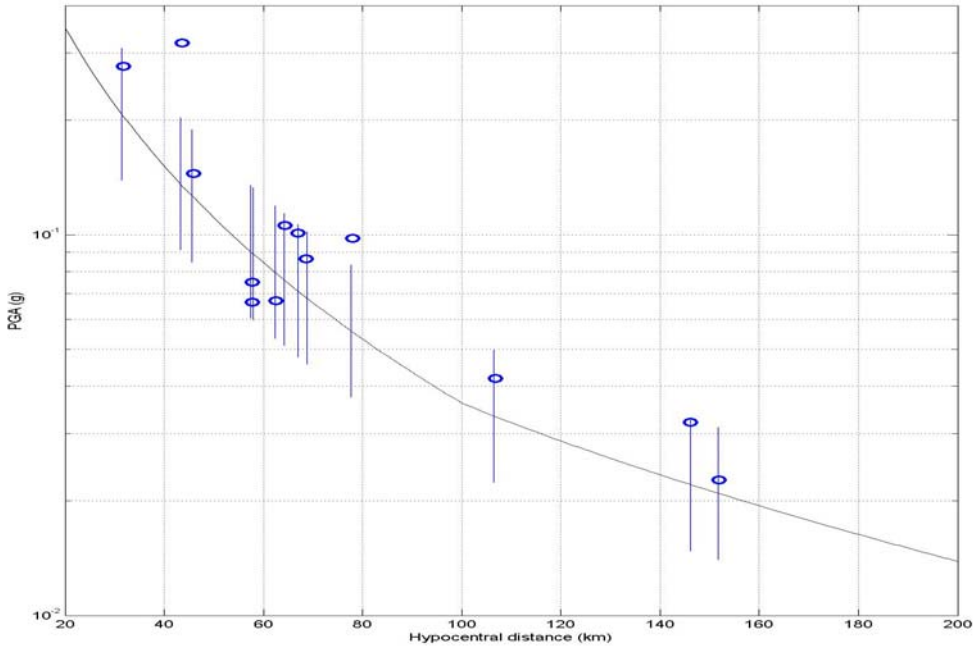

Fig. 4.10 Attenuation in the Himalayan region**.** Comparison between empirical estimates and recorded PGA data of the Uttarkashi earthquake (20th October 1991; M_w 6.8)

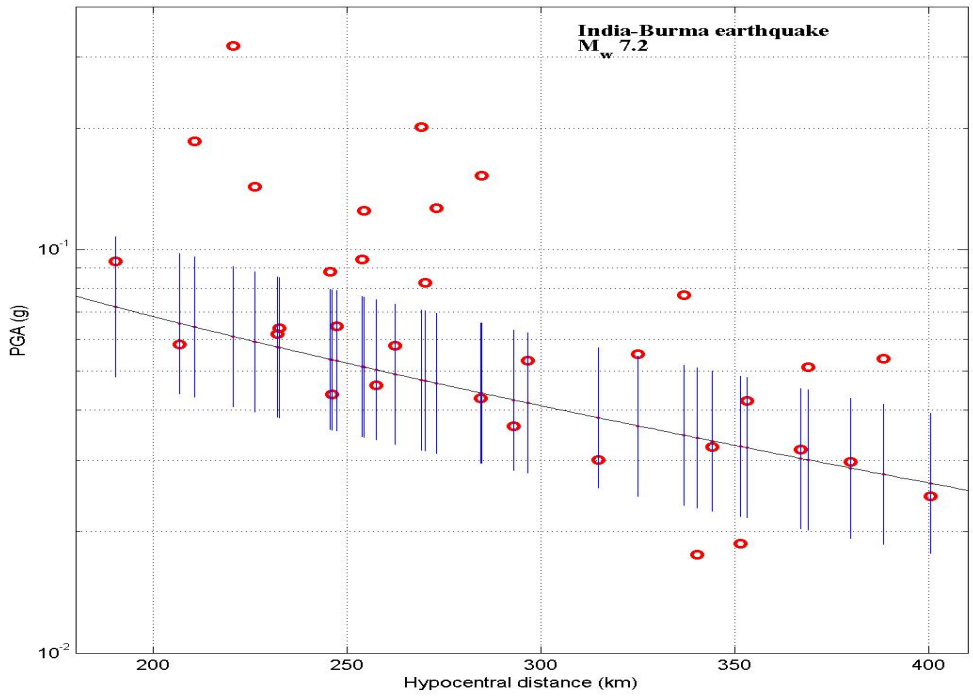

Fig. 4.11. Attenuation in North East India**.** Comparison between empirical estimates and recorded PGA data of **the** Indo-Burma earthquake (6^{th} August 1988; M_w 7.2)

Chapter 5

MAPPING THE SEISMIC HAZARD

5.1 Introduction

Characterization of the seismic source zones was presented in Chapters 2 and 3. In Chapter 4 effects of the path on ground vibration as the waves pass from the source to the site was studied. Now, it remains to link the assembled results together to arrive at the ground motion probabilities at every corner of the 0.2^0 x 0.2^0 grid that covers the whole country. Any site gets affected by events occurring within a radius of influence of 300 km (500 km near the Himalayas). Within this circle of influence, normally there will be several faults that can give rise to earthquakes of differing strength. As we have seen in Chapter 2 the faults are essentially in the demarcated 32 source zones of varying seismicity. This fact introduces two uncertain factors namely, the seismicity of the individual causative faults and the hypocentral distance to the site which sensitively depends on the geometry and orientation of the faults within the source zones. Similar to the recurrence relation for the source zones, one can ask for the G-R relation or (a, b) value for every fault in a source zone. However, this information is not available since accurate and acceptable slip rates for the faults are unknown. This gap in our knowledge is unlikely to be filled up in the near future even for well marked active faults. Hence, it is important to circumvent this difficulty in a reasonable way even if the arguments were to be heuristic (Iyengar and Ghosh 2004).

5.2 Fault Deaggregation

Let the number of earthquakes per year with $m > m_0$ in a given source zone consisting of n number of faults be denoted as $N(m_0)$. Since all these events are associated with the faults within the zone, it follows $N(m_0)= \sum N_s(m_0)$ where $N_s(m_0)$ stands for the annual frequency of event $(m > m_0)$ on the s-th fault (s=1,2,3,…n). This conservation property ca be heuristically used to develop G-R relations for each fault in the source zone. Here we take ($m_0 = 4$) for further work. The number of events $N_s(m_0)$ that can occur on a given fault depends on a variety of factors, the most important being the potential of the fault to break depending on its length and known past activity. This argument just reiterates that a long fault is capable of breaking into more number of smaller sections. At the same time a shorter fault might be more active contributing to more small magnitude events in the catalogue. Thus two parameters namely the fault length L_s and the number of past events n_s associated with the s-th fault have to be used as weights for finding $N_s(m_0)$. If N_z number of events is available in the zonal catalogue we get two weights for each fault within the zone as,

$$\alpha_s = L_s / \sum L_s \text{ and } \delta_s = n_s / N_z \qquad (5.1)$$

Taking the mean of the above two factors as indicating the seismic activity of the s-th fault in the zone we get

$$N_s(m_0) = 0.5\ (\alpha_s + \delta_s)\ N(m_0) \qquad (5.2)$$

as the *a*-value in the G-R relation of the *s*-th fault. The *b*-value for all the faults is taken to be constant equal to the zonal *b*-value already computed in Chapter 3. A further constraint appears in the form of the maximum possible magnitude m_u that can be foreseen on a given fault, depending on its length. This has to be less than the zonal potential but can be higher than the past magnitudes associated with the particular fault. Here it is taken to be half unit more than the past maximum magnitude. In the absence of past activity m_u is estimated depending on the length of the fault using the empirical relation proposed by Wells and Coppersmith (1994). As a typical example of the above approach the source zone 27 of Fig. 5.1 which mainly represents the Gujarat region is considered. This region consists of 23 faults with 138 past events in the catalogue. Already it has been found that $b = 0.87$; $N(m_0) = 1.31$ and $M_{max} = 8.0$. All the past events are apportioned to the 23 faults such that the $N(m_0)$ value is conserved as explained above. The resulting parameters for the individual faults are listed in Table 5.1. Similar to the above table fault deaggregation has been carried out for all the 32 source zones to cover the Indian land mass.

5.3 Probabilistic Seismic Hazard Analysis (PSHA)

The above characterization of all the faults in the 32 source zones forms the source data base for further work. We have developed in Chapter 4 the path characters quantified in terms of the attenuation relations for the seven regions corresponding to A-type site condition. With the help of the source and the path database we are now in a position to carry out PSHA for any grid point in Fig. 5.3. The procedure for carrying out PSHA is well known. The uncertainty in the magnitude of a future event is represented as an exponential random variable

$$p_M(m) = \frac{\beta e^{-\beta(m-m_0)}}{1-\beta e^{-\beta(m_u-m_0)}}; \quad (\mathrm{m}_0 \le \mathrm{m} \le \mathrm{m}_\mathrm{u}),\ \beta = 2.303\,\mathrm{b} \tag{5.3}$$

The other unknown factor is the distance *R* of the site to the future hypocenter The conditional probability distribution function of R, given that magnitude $M = m$ for a rupture segment uniformly distributed along a fault can be numerically computed following the method of Der Kiureghian and Ang (1977) . Referring to Fig.5.2 we have

$$\begin{aligned}
&P(R < r \mid M = m) = 0 \quad for\ R < \left(D^2 + L_o^2\right)^{1/2} \\
&P(R < r \mid M = m) = \frac{\left(r^2 - D^2\right)^{1/2} - L_o}{L - X(m)} \\
&\qquad for \left(D^2 + L_o^2\right)^{1/2} \le R < \left\{D^2 + \left[L + L_o - X(m)\right]^2\right\}^{1/2} \\
&P(R < r \mid M = m) = 1 \quad for\ R > \left\{D^2 + \left[L + L_o - X(m)\right]^2\right\}^{1/2}
\end{aligned} \tag{5.4}$$

The rupture length, $X(m)$, for an event of magnitude *m*, is given by

$$X(m) = MIN\left[10^{(-2.44+0.59m)}, fault\ length\right]$$

Probabilistic seismic hazard analysis estimates the probability of exceedance of spectral acceleration S_a at a site due to all possible future earthquakes as visualized by the previous hazard scenario. Assuming that the number of earthquakes occurring on a fault follows a stationary Poisson process, the probability that the control variable Y exceeds level y^*, in a time window of T years is given by

$$P(Y > y^* \text{ in T years }) = 1-\exp(-\mu_{y^*} T) \tag{5.5}$$

The rate of exceedance, μ_{y^*} is computed from the expression

$$\mu_{y^*} = \sum_{i=1}^{K} N_i(m_0) \int_m \int_r P(Y > y^* | m,r) p_{R|M}(r|m) p_M(m) \; dr dm \tag{5.6}$$

Here, κ is the total number of faults in the zone, $p_M(m)$ and $p_{R|M}(r|m)$ are the probability density functions of magnitude and hypocentral distance respectively. $P(Y>y^*|m, r)$ is the conditional probability of exceedance of the ground motion parameter Y. This is found as a lognormal random variable with mean value given by the attenuation equation conditioned on particular m and r values. The standard deviation of this variable is given by the standard error of the equation. These results have been presented in Chapter 4 for Indian regions. The reciprocal of the annual probability of exceedance gives the return period for the corresponding ground motion value. There will be sites which get affected by events originating in different zones and waves passing through regions with different quality factors. These variations have been handled through a suitably written computer program which incorporates all faults and regions around a site.

5.4 Comparison with Previous Results

Previously, Seeber *et al* (1999) have worked out PSHA map corresponding to B-C type sites having V_{30} in the range 1500-300 m/sec for the State of Maharashtra including Mumbai City. Raghukanth and Iyengar (2006) independently carried out PSHA for the city of Mumbai and arrived at results comparable to the values reported by Seeber *et al*. (1999). Hence it would be worthwhile to see how the present PSHA results compare with the values available in the literature. The seismic influence region for the grid point corresponding to Mumbai City is shown in Fig. 5.3. The ground motion at Mumbai can be caused by an event occurring in any of the four source zones 16, 19, 20 and 27. The probable causative faults and their important characters are shown in Table 5.2. In Table 5.3 the PGA and S_a results obtained from the present study are compared with the reported values of Raghukanth and Iyengar (2006). The present results and the previous estimates are in harmony when we keep in mind the differences in point source and finite source attenuation considered. It is generally expected finite source ground motion relations would show lower PGA values close to the fault.

Among the recent works of PSHA the results of Jaiswal and Sinha (2006) are notable. They followed the zoneless approach with logic tree incorporating the point source attenuation of central eastern united states (Toro et al 1997;Atkinson and Boore 1995) and Iyengar and Raghukanth (2004). They report higher acceleration values than what has been obtained in this report. For PI, Central India and Gujarat the range of PGA is in

between 0-0.36g, 0-0.2 and 0-0.36g respectively. Since the site condition used by them is not strictly as A-type and use of point source attenuation relation, it is possible that they have got a higher hazard value.

5.5 All India PSHA Maps

Probabilistic seismic hazard analysis for PGA, and spectral accelerations corresponding to periods 0.5 and 1.25 seconds has been carried out for all the grid points spread over the Indian land mass. The final results valid for A-type sites are presented as contour maps for return periods 475 (~500), and 2475 (~2500) years. These are shown in Figures 5.4-5.11. For developing design response spectrum as per the International Building Code IBC-2009, one needs spectral acceleration values at 0.2-second and 1-second periods corresponding to 2500 year return period. These results are shown in Figures 5.12 and 5.13 respectively. The PGA values at 48 important cities in India are also reported in Table 5.4 for two return periods.

Table 5.1 Zone 27 (b, = 0.87; $N(m_0)$,=1.31 and M_{max} = 8.0)

Fault number	Fault length (km)	No. of past seismic events associated with the fault	m_u	α_S	δ_S	$N_S(m_0)$
98	15.33	3	8.0	0.0055	0.0217	0.0178
106	205.52	11	6.1	0.0736	0.0797	0.1004
107	209.27	44	8.0	0.0750	0.3188	0.2579
108	47.12	7	7	0.0169	0.0507	0.0443
109	78.47	1	4.9	0.0281	0.0072	0.0232
110	168.58	1	5.5	0.0604	0.0072	0.0443
111	422.09	3	6.7	0.1512	0.0217	0.1133
144	144.51	4	6.1	0.0518	0.0290	0.0529
334	16.54	0	6.7	0.0059	0	0.0039
414	29.64	0	7.1	0.0106	0	0.0070
415	19.74	4	6.2	0.0071	0.0290	0.0236
416	113.75	3	5.6	0.0407	0.0217	0.0409
417	26.57	0	7.0	0.0095	0	0.0062
418	37.95	2	4.6	0.0136	0.0145	0.0184
420	25.82	0	6.98	0.0093	0	0.0061
699	40.87	0	7.28	0.0146	0	0.0096
700	293.26	5	4.7	0.1050	0.0362	0.0925
753	60.09	5	6.2	0.0215	0.0362	0.0378
754	188.19	1	4.9	0.0674	0.0072	0.0489
759	311.71	13	6.5	0.1116	0.0942	0.1348
780	41.49	3	5.5	0.0149	0.0217	0.0240
781	184.03	1	4.7	0.0659	0.0072	0.0479
782	111.33	27	6.3	0.0399	0.1957	0.1543

Table 5.2 Fault characteristics for grid point Mumbai

Fault No.	Fault Name	Source zone	b	$N_s(m_o)$	M_{max}
34	Upper Godavari fault	29	1.19	4.86E-02	6.8
35	West Coast fault	20	0.76	3.49E-02	5.9
36	Chiplun fault - south	20	0.76	1.23E-02	6.8
792	Chiplun fault - north	20	0.76	8.13E-02	6.2
38	Warna fault	29	1.19	2.41E-02	6
93	Tapti North fault	16	0.64	3.17E-02	5.4
110	Kim fault	27	0.87	4.48E-02	5.5
416	Neotectonic fault	27	0.87	4.13E-02	5.6
423	Neotectonic fault	20	0.76	4.63E-03	5.8
520	Fault involving basement and cover	20	0.76	3.81E-03	5.2
521	Neotectonic fault	29	1.19	1.38E-02	5
522	Fault involving basement and cover	20	0.76	4.45E-03	6.5
718	Fault involving cover	20	0.76	5.65E-03	6.8
719	Fault involving cover	20	0.76	1.11E-02	6.5
720	Fault involving cover	20	0.76	1.34E-02	4.6
721	Fault involving basement and cover	20	0.76	9.37E-04	6.8
722	Fault involving basement and cover	20	0.76	1.23E-02	5.3
723	Fault involving basement and cover	20	0.76	1.49E-02	7
727	Fault involving cover	29	1.19	8.45E-04	6.8
728	Fault involving cover	20	0.76	2.76E-03	5.3
767	Fault involving basement and cover	20	0.76	3.86E-03	6.8
768	Fault involving basement and cover	20	0.76	3.65E-03	6.8
769	Neotectonic fault	20	0.76	3.83E-03	6.2
770	Panvel flexure	20	0.76	3.51E-03	6.8
786	Fault involving cover	16	0.64	1.06E-03	6.8

Table 5.3 Comparison of spectral acceleration at Type A level for Mumbai city

Mean return period	ZPA (g)	
	Raghukanth and Iyengar (2006)	Present Study
475 years	0.13	0.09
2475 years	0.25	0.19

Table 5.4 Relative Seismic Hazard of Indian Cities on A-type Sites in terms of PGA

No.	Agglomeration	Lat.	Long.	PGA(g) (T_R=500)	PGA(g) (T_R=2500)	PGA(g) (T_R=5000)	PGA(g) (T_R=10000)
1	Guwahati	26.17	91.77	0.23	0.37	0.42	0.51
2	Chandigarh	30.75	76.78	0.10	0.19	0.25	0.32
3	Kolkata	22.55	88.37	0.09	0.19	0.24	0.31
4	Mumbai	19.00	72.80	0.09	0.19	0.25	0.32
5	Jabalpur	23.15	79.93	0.08	0.18	0.24	0.31
6	Asansol	23.68	86.98	0.08	0.17	0.21	0.27
7	Delhi	28.62	77.22	0.08	0.17	0.22	0.29
8	Srinagar	34.08	74.78	0.08	0.16	0.21	0.26
9	Jaipur	26.92	75.82	0.07	0.16	0.17	0.28
10	Meerut	28.99	77.70	0.06	0.14	0.18	0.23
11	Agra	27.18	78.02	0.06	0.14	0.18	0.25
12	Ahmedabad	23.03	72.57	0.07	0.14	0.17	0.24
13	Vijayawada	16.51	80.61	0.07	0.13	0.15	0.21
14	Jamshedpur	22.80	86.18	0.07	0.12	0.14	0.20
15	Dhanbad	23.80	86.45	0.06	0.11	0.13	0.18
16	Pune	18.52	73.85	0.06	0.11	0.13	0.16
17	Kozhikode	11.25	75.77	0.05	0.10	0.09	0.17
18	Kolhapur	16.70	74.23	0.05	0.10	0.11	0.11
19	Rajkot	22.30	70.78	0.05	0.09	0.11	0.13
20	Vadodara	22.30	73.20	0.05	0.09	0.10	0.16
21	T'nanthapuram	8.480	76.95	0.04	0.08	0.10	0.11
22	Kochi	9.970	76.27	0.03	0.08	0.11	0.13
23	Ludhiana	30.91	75.85	0.04	0.08	0.10	0.14
24	Indore	22.42	75.54	0.04	0.08	0.10	0.12
25	Patna	25.60	85.12	0.04	0.08	0.11	0.13
26	Lucknow	26.83	80.92	0.04	0.08	0.11	0.17
27	Kanpur	26.46	80.33	0.03	0.08	0.11	0.17
28	Surat	21.23	72.78	0.04	0.08	0.09	0.14
29	Trichy	10.81	78.69	0.04	0.07	0.09	0.11
30	Ranchi	23.35	85.33	0.03	0.07	0.09	0.11
31	Allahabad	25.45	81.85	0.03	0.07	0.09	0.13
32	Amritsar	31.64	74.86	0.03	0.07	0.09	0.11
33	Coimbatore	11.04	76.96	0.04	0.07	0.09	0.11
34	Nagpur	21.15	79.08	0.04	0.07	0.09	0.10
35	Jodhpur	26.28	73.02	0.03	0.06	0.08	0.11
36	Nashir	20.00	73.78	0.03	0.06	0.08	0.10
37	Gwalior	26.14	78.10	0.02	0.05	0.07	0.10
38	Madurai	9.800	78.10	0.03	0.05	0.07	0.10
39	Varanasi	25.32	82.98	0.02	0.05	0.06	0.07
40	Bhopal	23.25	77.42	0.03	0.05	0.07	0.09
41	Hyderabad	17.37	78.48	0.02	0.05	0.06	0.07
42	Chennai	13.05	80.27	0.03	0.05	0.06	0.07
43	Solapur	17.68	75.92	0.02	0.04	0.05	0.06
44	Bhubaneswar	20.27	85.84	0.02	0.04	0.05	0.06
45	Bangalore	12.97	77.58	0.02	0.04	0.05	0.06
46	Aurangabad	19.78	75.29	0.02	0.03	0.03	0.04
47	Visakhapatnam	17.07	83.25	0.02	0.03	0.04	0.04
48	Raipur	21.23	81.63	0.01	0.02	0.02	0.03

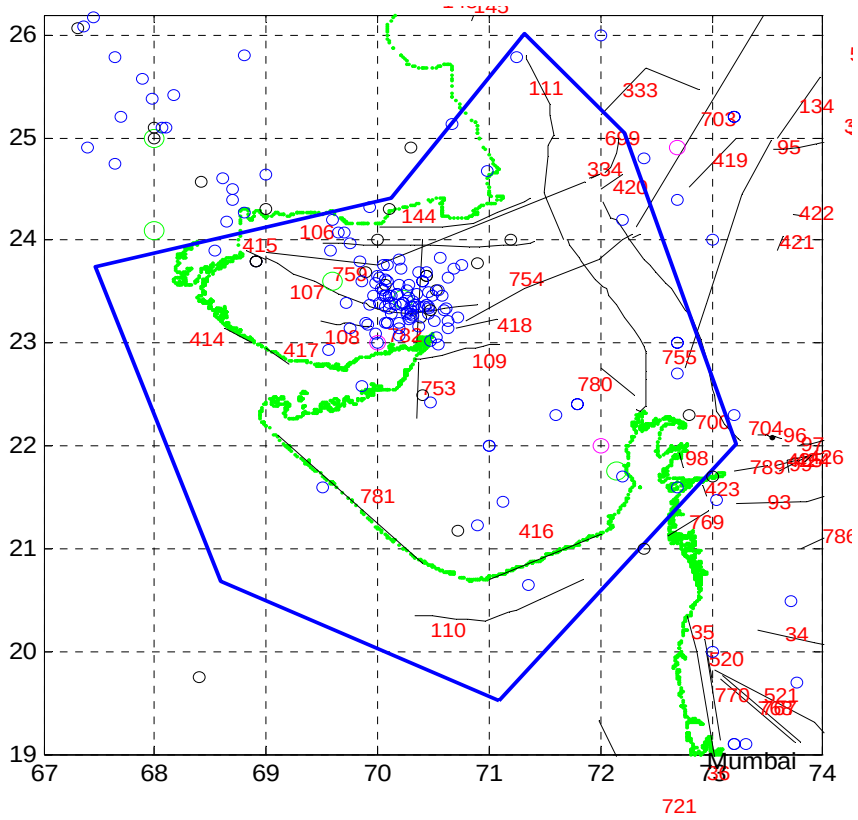

Figure 5.1 Faults and epicenters in source zone 27

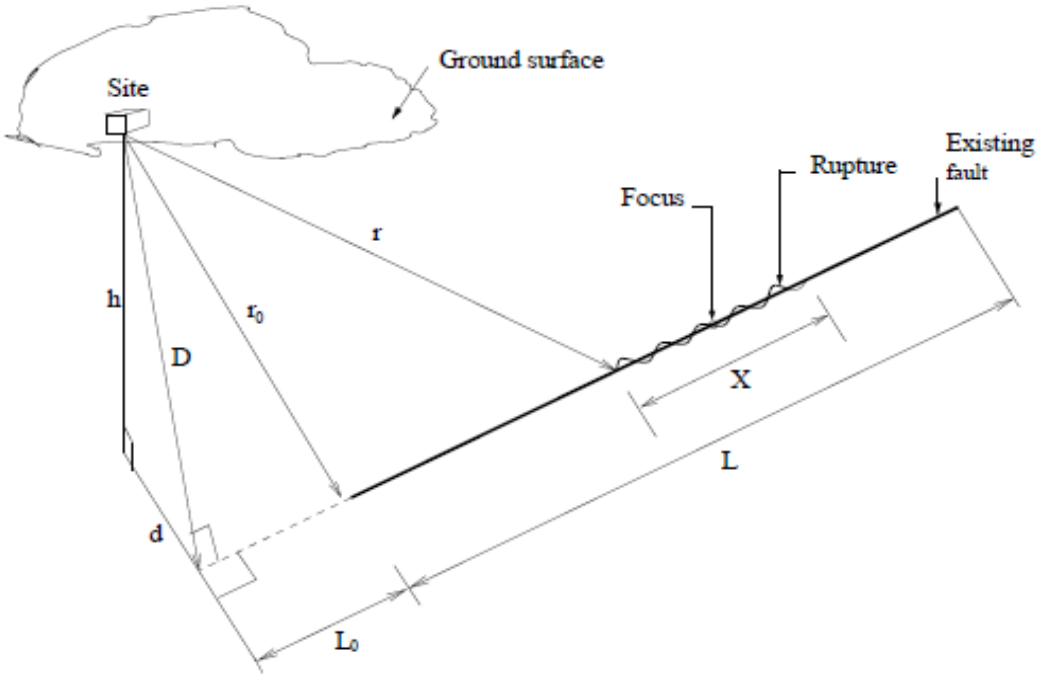

Figure 5.2 Source, Site and Path for PSHA

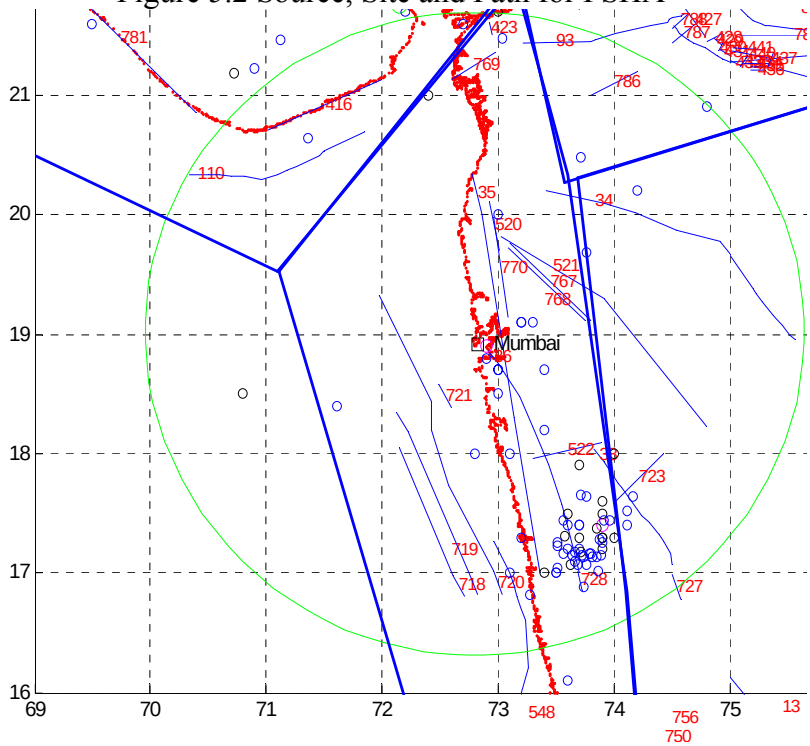

Fig 5.3. Seismic influence zone for Mumbai. Blue lines indicate the boundaries of different source zones

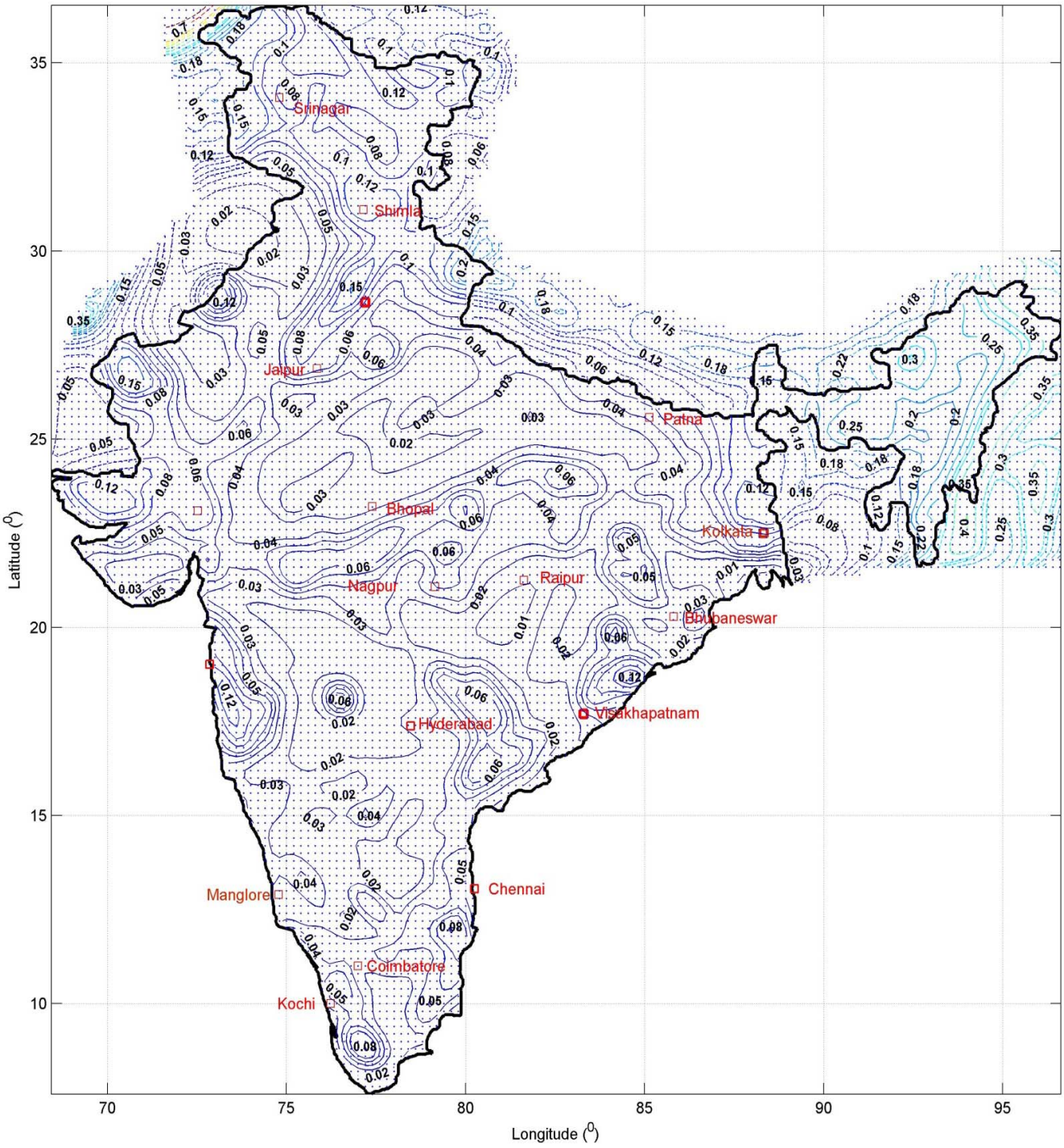

Fig 5.4 PGA Contours with 10% probability of exceedence in 50 years (Return Period ~500 years) on A-type Sites

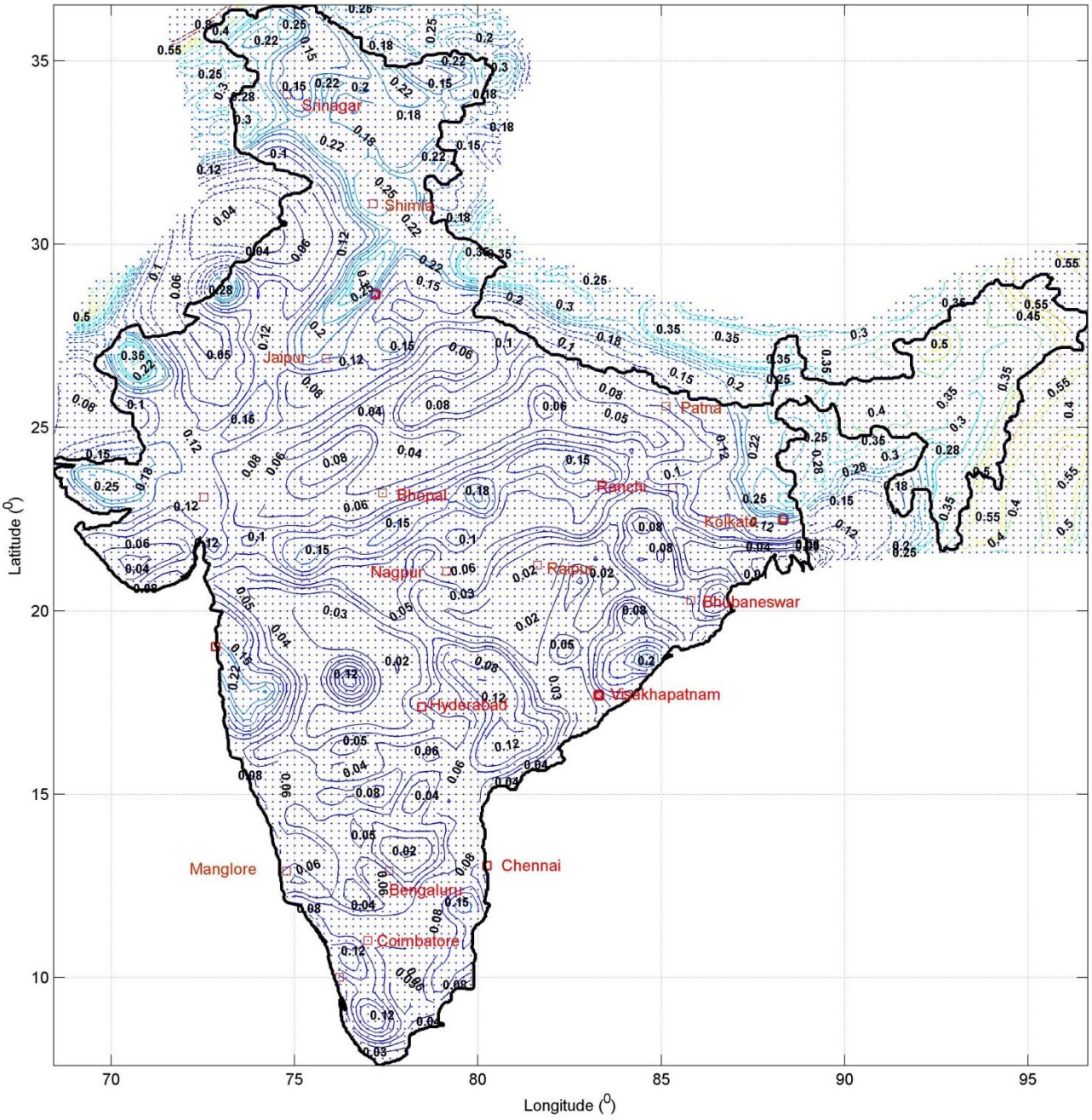

Fig 5.5 PGA Contours with 2% probability of exceedence in 50 years (Return Period ~2500 years) on A-type Sites

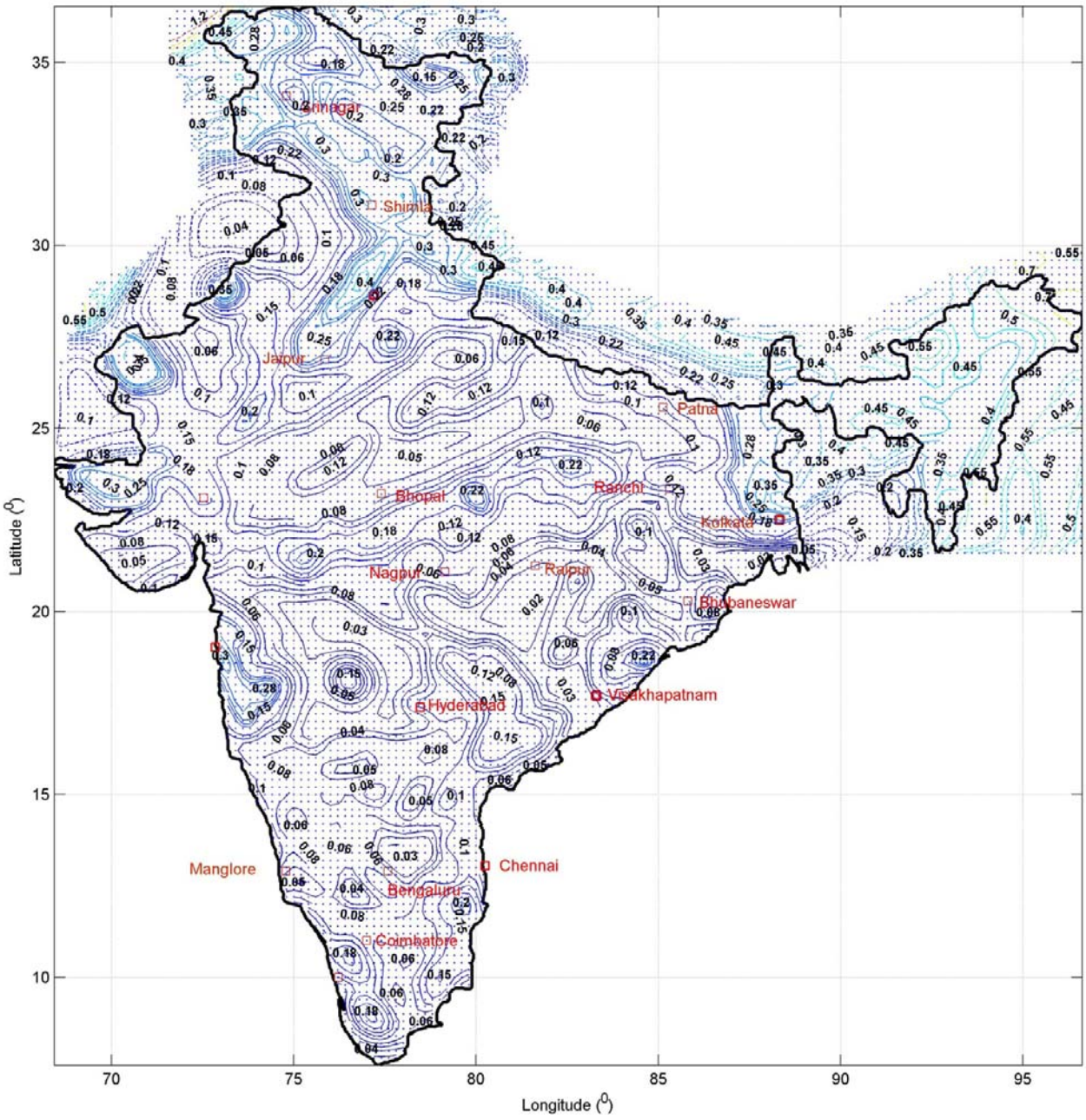

Fig 5.6 PGA Contours with Return Period of ~5000 years on A-type Sites

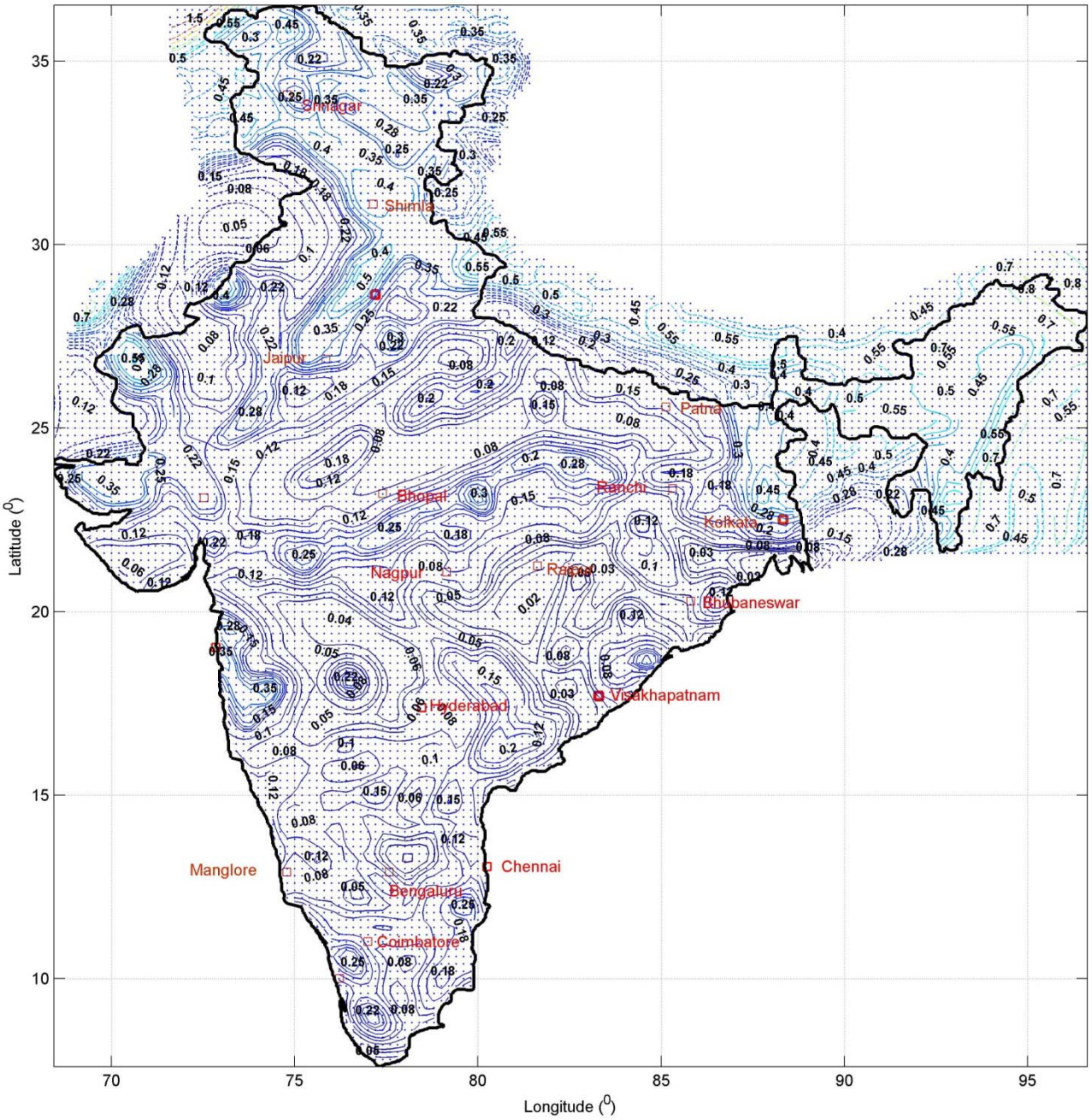

Fig 5.7 PGA Contours with Return Period of ~10,000 years on A-type Sites

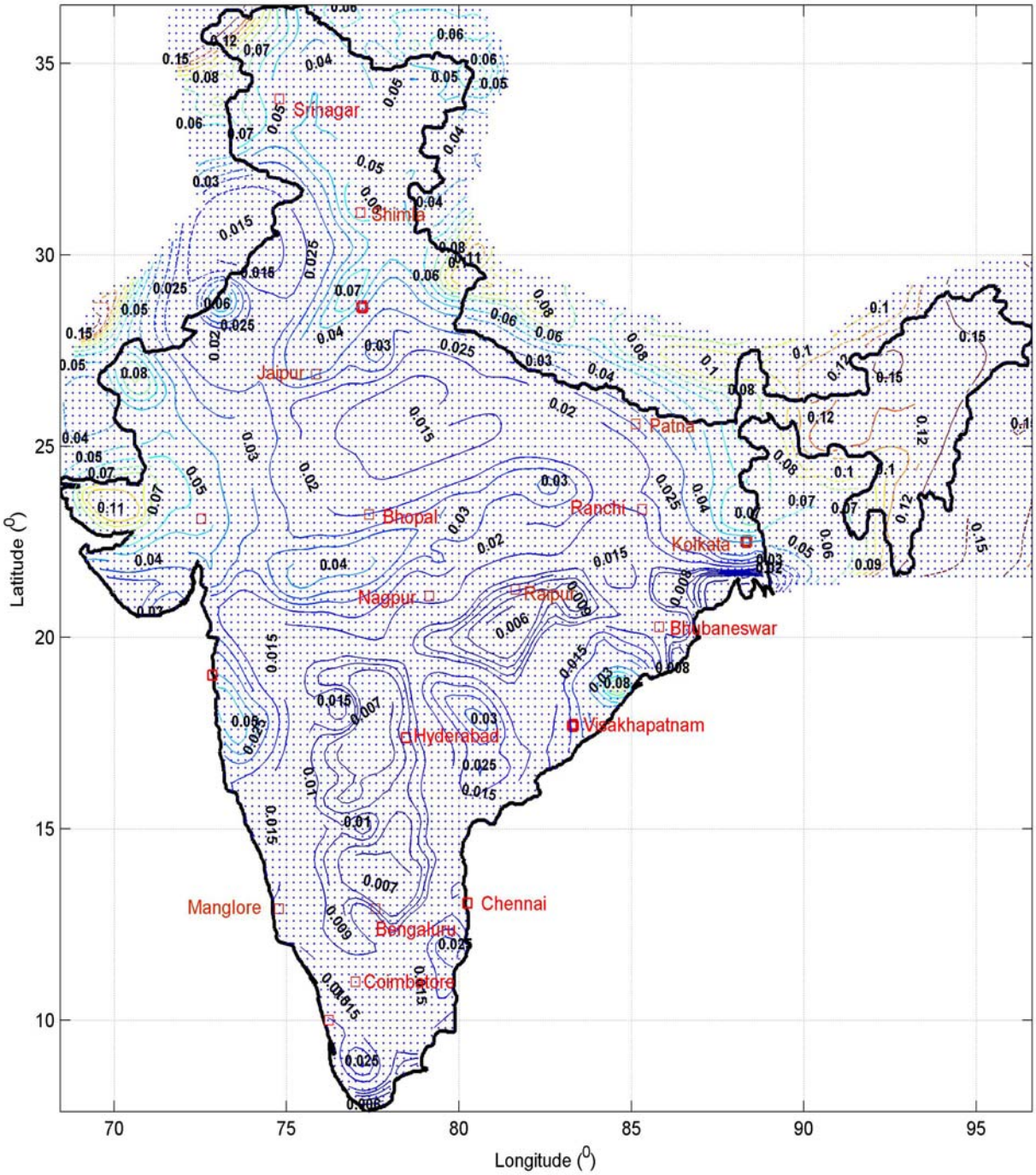

Fig. 5.8 Spectral Acceleration at T =0.5sec and 5% damping with 10% probability of Exceedence in 50 years (Return Period ~ 500 years) on A-type sites

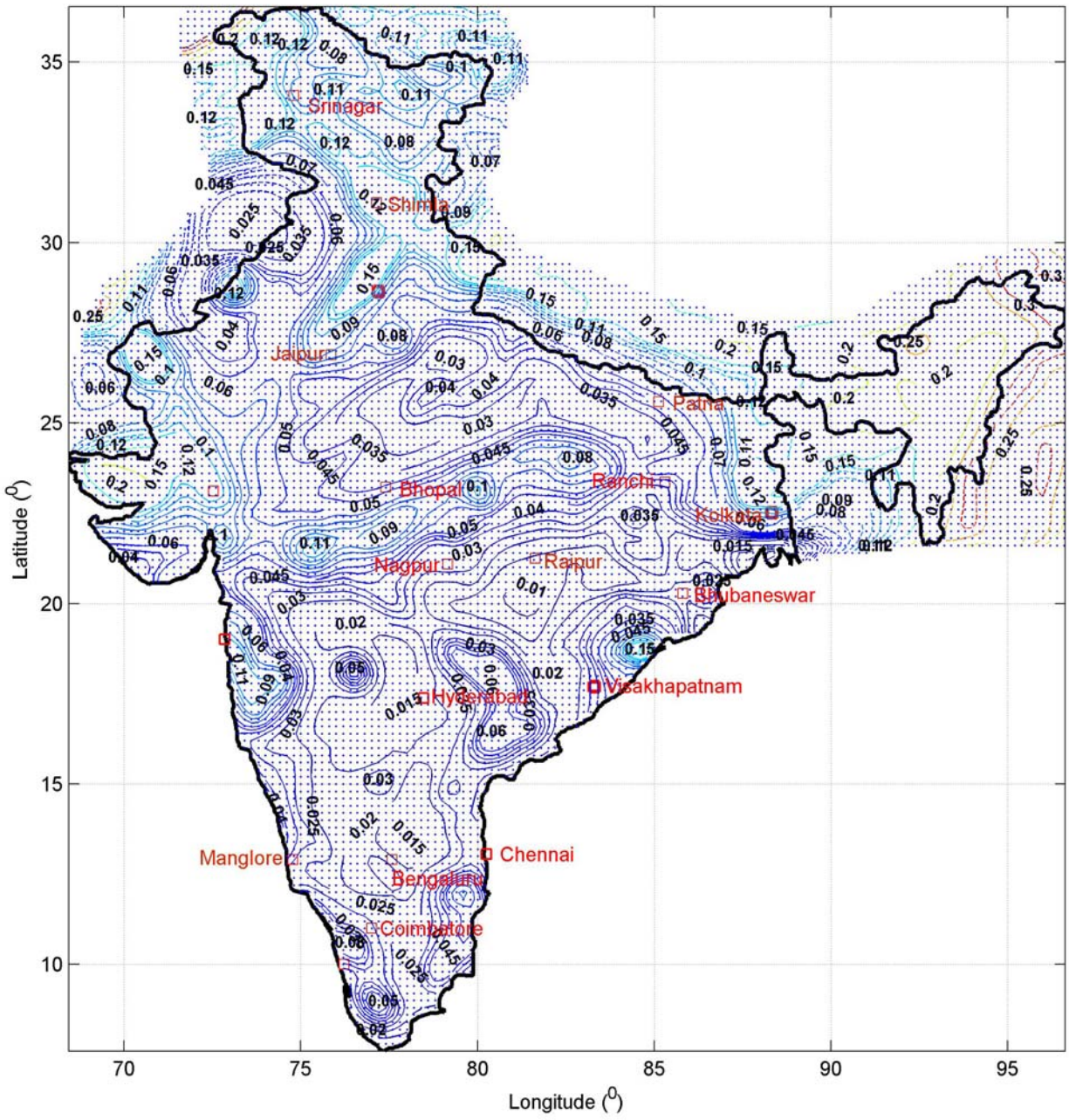

Fig. 5.9 Spectral Acceleration at T =0.5sec and 5% damping with 2% probability of exceedence in 50 years (Return Period ~2500 years) on A-type sites

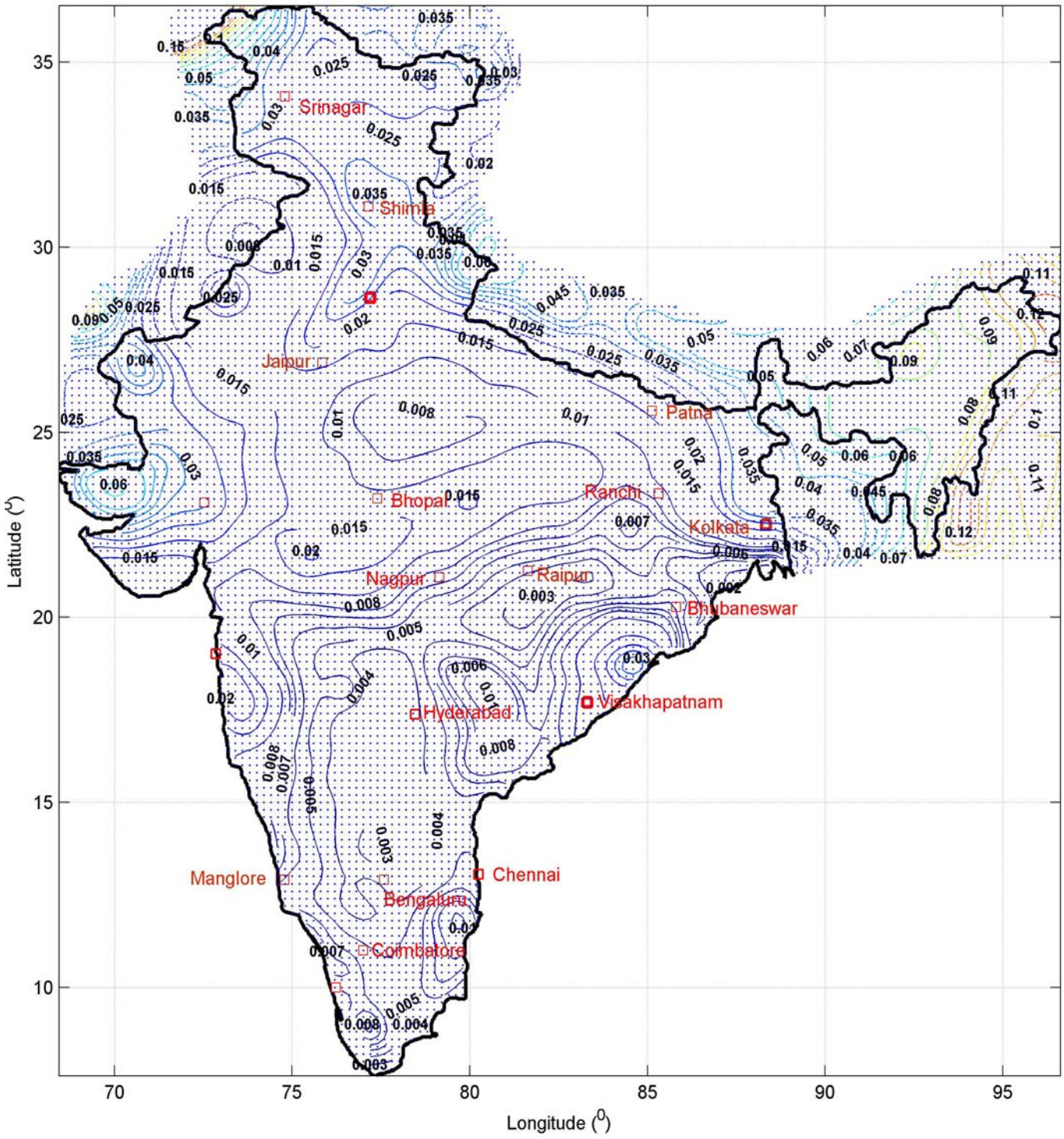

Fig. 5.10 Spectral Acceleration at T =1.25 sec and 5% damping with 10% probability of exceedence in 50 years (Return Period ~500 years) on A-type Sites

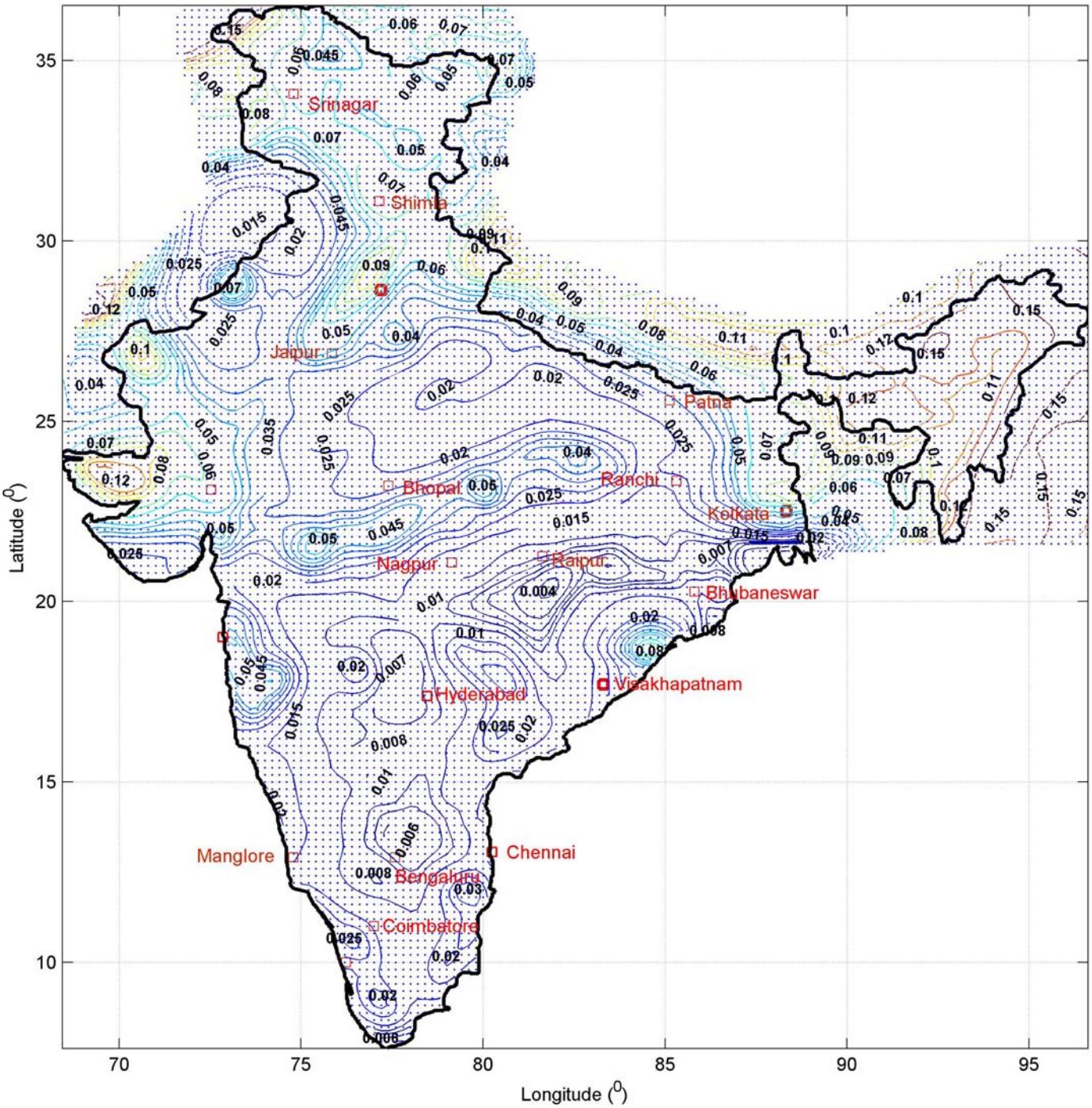

Fig. 5.11 Spectral Acceleration at T =1.25sec and 5% damping with 2% probability of exceedence in 50 years (Return Period ~2500 years) on A-type Sites

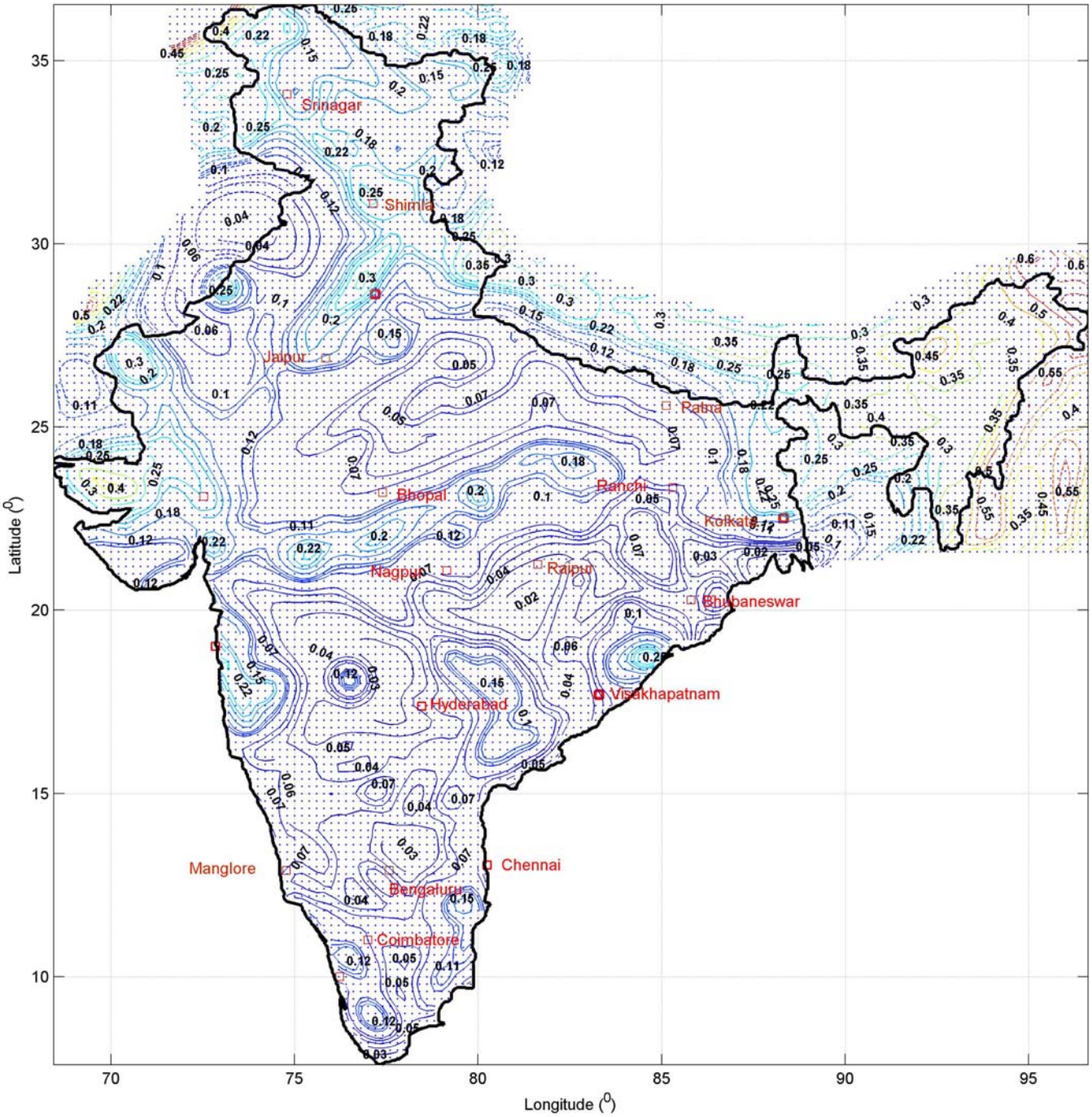

Fig. 5.12 Short Period Spectral Acceleration at T = 0.2 second with Return Period of 2500 years on A-type Sites (5% damping)

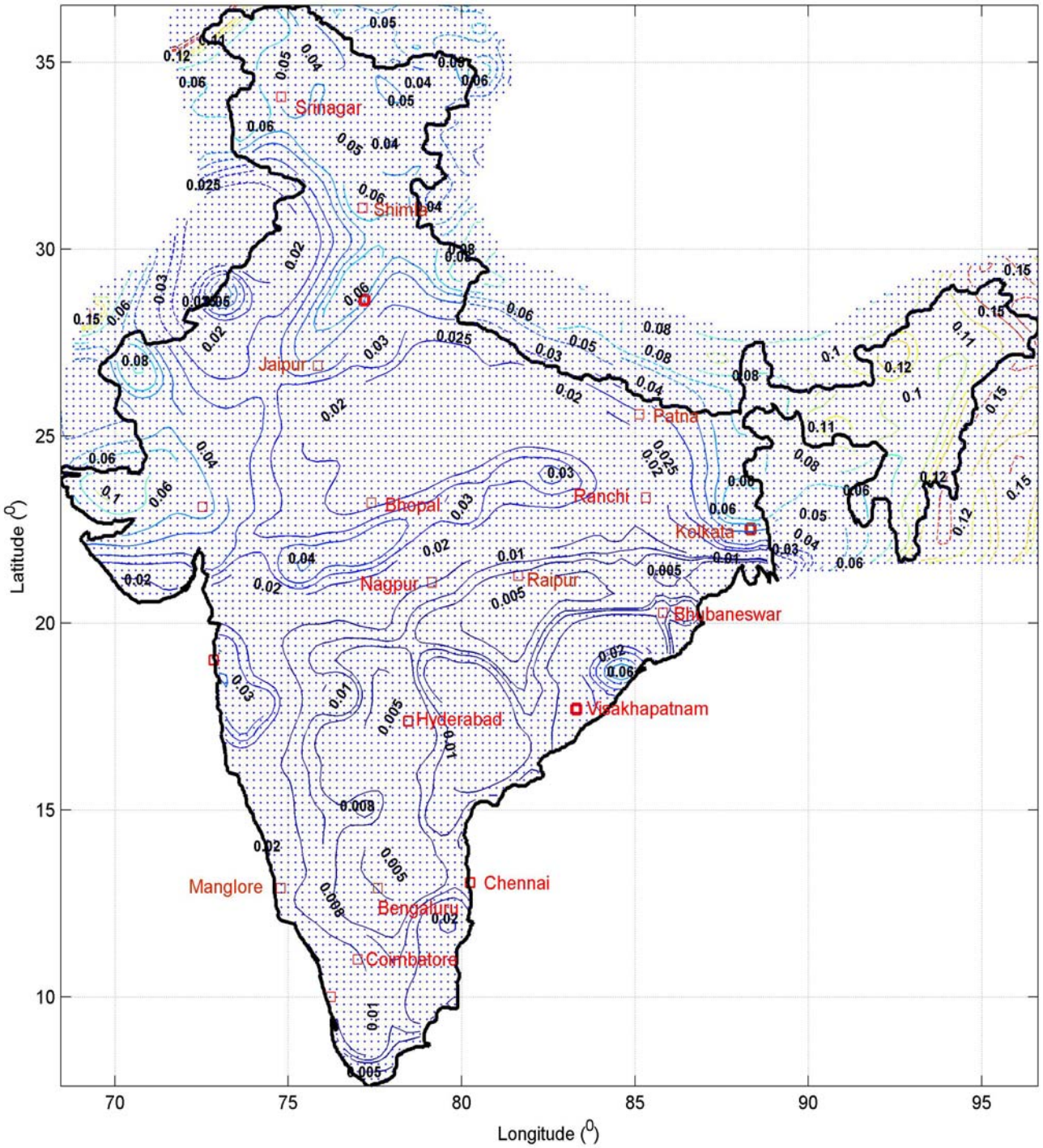

Fig. 5.13 Long Period Spectral Acceleration at T = 1 second with Return Period of 2500 years on A-type Sites (5% damping)

REFERENCES

1.Abrahamson N.A., Litcheister J.J. (1989). Attenuation of vertical peak acceleration. *Bull Seismol Soc Am* 79:549–580

2.Algermissen, S.T. and Perkins, D.M. (1976), *A probabilistic estimate of maximum acceleration in rock in the contiguous United States*, U.S. Geol. Surv. Open-file Report, 76–416, 45 pp.

3. Ambraseys, N. and Bilham, R. (2009), The tectonic setting of Bamiyan and seismicity in and near Afghanistan for the past twelve centuries. *UNESCO Special Publication:The Destruction of the Giant Buddha Statues in Bamiyan, Central Afghanistan, UNESCO's emergency activities for the recovering and rehabilitation of cliff and niches*. Ed. Claudio Margottini, ISBN 978-448-0375-5. 158 p.

4. Ambraseys, N. and Jackson, D. (2003), A note on early earthquakes in northern India and southern Tibet, *Curr. Sci.*, 84:570-582.

5.Anderson, J.G. and Trifunac, M.D. (1978), Uniform risk functionals for characterization of strong earthquake ground motion, *Bulletin of the Seismological Society of America*, 68(1):205–218.

6.Bapat, A. Kulkarni, R.C. and Guha, S.K. (1983). Catalogue of earthquakes in India and Neighborhood from historical period up to 1799. *Indian Society of Earthquakes Technology,* pp. 211.

7.Balakrishnan, T. S., Unnikrishnan, P., and Murthy, A.V.S. (2009). The tectonic map of India and contiguous areas. *Journal of Geological Society of India.* 74, 158-170.

8.Baumbach, M., Grosser, H., Schmidt, H.G., Paulat, A., Rietbrock, A., Ramakrishna Rao, C.V., Solomon Raju, P., Sarkar, D. and Mohan, I. (1994), Study of foreshocks and aftershocks of the intraplate Latur earthquake of September 30, 1993, India; In: *Latur Earthquake* (ed) H K Gupta, *Geol. Soc.India Mem.*, 35:33-63.

9.Bhatia, S.C., Kumar, M.R. and Gupta, H.K. (1999), A probabilistic seismic hazard map of India and adjoining regions, *Annali di Geofisica*, 42:1153-1166.

10.Bilham, R. (2004), Earthquakes in India and the Himalaya: tectonics, geodesy and history, *Annals of Geophysics*, 47(2):839-858.

11.Bilham, R. and Szeliga, W. (2008), Interaction between the Himalaya and the flexed Indian plate-spatial fluctuations in seismic hazard in India in the past millennium?, *2008 Seismic enginering conference commemorating the 1908 Messina and Reggio Calabria earthquake*. Santini A, Moraci N (eds) American Institute of Physics Conference Proceeding 1020(1), pp 224–231, (978-0-7354-0542-4/08).

12.Bodin, P. *et al.* (2004), Ground motion scaling in the Kachchh basin, India, deduced from aftershocks of the 2001 Mw 7.6 Bhuj earthquake, *Bulletin of the Seismological Society of America,* 94(5):1658-1669.

13.Boominathan, A. (2004). Seismic site characterization for nuclear structures and power plants. *Current Science*, 87(10), 1388–1397.

14.Boore, D.M. (1983), Stochastic simulation of high - frequency ground motions based on seismological models of the radiated spectra, *Bull. Seism. Soc. Am.*, 73:1865 – 1894.

15. Boore, D.M. (2003), Simulation of ground motion using the stochastic model, *Pure and Applied Geophysics*, 160:635 – 676.

16. Boore, D.M. (2009). Comparing stochastic point-source and finite-source ground motion simulations: SMSIM and EXSIM, *Bull. Seism. Soc. Am*. 99(6):3202-3216.

17. Boore, D.M. and Atkinson, G.M. (1987), Stochastic prediction of ground motion and spectral response parameters at hard-rock sites in Eastern North America, *Bull. Seismol. Soc. Am.*, 77:440–467.
18. Boore, D.M. and Boatwright, J. (1984), Average bodywave radiation coefficients; *Bull. Seism. Soc. Am.,* 74:1615–1621.
19. Boore, D.M., and Joyner, W.B. (1997). Site amplifications for generic rock sites, *Bull. Seism. Soc. Am.*, 87(2):327-341.
20. Brune, J.N. (1970), Tectonic stress and spectra of seismic shear waves from earthquakes, *Journal of Geophysical Research*, 75:4997 – 5009.
21. Campbell, K. W. (2003). Prediction of strong ground motion using the hybrid empirical method in Eastern North America. *Bull. Seism. Soc. Am.*, 93,1012-1033.
22. Chandra, U (1977). Earthquakes of Peninsular India - A seismotectonic study *Bull. Seism. Soc. Am* 67:5, 1387-1413.
23. Chandra, U. (1978), Seismicity, earthquake mechanisms and tectonics along the Himalayan mountain range and vicinity, *Phys. Earth Planet. Inter*., 16:109-131.
24. Chandra, U. (1992), Seismotectonics of Himalaya, *Current Science*, 62 (1–2), 40–71.
25. Chandrasekaran, A.R. and Das, J.D. (1992), Strong motion arrays in India and analysis of data from Shillong array, *Current Sci.*, 62:233-250.
26. Chen, W.-P. and Molnar, P. (1990), Source parameters of earthquakes and intraplate deformation beneath the Shillong Plateau and northern Indoburman Ranges, *J. Geophys. Res.*, 95:12527-12552.
27. Cornell, C.A. (1968), Engineering seismic risk analysis, *Bulletin of Seismological Society of America*, 58, 1583-1606.
28. Cornell, C.A. (1970), Probabilistic analysis of damage to structures under seismic loads. In *Dynamic Waves in Civil Engineering*, Chapter 27, Howells DA, Haigh IP
29. Taylor C (eds). Wiley-Interscience: New York, 1970; *Proceedings of Conference on Earthquake and Civil Engineering Dynamics*, University College at Swansea, 7–9 July 1970.
30. Cornell, C.A. and Merz, H.A. (1974). Seismic risk analysis of Boston, *Journal of Structural Division, ASCE*, 101, 2027-2043.
31. Cornell, C.A. and Vanmarcke, E.H. (1969), The major influences on seismic risk, *Proceedings of the Fourth World Conference on Earthquake Engineering*, Santiago, Chile, Vol. A-1, pp. 69–93.
32. Curray, J.R., Moore, D.G., Lawver, L.A., Emmel, F.J., Raitt, R.W., Henry, M. and Kieckhefer, R. (1979), Tectonics of the Andaman Sea and Burma, in Watkins J.S., Montadert L. and Dickenson P.,(ed.) *Geological and Geophysical Investigations of Continental Margins*, American Association of Petrochemical Geology Memoir 29, 189–198.
33. Das, S., Gupta, I.D. and Gupta, V.K. (2006), A probabilistic seismic hazard analysis of Northeast India, *Earthquake Spectra*, 22(1):1-27.
34. Der Kiureghian, A. and Ang, A. H.-S. (1977), A fault rupture model for seismic risk analysis. *Bull. Seismol. Soc. Am.*, 67:1173–1194.
35. Fitch, T.J. (1970), Earthquake mechanisms in the Himalaya, Burmese, and Andaman regions and continental tectonics in Central Asia, *J. Geophys. Res.*, 75:2699–2709.
36. Frankel, A. (1995), Mapping seismic hazard in the Central and Eastern United States, *Seismological Research Letters*, 66(4):4–8.

37. Gansser, A. (1974), The Ophiolitic Melange, a world-wide Problem on Tethyan examples, *Eclogae geol. Helv.*, 67:479-507.
38. Gardner, J.K. and Knopoff, L. (1974), Is the sequence of earthquakes in Southern California, with aftershocks removed, Poissonian?. *Bull. Seism. Soc. Am.* 64, 1363–1367.
39. Gaull, B.A., Michael-Leiba, M.O. and Rynn, J.M.W. (1990), Probabilistic earthquake risk maps of Australia, *Australian Journal of Earth Sciences*, 37:169-187.
40. Giardini, G., Wiemer, S., Fäh, D. and Deichmann, N. (2004), *Seismic Hazard Assessment of Switzerland*, Publication Series of the Swiss Seismological Service, ETH Zürich, 91 p.
41. GSI (2000), *Seismotectonic Atlas of India and its Environs*. Geological Survey of India.
42. Grady, J.C. (1971) Deep main faults in south India, *J. Geol. Soc. India*, v. 12, pp. 56-62.
43. Gubin, I.E. (1968). Seismic zoning of Indian peninsula, *Bulletin of International Institute of Seismology and Earthquake Engineering*, 5, 109-139.
44. Guha, S.K. and Basu (1993). *Catalogue of earthquakes (> 3.0) in Peninsular India*, AERB Technical Document No. TD/CSE -1, pp. 1- 70.
45. Guha, S.K., Gosavi, P.D., Varma, M.M. , Agarwal, S P., Padale, J.G. and Marwadi, S.C. (1968). *Recent seismic disturbances in the Shivaji isagar Lake area of the Koyna hydroelectric project, Maharashtra, India*, Comprehensive report up to June 1969,Central Water and Power Research Station, Khadakwasla, Poona-24, India.
46. Gupta, I. D., R. G. Joshi, and V. Rambabu (1992). Analysis of Some Significant Accelerograms of Koyna Dam Earthquakes Using Improved Data Processing Techniques, Technical Memorandum, Ministry of Water Resources, Central Water and Power Research Station.
47. Gupta, I.D. (2006). Delineation of probable seismic sources in India and neighbourhood by a comprehensive analysis of seismotectonic characteristics of the region, *Soil Dynamics and Earthquake Engineering,* 26,766–790.
48. Hasegawa H.S., Basham P.W., Berry M.J. (1981) Attenuation relations for strong seismic ground motion in Canada. *Bull Seismol Soc Am* 71:1943–1962
49. IBC. (2003). *International Building Code*. International Code Council.
50. Idriss, I.M. (1985). Evaluating seismic risk in engineering practice. *Proc. of the 11th Intl. Conf. on Soil Mechanics and Foundation Engineering,* San Francisco, 1, 255–320.
51. Iman, R.L. and Conover, W.J. (1980), Small sample sensitivity analysis techniques for computer models, with an application to risk assessment, *Communications in Statistics*, A9(17):1749-1842. Rejoinder to Comments, 1863-1874.
52. IS 1893-2002 (2002). *Criteria for earthquake resistant design of structures: Part 1 - General provisions and buildings*, Bureau of Indian Standards, BIS, New Delhi.
53. Iyengar, R. N. (1997) Strong motion: Analysis, Modelling and Applications. *Bull. ISET,* Paper no. 370, **34**, 4, 171-208
54. Iyengar, R.N, Sharma, D, and Siddiqui, J.M. (1999), Earthquake history of India in medieval times, *Indian Journal of history Science*, 34 (3).
55. Iyengar, R.N. (2000). Seismic status of Delhi Megacity, *Current Science*, 78, 568-574.
56. Iyengar, R.N. and Raghukanth, S.T.G. (2004), Attenuation of strong ground motion in peninsular India, *Seismological Research Letters*, 75(4), 530-540.

57. Iyengar, R.N., Ghosh, S. (2004). Microzonation of earthquake hazard in Greater Delhi area, *Current Science*, 87(9).
58. Jaiswal, K. and Ravi Sinha (2007). Probabilistic seismic-hazard estimation for peninsular India, *Bull. Seism. Soc. Am.* 91(1B), 318-330.
59. Joyner, W.B. and Boore, D.M. (1981), Peak horizontal acceleration and velocity from strong-motion records including records from the 1979 Imperial Valley, California, Earthquake, *Bull. Seism. Soc. Am.*, 71:2011–2038.
60. Kaila, K.L., Gaur, V.K. and Narain Hari (1972), Quantitative seismicity maps of India. *Bull Seismol Soc Am.*, 62:1119–1131.
61. Katti, R. K., Kulkarni, K. R., Chandrasekaran, V. S., Venkatachalam, G., and Dewaikar, D. M. (1975). Regional soil deposits of India. Proc., 5th Asian regional conference on Soil mechanics and Foundation engineering, Bangalore, India.
62. Kayal J.R. (2008), *Microearthquake Seismology and Seismotectonics of South Asia*. Capital Publishing Company, New Delhi.
63. Khattri, K.N. (1994). Earthquake hazard in Indian region, *Sadhana*, 19(4):609-614.
64. Khattri, K.N., Rogers, A.M., Perkins, D.M. and Algermissen, S.T. (1984), A seismic hazard map of India and adjacent areas, *Tectonophysics*, 108:93–134.
65. Kijko, A. (2002), Statistical estimation of maximum regional magnitude *mmax*. In: *Proceedings of the 12th European Conference on Earthquake Engineering*, London, Sept. 9-13, Elsvier Science, paper Reference FW:022.
66. Kijko, A. and Graham, G. (1998), Parametric-historic procedure for probabilistic seismic hazard analysis: Part I - estimation of maximum regional magnitude *mmax*. *Pure Appl. Geophys.*, 152:413-442.
67. Kijko, A. and Graham, G. (1999), "Parametric-historic" procedure for probabilistic seismic hazard analysis, Part II: assessment of seismic hazard at specified site, *Pure and Appl. Geophys.*, 154:1–22.
68. Kijko, A. and Sellvoll, M.A., (1989). Estimation of seismic hazard parameters from incomplete data files. Part-1: Utilization of extreme and complete catalogues with different threshold magnitudes, *Bull. Seism. Soc. Am.*, 79:645-654.
69. Knopoff, L. and Kagan, Y. (1977), Analysis of the theory of extremes as applied to earthquake problems, *J. Geophys. Res.*, 82:5647-5657.
70. Kumar, S., Wesnouskey, S.G., Rockwell, T.K., Ragona, D., Thakur V.C. and Seitz, G.G. (2001), Earthquake reoccurrence and rupture dynamics of Himalayan Frontal Thrust, India, *Science*, 294:2328–2331.
71. Lave, J., Yule, D., Sapkota, S., Basant, K., Madden, C., Attal, M., Pandey, R. (2005), Evidence for a great medieval earthquake (1100 A.D.) in the Central Himalayas, *Nepal. Science*, 307:1302–1305.
72. Mahajan, A. K., Thakur, V.C.,Sharma, M. L., Chauhan, M. (2010). Probabilistic seismic hazard map of NW Himalaya and its adjoining area, India, Natural Hazards,53, 443-457.
73. Malik, J.N., Nakata, T., Philip, G. and Virdi, N.S. (2003), Preliminary observations from trench near Chandigarh, NW Himalaya and their bearing on active faulting. *Current Science*, 85 (12):1793-1799.
74. McCalpin, J. (2009), *Paleoseismology*, Volume 95 of International geophysics series, Academic Press, 2nd Edition, 613 p.

75. Menon, A., Ornthammarath, T., Corigliano, M. and Lai, C. G., (2010) Probabilistic Seismic Hazard Macrozonation of Tamil Nadu in Southern India, *Bulletin of the Seismological Society of America,* 100(3):1320-1341.
76. Milne, J. (1911), *A catalogue of destructive earthquakes: A.D. 7 to A.D. 1899*, British Association for the Advancement of Science London, 92 p.
77. Mitra, S., Priestley, K., Bhattacharyya, A.K., et al., (2005), Crustal structure and earthquake focal depths beneath northeastern India and southern Tibet: *Geophysical Journal International*, 160:227-248.
78. Mohanty, W.K., Prakash, R., Suresh, G., Shukla, A.K., Walling, M.Y. and Srivastava, J.P. (2009), Estimation of coda wave attenuation for the national capital region, Delhi, India using local earthquakes, *Pure and Applied Geophysics*, 166(3): 429-449.
79. Oldham, T. (1883). A catalogue of Indian earthquakes from the earliest times to the end of 1869 A.D. *Mem. Geol. Surv. India.* XIX, Part. 3.
80. Parvez, I.A, Sutar, A.K, Mridula, M., Mishra, S.K. and Rai, S.S. (2008), Coda Q estimates in the Andaman Islands using local earthquakes, *Pure and Applied Geophysics,* 165:1861–1878.
81. Parvez, I.A., Vaccari, F. and Panza, G.F. (2003), A deterministic seismic hazard map of India and adjacent areas. *Geophysical Journal International*, 155:489-508
82. PMD (2007), Seismic Reports, Pakistan Meteorological Department, url: www.pakmet.com.pk
83. Quittmeyer, R.C. and Jacob, K.H.(1979). Historical and modern seismicity of Pakistan, Afghanistan, north-western India and south-eastern Iran, *Bull. Seism. Soc. Am.* 69:773-823.
84. Raghukanth S.T.G. and Iyengar R.N. (2006), Seismic hazard estimation of Mumbai city, *Current Science*, 92(11):1486-1494.
85. Raghukanth S.T.G. and Somala S N, Modeling of strong motion data in Northeastern India: Q, stress drop and site amplification (2009), *Bulletin of the Seismological Society of America,* 99(2A):705-725.
86. Raghukanth, S.T.G and Iyengar, R.N. (2007), Estimation of seismic spectral acceleration in Peninsular India, *Journal of Earth System Science*, 116(3):199 – 214.
87. Rajendran, C.P., Rajendran, K., Thakkar, M. and Goyal, B. (2008), Assessing the previous activity at the source zone of the 2001 Bhuj earthquake based on the near source and distant paleoseismological indicators. *Jour. Geophy. Res.*, 113(B05311):1–17.
88. Rajendran, C.P.K., Rajendran, Duarah B. P., Baruah S., and Earnest A., (2004), Interpreting the style of faulting and paleoseismicity associated with the 1897 Shillong, northeast India, earthquake: Implications for regional tectonism. *Tectonics*,23(4),TC4009.
89. Rao, B. R., and Rao, P. S. (1984). Historical seismicity of peninsular India. *Bull. Seism.Soc. Am.,* 74(6), 2519-2533.
90. Rao, B. R. (2005). Monograph on history of Indian earthquakes from earliest to 2005; http://seisinfo-india.org/seismocity.html.
91. Rao, R., Seshamma, C.V. and Mandal, P. (1998). *Estimation of Coda Qc and spectral characteristics of some moderate earthquakes of southern Indian peninsula*. Unpublished Report.
92. Reasenberg, P. (1985), Second-order moment of central California seismicity, 1969-1982, *J. Geophys. Res.* 90, 5479–5495.

93. Sadigh, K., Chang, C. Y., Egan, J. A., Makdisi, F., and Youngs, R. R., (1997). Attenuation relationships for shallow crustal earthquakes based on California strong motion data, *Seismol. Res. Lett.* **68**, 180–189.
94. Saragoni, G.R. and Hart, G.C. (1974), Simulation of artificial earthquakes, *Earthq. Eng. Struct. Dyn.*, 2, 249–267.
95. Scholz, C.H. (1997). Size distributions for large and small earthquakes. *Bull. seism. Soc. Am.*, 87:1074-1077.
96. Scordilis, E. M. (2006), Empirical global relations converting M*s* and m_b to moment magnitude. *Journal of Seismology*, 10, 225-236.
97. Seeber, L., Armbruster, J.G. and Jacob, K.H. (1999), *Probabilistic assessment of earthquake hazard for the state of Maharashtra*. Report to Government of Maharashtra Earthquake Rehabilitation Cell Mumbai.
98. Shanker, D. and Sharma, M.L. (1998), Estimation of seismic hazard parameters for the Himalayas and its vicinity from complete data files, *Journal of Pure and Applied Geophysics*, 152(2):267-279.
99. Sharma, B., Teotia, S.S. and Dinesh Kumar (2007), Attenuation of P, S, and coda waves in Koyna region, India, *Journal of Seismology,* 11:327–344.
100. Sharma, M.L. (1998). Attenuation relationship for estimation of peak ground horizontal acceleration using data from strong-motion arrays in India, *Bull. seism. Soc. Am.*, 88:1063-1069.
101. Shukla, A. K., Prakash, R., Singh, R. K., Mishra, P.S. and Bhatnagar, A. K. (2007). Seismotectonic implications of Delhi region through fault plane solutions of some recent earthquakes, *Current Science*, 93(12), 1848-1853.
102. Singh, S.K., Bansal, B.K., Bhattacharya, S.N., Pacheco, J.F., Dattratrayam, R.S., Ordaz, M., Suresh, G., Kamal and Hough, S.E. (2003), Estimation of ground motion for Bhuj (26th January 2001. Mw = 7.6) and for future earthquakes in India, *Bull. Seismol. Soc. Am.*, 93(1):353–370.
103. Singh, S.K., Dattatrayam, R.S., Shapiro, N.M., Mandal, P., Pacheco J.F., and Midha, R.K. (1999), Crustal and upper mantle structure of peninsular India and source parameters of the 21 May 1997 Jabalpur earthquake (Mw = 5.8): Results from a new regional broadband network, *Bull. Seismol. Soc. Am.*, 89:1631–1641.
104. Singh, S.K., Garc, D., Pacheco, J.F., Valenzuela, R., Bansal, B.K. and Dattatrayam, R.S. (2004), Q of the Indian Shield, *Bull. Seismol. Soc. Am.*, 94(4):1564-1570.
105. Singh, S.K., Ordaz, M., Dattatrayam, R.S. and Gupta, H.K. (1999), A spectral analysis of the May 21, 1997, Jabalpur, India earthquake (*M*w 5.8) and estimation of ground motion from future earthquakes in the Indian shield region, *Bull. Seismol. Soc. Am.*, 89(6):1620–1630.
106. Stepp, J.C. (1972), Analysis of completeness of the earthquake sample in the Puget sound area and its effect on statistical estimates of earthquake hazard. In *International Conference on Microzonation*, II, 897–909.
107. Sukhija B.S., Laxmi, B.V., Rao, M.N., Reddy, D.V., Nagabhushanam, P., Hussain, S. and Gupta, H.K. (2006), Wide spread geologic evidence of a large paleoseismic event near the Meizoseismal area of the 1993 Latur earthquake, Deccan shield. *India. Jour. Indian Geophys. Union*, 10:1–14.

108. Sukhija, B.S., Rao, M.N., Reddy, D.V., Nagabhushanam, P., Hussain, S., Chadha, R.K. and Gupta, H.K. (1999), Paleoliquefaction evidence and periodicity of large prehistoric earthquakes in Shillong Plateau, *Indian Earth Planet. Sci. Lett.*, 167:269–282
109. Tandon, A.N. and Chaudhury, H.M. (1968). Koyna earthquake of December, 1967, *India Meteorol. Dept., Scientific Report No.* 59.
110. Toro, G., Abrahamson, N., and Schneider, J. (1997). Attenuation relations of ground motion for rock and soil sites in Eastern United States. *Seismological Research Letters*,68, 41–57.
111. Turner, H.H. (1911), *Seismological investigations XII, seismic activity, 1899–1903 inclusive*, British Association for the Advancement of Science, London, 57–65.
112. Uhrhammer, R. (1986). Characteristics of northern and southern California seismicity, *Earthq. Notes* **57,** 21
113. USNRC (1997). Regulatory guide 1.165: Identification and characterization of seismic sources and determination of safe shutdown earthquake ground motion. Report No. DG- 1032(RG 1.165), USA.
114. Valdiya, K.S. (1976), Himalayan transverse faults and folds and their parallelism with subsurface structures of the Northern Indian Plains. *Tectonophysics*, 32:353-386.
115. Valdiya, K.S. (2001), *Himalaya: emergence and evolution*, Universities Press, Hyderabad.
116. Wells, D.L. and Coppersmith, K.J. (1994), Empirical relationships among magnitude, rupture length, rupture width, rupture area and surface displacements, *Bull. Seismol. Soc. Am.*, 84(4):974-1002.

******